Chameleon Models with Field-dependent Couplings

Hans Arnold Winther

Thesis submitted for the degree of
Master of Science

Institute of Theoretical Astrophysics
University of Oslo

June 2010

Abstract

Certain scalar-tensor theories exhibit the so-called chameleon mechanism, whereby observational signatures of scalar fields are hidden by a combination of self-interactions and interactions with ambient matter. Not all scalar-tensor theories exhibit such a chameleon mechanism, which has been originally found in models with inverse power run-away potentials and field independent couplings to matter. In this thesis we investigate field-theories with field-dependent couplings for the scalar field together with an appropriate potential in each case. We show that the thin-shell suppression mechanism is present for these new models, and the theory is indeed a chameleon field theory. We find the thin-shell solutions for a spherical body and investigate the consequences for the Eöt-Wash experiment, fifth-force searches and Casimir force experiments. Requiring that the scalar-field evades gravitational tests, we find that the coupling is sensitive to a mass-scale which is of order of the Hubble scale today. The cosmology of the theory is studied and its found that the chameleon can act as a dark energy fluid, and cause the late time acceleration of the universe. When local gravity bounds are satisfied the background evolution will be indistinguishable from ΛCDM. The linear matter perturbations will, for some values of the parameters exhibit a scale dependent growth which may allow future experiments of the large scale structure to discriminate our models from ΛCDM. However, in order to have this effect local gravity experiments forces us to have a coupling to dark matter only.

Acknowledgment

I would like to thank:

1. **David Fonseca Mota:** My supervisor and the man behind the ideas.
2. All the people I have been working with during this thesis.
3. My family, a specially my grandmother **Margot Johansen**, for funding this thesis.
4. My fellow students at the Institute of Theoretical Astrophysics and at the Theory group at the Department of Physics for making this a pleasant experience. Special thanks to **Jan Lindroos** and **Mikjel Thorsrud** for reading through this thesis.
5. **Larry David** for making me a better person.

Contents

Chapter 1

Introduction

1.1 Introduction

A host of observations [2, 3] concord with the existence of a dark energy component with negative pressure, which accounts for more than two thirds of the current total energy density in the universe. The data is so far consistent with the dark fluid being a cosmological constant, but it is nevertheless interesting to consider the possibility that we one day might find that the equation of state differs from -1.

This would imply that the vacuum energy is time-dependent, and from the principle of general covariance and locality it should also be a function of space; i.e. it is a field. The simplest possible field is a scalar field, and scalar field models of dark energy generally are referred to as quintessence, 'the fifth element'. The above argument of course assumes that gravity is well described by general relativity. It is however possible that the late time acceleration of the universe is due to some breakdown of general relativity on large scales.

If the equation of state differs -1, the vacuum energy must have varied significantly over the last Hubble time. This requires the scalar field to have a tiny mass of order $H_0 \sim 10^{-32} eV$, and which comes from the field equation for the scalar field: if the mass is much smaller then H_0 then the solution would be overdamped and the corresponding ω would be unmeasurable close to to -1. Similar if the mass is much larger than H_0 then the field would be rolling too rapidly to cause cosmic acceleration [26].

If a field with such a small mass exist then why has it not been detected in local tests of the equivalence principle (EP) and fifth force searches? From string theory it is known that in effective theories such scalar fields couple to matter with gravitational strength, leading to unacceptably large violation of EP and a fifth-force.

It is here the chameleon mechanism comes to the rescue. Originally proposed by Justin Khourey and Amanda Weltman [1], where they showed that a scalar field non-minimally coupled to matter can evolve on a Hubble time today and cause cosmic acceleration, having a coupling to matter with gravitational strength and still evade current bounds from local gravity experiments.

The basic idea behind the mechanism is that the scalar field acquires a mass which depends on the local matter density. On Earth, where the density is high, the mass will be large, but on cosmological scales where the density is much smaller the mass will be be much smaller and the field can act as a dark energy fluid and cause cosmic acceleration. This also explains its name of the model: the field act as a chameleon, hiding in high density environments.

Also, an important feature of the chameleon is that it makes unambiguous and testable predictions for near future test of gravity in space, namely for the three satellite experiments MICROSCOPE, STEP and GG [4, 5,

6]. In the solar system the chameleon is essentially a free field and thus mediates a long-range force. Due to the thin-shell mechanism[1] this force will be very weak for large bodies, such as planets, therefore not affecting planetary orbits. The thin-shell mechanism is essentially the effect that only a thin-shell near the surface will contribute to the resulting fifth-force. This is a breakdown of the superposition principle and is due to the non-linear self-interactions of the field.

Typically test-masses in the above satellite experiments don't necesarilly have a thin-shell and therefore the extra force due to the scalar field will be of the same order as gravity. This means that MICROSCOPE, STEP and GG could measure violations of EP stronger than currently allowed by laboratory experiments. Furthermore the SEE-project could measure an effective gravitational constant that differs by $\mathcal{O}(1)$ from the value measured on earth. Such an outcome of the experiment would constitute strong evidence for the existence of chameleons in our universe.

1.2 Outline

In the first part of this thesis we will give a short review of the theoretical foundations which is required in the study of the chameleon model from Lagrangian field theory to general relativity and its applications in cosmology. The focus has been on the principles behind the models, and the mathematical equations are just stated without to much justification since this can be found in any good text book on the subject. We have also added a short review of the PPN-formalism which is a useful tool for analyzing modified gravitational models, but can be very technical. This chapter can serve as a reference, when used together with [19], to learn the methods of the PPN formalism since C. Will's book is very compact. After the prerequisite we give a short review of the Chameleon model.

In the literature the chameleon mechanism have only been studied with a constant coupling. The first original production comes in chapter 4 and is a study of the linear matter perturbations in this model. In chapter 5 we generalize this coupling to an inverse power law, ϕ^{-n}, where $n > 0$. We have looked at the theoretical predictions of this new model and worked out the experimental bounds constraining the free parameters in the model. The case $n < -1$ was discussed in [11], and their result is that this coupling is bothered with singularities. However this result is based on some false assumptions. We will derive the correct equations in chapter 6 and show that there do indeed exist a chameleon (thin-shell) mechanism in these models. In chapter 7 we study the cosmology of this new models, since we would like it to be a natural dark energy candidate, and where our main interest is to

[1] The thin-shell mechanism is discusses in section III: 'Review of the Chameleon Model'.

see whether the chameleon can have an effect on the growth of the matter perturbations.

In working with this thesis I have been involved in three projects which will hopefully resulted in three papers. The first paper, 'On the growth of matter perturbations in chameleon models', is a collaboration with Radouane Gannouji, Bruno Moraes, David F. Mota, David Polarski and Shinji Tsujikawa. We have studied the perturbations in the standard chameleon model with an exponential potential and my work has mainly been to calculate the local gravity bounds for this model and do some cosmological numerics. This paper is in preparation and the results shown in chapter 4 are the preliminary results and might seem a little amputated. The second paper is a collaboration with David Mota, Phillippe Brax, Carsten van de Bruck and Nelson Nunes on 'Chameleons with Field-dependent Couplings' and will be sent for publication to Phys.Rev. D. in the very recent future. This has been the main project of this thesis, the work shown here is mostly my own work, but the results have been checked and the paper have been edited by the collaboration. The last project is 'Cosmology of Chameleons with Field-dependent Couplings' and is the work of David Mota and myself.

1.3 Notation

1.3.1 Units

We will always work in units of $\hbar = c \equiv 1$. This makes sure that all basic quantities (length, time, mass, energy) can be expressed in terms of a single mass unit

$$\text{mass} = \text{energy} = \text{length}^{-1} = \text{time}^{-1} \tag{1.1}$$

Conversion factors, which is used in transforming from SI-units to the $\hbar = c = 1$ units, are:

$$\begin{aligned} \text{kg} &= 5.65 \cdot 10^{26}\text{GeV} \\ \text{m} &= 5.07 \cdot 10^{15}\text{GeV}^{-1} \\ \text{s} &= 1.52 \cdot 10^{24}\text{GeV}^{-1} \\ \text{N} &= 1.24 \cdot 10^{-6}\text{GeV}^{2} \\ \text{J} &= 6.24 \cdot 10^{9}\text{GeV} \end{aligned}$$

When speaking about the Planck-mass we use the following convention

$$M_p \equiv \frac{1}{\sqrt{8\pi G}} = 2.4 \cdot 10^{18} GeV$$

In some parts of this thesis we will apply Planck-units in which $M_p = 2.4 \cdot 10^{18}\text{GeV} \equiv 1$. This corresponds to putting $GeV \rightarrow 4.16 \cdot 10^{-19}$ in

the conversion factors above.

The metric is given the signature $(-,+,+,+)$.

1.3.2 Einstein Summation Convention

Any expression where there are equal upper and lower indices, the indices should be summed over

$$g_{\mu\nu}A^{\mu} = \sum_{x=0}^{3} g_{x\nu}A^{x}$$

Greek indices implies a summation over all four components of spacetime, and Latin indices implies a summation over only the three space indices.

1.3.3 Derivatives

The following notation for different typed of derivatives are used:

$$\begin{array}{ll} \text{A total derivative:} & \frac{df}{dx},\ \dot{f},\ f' \\ \text{Partial derivatives:} & \frac{\partial f}{\partial x} \equiv f_{,x} \\ \text{Covariant derivatives:} & \nabla_{\mu} f \equiv f_{;\mu} \\ \text{d'Alembert operator:} & \Box \equiv \nabla_{\mu}\nabla^{\mu} \\ \text{Laplacian operator:} & \nabla^2 \equiv \sum_i \frac{d^2}{dx_i^2} \end{array} \tag{1.2}$$

When derivatives are to be evaluated at a particular point the notation $f_{,\phi_i} \equiv \left.\frac{\partial f}{\partial \phi}\right|_{\phi=\phi_i}$ will sometimes be used.

1.3.4 Acronyms

The following acronyms will be used throughout this thesis:

- BBN - Big Bang nucleosynthesis
- BD - Brans-Dicke
- CMB - Cosmic microwave background radiation
- DE - Dark energy
- EEP - Einstein equivalence principle
- EP - Equivalence principle
- FLRW - Friedmann-Lemaître-Robertson-Walker
- GR - General relativity

- IPLC - Inverse power coupling
- LLI - Local Lorentz Invariance
- LLR - Lunar laser ranging
- LPI - Local Position Invariance
- PLC - Power-law coupling
- PPN - Parametrized Post-Newtonian formalism
- SCM - Standard chameleon model
- SR - Special relativity
- WEP - Weak equivalence principle

Chapter 2

Preliminaries

2.1 Field Theory

In physics, a field is a physical quantity associated to each point of spacetime. A field can be classified as a scalar field, a vector field, or a tensor field, according to whether the value of the field at each point is a scalar, a vector, or, more generally, a tensor, respectively. For example, the Newtonian gravitational field is a vector field: specifying its value at a point in spacetime requires three numbers, the components of the gravitational field vector at that point. Moreover, within each category a field can be either a classical field or a quantum field, depending on whether it is characterized by numbers or quantum operators respectively. We will only consider classical fields, and for an introduction to Lagrangian field theory in the context of quantum field theory see [30]. This section is based on [7, 8].

2.1.1 The Lagrangian Formalism

The framework of modern theoretical physics today such as particle physics, gravitational physics and cosmology are generally expressed in terms of a Lagrangian and an action. The equations describing the dynamics of a physical system are derived from the action by using an invariant action principle. We introduce the Lagrangian formalism for classical mechanics and show how it carries over to classical fields.

Classical Mechanics

There are often many different ways of formulating the same physics in the language of mathematics. Richard Feynman once said that *'every theoretical physicist who is any good knows six or seven different theoretical representations for exactly the same physics'*. Classical mechanics is often formulated by using *Newton's second law* which states

- **Newtons second law:** In an inertial frame, the net external force on a body is equal to the mass of that body times its acceleration, $F = ma$.

This formulation is the simplest to use when dealing with small and predicable systems, but when the complexity of the system increases it becomes difficult to use. Fortunately the same dynamics produced by Newton's second law can be derived from a more abstract principle which can also be used to formulate theories of nature where Newton's laws breaks down, namely *Hamilton's Principle* which states

- **Hamilton's Principle:** The motion of a system from time t_1 to t_2 is such that the action-integral

$$S = \int_{t_1}^{t_2} L dt \tag{2.1}$$

where $L = T - V$, has a stationary value for the actual path of motion.

L is called the Lagrangian of the system and is defined as the kinetic energy T minus the potential energy V. The Lagrangian is a function of the degrees of freedom of the system q_i and time derivatives $\dot{q}_i$, the variables that describe the position and velocity of the particles making up the system.[1]

Using Hamilton's principle we can find the equations of motion for the system in terms of the Lagrangian. We start with the action for a general path $q = q_1, ..., q_N$ and introduce a small variation in the path $q \to q + \delta q$ where we keep the endpoints fixed: $\delta q_i(t_1) = \delta q_i(t_2) = 0$. This leads to a variation in L given by

$$\delta L = \frac{\partial L}{\partial q_i}\delta q_i + \frac{\partial L}{\partial \dot{q}_i}\delta \dot{q}_i \tag{2.2}$$

$$= \left[\frac{\partial L}{\partial q_i} - \frac{d}{dt}\left(\frac{\partial L}{\partial \dot{q}_i}\right)\right]\delta q_i + \frac{d}{dt}\left[\frac{\partial L}{\partial \dot{p}_i}q_i\right] \tag{2.3}$$

The variation in the action S becomes

$$\delta S = \int_{t_1}^{t_2}\left[\frac{\partial L}{\partial q_i} - \frac{d}{dt}\left(\frac{\partial L}{\partial \dot{q}_i}\right)\right]\delta q_i dt + \left[\frac{\partial L}{\partial \dot{p}_i}q_i\right]_{t_1}^{t_2} \tag{2.4}$$

where the last term vanishes due to the boundary conditions stated above. If we have a stationary path the first integral should vanish for arbitrary δq_i, but this is only possible if

$$\frac{\partial L}{\partial q_i} - \frac{d}{dt}\left(\frac{\partial L}{\partial \dot{q}_i}\right) = 0 \tag{2.5}$$

This are the equations of motion for the system, called the *Euler-Lagrange equation* (EL).

To show that this formulation is equivalent to Newton's formulation (in the case of conservative forces) is seen by looking at a non-relativistic particle traveling in a potential $V(|\vec{x}|)$. Denoting its position by $\vec{x}(t)$, its kinetic energy is then given by the usual expression $T = \frac{1}{2}m\dot{\vec{x}}^2$. This gives the Lagrangian

$$L = \frac{1}{2}m\dot{\vec{x}}^2 - V(|\vec{x}|) \tag{2.6}$$

By applying the EL equation we find

$$m\ddot{\vec{x}} = -\vec{\nabla}V(|\vec{x}|) \tag{2.7}$$

[1] The reason one rearly considers a Lagrangian with higher order derivatives is due to the Ostrogradskian instability: Both positive and negative energy modes can grow without bounds [68].

which is Newton's second law for conservative forces. The generalization to fields can be done formally by first defining the field discreetly in some region Ω of space by $\Phi(x = i\Delta x, t) = q_i(t)$ and then taking the limit $\Delta x \to 0$. This is a dippy process, but it can serve as a justification of the generalization of the Lagrangian formalism from classical mechanics to classical fields. We refer the reader to [8] for a more thorough discussion.

Classical Field Theory

One problem with the classical mechanical Lagrangian is that the action following from it fails to be relativistic invariant (Lorentz-invariant), and thus it cannot be used in a general setting according to the principle of special relativity. This can be solved by introducing a Lagrangian density $\mathcal{L}$ via

$$L = \int dx^3 \mathcal{L} \tag{2.8}$$

Now the action $S = \int dt L = \int_\Omega dx^4 \mathcal{L}$, where Ω is some region of spacetime, is Lorentz-invariant as long as $\mathcal{L}$ is. Let us consider a system which requires several fields $\Phi_i(x,t)$, $i = 1, .., N$ to specify it. The index may label components of the same field, for example the components of the vector potential $\vec{A}(x)$, or it may refer to different independent fields. Under a variation of the fields $\Phi_i \to \Phi_i + \delta\Phi_i$, which vanish on the surface $\Gamma(\Omega)$ bounding the region Ω,

$$\delta\Phi_r(x) = 0 \text{ for } x \in \Gamma(\Omega) \tag{2.9}$$

will lead to a variation $\delta\mathcal{L}$ in $\mathcal{L}$. Using Hamilton's principle we demand that the action for an arbitrary region Ω has a stationary value $\delta S(\Omega) = 0$. $\delta S(\Omega)$ is given by

$$\delta S(\Omega) = \int_\Omega dx^4 \left[\frac{\partial \mathcal{L}}{\partial \Phi_i} - \partial_\mu \left(\frac{\partial \mathcal{L}}{\partial \Phi_{i,\mu}}\right)\right] \delta\Phi_i + \int_\Omega dx^4 \partial_\mu \left[\frac{\partial \mathcal{L}}{\partial \Phi_{i,\mu}} \delta\Phi_i\right] \tag{2.10}$$

and the last term can be written as a surface integral over $\Gamma(\Omega)$ by using Gauss's theorem in four dimensions and since $\delta\Phi_i$ vanishes on $\Gamma(\Omega)$ this term is zero. If $\delta S(\Omega)$ is to vanish for arbitrary variations $\delta\Phi_i$ we must require

$$\frac{\partial \mathcal{L}}{\partial \Phi_i} - \partial_\mu \left(\frac{\partial \mathcal{L}}{\partial \Phi_{i,\mu}}\right) = 0 \tag{2.11}$$

which are the EL equations for fields.

2.1.2 Symmetries and conservation laws

For a field theory derived from a Lagrangian density $\mathcal{L}$, one can construct conserved quantities from the invariance of $\mathcal{L}$ under symmetry transformations. This is known as *Noether's theorem* and in physics it is often formulated in the following way:

- **Noether's theorem:** For every continuous symmetry-transformation that leaves the Lagrangian unchanged there exist a conserved current.

To show why this is true, consider a transformation $\Phi_i \to \Phi_i'$ of the fields. Because the transformation is assumed to be continuous we need only look at an infinitesimal transformation $\Phi_i' = \Phi_i + \delta\Phi_i$. The change induced in $\mathcal{L}$ is given by

$$\delta\mathcal{L} = \frac{\partial\mathcal{L}}{\partial\Phi_i}\delta\Phi_i + \frac{\partial\mathcal{L}}{\partial\Phi_{i,\mu}}\delta\Phi_{i,\mu} = \partial_\mu\left[\frac{\partial\mathcal{L}}{\partial\Phi_{i,\mu}}\delta\Phi_i\right] \tag{2.12}$$

where the last equality follows from the EL equations. If $\mathcal{L}$ is invariant under the transformation then $\delta\mathcal{L} = 0$ giving

$$\partial_\mu\mathcal{F}^\mu = 0 \tag{2.13}$$

where $\mathcal{F}^\mu = \frac{\partial\mathcal{L}}{\partial\Phi_{i,\mu}}\delta\Phi_i$. Defining $F^\mu = \int dx^3\mathcal{F}^\mu$ we can write

$$\frac{dF^0}{dt} = -\int dx^3\partial_i\mathcal{F}^i = 0 \tag{2.14}$$

where the last equality follows by using Gauss's divergence theorem and assuming that the fields tend to zero at infinity. Or if we use a finite normalization volume for our system this term vanishes by periodic boundary conditions. The derivation above shows that F^0 is a conserved quantity which proves Noether's theorem in this special case. Going further we can show that invariance under spacetime translations yields energy and momentum conservation and invariance under rotations yields conservation of angular momentum. The close relationship between symmetries and conserved quantities in the Lagrangian formalism makes it the natural choice to work within.

2.2 Gravitational Theory

2.2.1 Introduction

Gravitational theory has roots all the way back to the era where the modern physics and mathematics was born. Issac Newton, in his famous book 'Principia' of 1686, stated that gravity was a force which falls off as the square of the distance from the center of mass. Newton demonstrated that such a force would naturally lead to circular and elliptical orbits of planets in agreement with what was observed. This section is mainly based on [9, 19, 24].

Newtons' law of gravitation can be stated mathematically as

$$F = \frac{GmM}{r^2} \tag{2.15}$$

where m is the (inertial) mass of the body in which the force acts on, M is the mass of the source generating the gravitational force, r is the center-center distance between the bodies and G is the gravitational constant. The (experimental) result that the gravitational force on a mass is proportional to the inertial mass has become a principle, now called the *weak principle of equivalence*

- **The Weak Principle of Equivalence (WEP):** *The gravitational mass equals the inertial mass.*

To Newton this was such a cornerstone in his theory that he devoted the opening part of the 'Principia' to a detailed discussion of it. Note that in the literature this principle is sometimes stated as the *universality of free fall*,

- **Universality of free fall:** *Any two test bodies must fall with the same acceleration in a given external gravitational field.*

but the two formulations are equivalent. Newton performed pendulum experiments to verify this principle, and in modern days this principle has been tested to such a great accuracy that we believe it to be true. For a through review on the experimental situation see [19].

2.2.2 Special Relativity

When Maxwell in the 1860's discovered the laws of classical electrodynamics it was found that the laws was not invariant under the usual Galilean coordinate transformations [17]. If we start with Maxwell's wave-equation for the electric field

$$\frac{\partial^2 E}{\partial x^2} = \frac{1}{c^2}\frac{\partial^2 E}{\partial t^2} \tag{2.16}$$

and make a translation $x' = x + vt$ with $t' = t$ we find that the E-field in this new frame is determined by

$$\frac{\partial^2 E'}{\partial x'^2}\left(1 - \frac{v^2}{c^2}\right) + \frac{2v}{c^2}\frac{\partial^2 E'}{\partial x' \partial t'} = \frac{1}{c^2}\frac{\partial^2 E'}{\partial t^2} \tag{2.17}$$

which is not the same equation. This was explained by postulating that there existed a universal rest frame, the ether, in which light moved relative to and the wave-equation only takes the form (2.16) in this frame. The laws of mechanics and electrodynamics was treated separately in the sense that *Galileo's principle of relativity*

- **Galileo's principle of relativity:** *All uniform motion is relative and there is no absolute and well-defined state of rest*

was thought to be valid only for the laws of mechanics.

This changed in 1905 when Einstein put forward his special theory of relativity (SR) where he generalized the Galilean principle to all the laws of physics, including the laws of electrodynamics. The theory is termed 'special' because it applies the principle of relativity, defined below, only to frames in uniform relative motion. Einstein put forward two fundamental propositions that the theory is build on

- **The Principle of Relativity:** *The laws of physics are the same in all inertial frames.*
- **The Principle of Invariant Light Speed:** *The speed of light in empty space is the same in all inertial frames and independent of the motion of the light source.*

and with these principles he was able to deduce the mathematical formulation of the theory. We assume the reader is familiar with the mathematical formulation of SR. See [24] for a thorough review.

This theory has a wide range of consequences which have been experimentally verified. Some consequences are counter-intuitive ones such as time dilation and the relativity of simultaneity, contradicting the classical notion that the duration of the time interval between two events is equal for all observers. Combined with other laws of physics, the two postulates of special relativity predict the equivalence of matter and energy, as expressed in the famous mass-energy equivalence formula $E = mc^2$. The theory gives a new law of velocity addition and one of the consequences of this is that it is impossible for any particle that has rest mass to be accelerated to the speed of light. In the limit where the velocities in play are small compared to the speed of light the theory reduces to the well knows laws of Newtonian mechanics.

2.2.3 Differential Geometry

Geometry is one of the oldest discipline in pure mathematics and has a rich history. Euclid, in the 3rd century BC, gave geometry a firm mathematical foundation by the introduction of the basic axioms, and the result - Euclidean geometry - set a standard for many centuries to follow. Coordinates as we use for almost everything today was introduced by René Descartes and the concurrent development of algebra marked a new stage for geometry, since geometric figures, such as plane curves, could now be represented analytically with functions and equations. The subject of geometry was further enriched by the study of intrinsic structure of geometric objects that originated with Euler and Gauss and led to the creation of topology and differential geometry. In Euclid's time there was no clear distinction between the physical space and the geometrical space: It was thought to be the same. But this changed by the discovery of non-Euclidean geometry, by Bernhard Riemann in 1854. Riemann went back to the axioms proposed by Euclid and showed that if one changed one of them, one could produce a completely different geometry. In doing so the concept of space, point, line, etc. lost its intuitive contents, so today we have to distinguish between physical space and geometrical spaces (in which the concepts space, line etc. still have their intuitive meaning). Modern geometry considers manifolds, spaces that may be considerably more abstract than the familiar Euclidean space, which they only approximately resemble at small scales. These spaces may be endowed with a metric, allowing one to speak about length. Modern geometry has strong bonds with physics, and Einstein had to use non-euclidean geometry when developing general relativity.

Einstein's equation is the centerpiece of general relativity, and is formulated using the concepts of Riemannian geometry. The geometric properties of a spacetime are described by a quantity called the metric. The metric encodes the information needed to compute the fundamental geometric notions of distance and angle in a curved spacetime. The principle of general covariance implies that the laws should be written in a form which does not depend on the frame of reference used, and it guides us in choosing the appropriate mathematical objects for the formulation of the laws, namely tensors.

In a Riemannian manifold, we can define a metric tensor g which gives the inner product of two vectors a and b by

$$g(a,b) = a \cdot b = g_{\mu\nu} a^\mu b^\nu \tag{2.18}$$

Here $g_{\mu\nu}$ is the components of the tensor given by $g_{\mu\nu} = \vec{e}_\mu \cdot \vec{e}_\nu$ where $\vec{e}_\mu$ is an arbitrary basis. In general relativity the metric is often stated by using the *line-element*

$$ds^2 = g_{\mu\nu} dx^\mu dx^\nu \tag{2.19}$$

Given a vector, $\vec{A} = A^\mu \vec{e}_\mu$, then under a change of coordinates the ordinary derivative, $A^\mu{}_{,\nu}$, of the vector transforms as

$$A^{\mu'}{}_{,\nu'} = \frac{\partial x^\nu}{\partial x^{\nu'}} \frac{\partial x^{\mu'}}{\partial x^\mu} A^\mu{}_{,\nu} + \frac{\partial x^\nu}{\partial x^{\nu'}} A^\mu \frac{\partial^2 x^{\mu'}}{\partial x^\nu \partial x^\mu} \tag{2.20}$$

The existence of this last term shows that $A^\mu{}_{,\nu}$ do not transform as a tensor for general coordinate transformations. But one can introduce the *covariant derivative*

$$\nabla_\nu A^\mu \equiv A^\mu_{;\nu} = A^\mu{}_{,\nu} + \Gamma^\mu_{\alpha\nu} A^\nu \tag{2.21}$$

which do transform as a tensor. Γ is the Christoffel-symbols defined by

$$\Gamma^\mu_{\alpha\beta} = \frac{1}{2} g^{\mu\delta} (g_{\alpha\delta,\beta} + g_{\delta\beta,\alpha} - g_{\alpha\beta,\delta}) \tag{2.22}$$

in a coordinate basis and describes the derivatives of the basis vectors. Given a general curve with tangent vector, $\vec{u}(\tau)$ and parametrized by τ, the covariant derivative of a vector field $\vec{A}$ along the curve is defined by

$$\nabla_{\vec{u}} \vec{A} = A^\mu_{;\nu} u^\nu \vec{e}_\mu \tag{2.23}$$

Vectors in the vector field are said to be *connected by parallel transport* along the curve if

$$A^\mu_{;\nu} u^\nu = 0 \tag{2.24}$$

In Euclidean geometry, the shortest path between two points is a straight line. In curved spacetime the generalization of a 'straight line' is called the *geodesic* and is defined as

- **Geodesic curve:** A curve whose tangent vectors are connected by parallel transport: $u^\mu_{;\nu} u^\nu = 0$.

By using (2.21) and (2.24) one can express the geodesic equation in more familiar terms

$$\frac{d^2 x^\mu}{d\tau^2} + \Gamma^\mu_{\alpha\beta} \frac{dx^\alpha}{d\tau} \frac{dx^\beta}{d\tau} = 0 \tag{2.25}$$

The intrinsic curvature of the manifold can be quantified by looking on how four-vectors change when they are parallel-transported around an infinitesimal loop, the result is

$$\Delta \vec{A} = \frac{1}{2} A^\nu R^\mu_{\nu\alpha\beta} \Delta S^{\alpha\beta} \vec{e}_\mu \tag{2.26}$$

where $|\Delta \vec{S}| = |\vec{\Delta u} \times \vec{\Delta v}|$ is the area of the loop and $R^\mu_{\nu\alpha\beta}$ is the Riemann-curvature tensor. A second order curvature tensor can be constructed by

contracting two indices in the Riemann-curvature tensor.[2] This gives us the Ricci-tensor, $R_{\nu\beta} = R^{\mu}_{\nu\mu\beta}$, which in a coordinate basis is given explicitly by

$$R_{\mu\nu} = \Gamma^{\alpha}_{\mu\nu,\alpha} - \Gamma^{\alpha}_{\mu\alpha,\nu} + \Gamma^{\alpha}_{\mu\nu}\Gamma^{\lambda}_{\lambda\alpha} - \Gamma^{\alpha}_{\mu\lambda}\Gamma^{\lambda}_{\nu\alpha} \tag{2.27}$$

For an introduction to differential geometry in the context of general relativity see [24, 46] which this section is based on.

2.2.4 General Relativity

Special relativity states that the laws of physics should be the same for all inertial observers, but for Einstein this was not enough. He had the strong belief that the laws of physics should be the same for all observers, inertial or not, and this lead him to a new principle which is a generalization of the principle of relativity

- **The Principle of General Covariance:** *The laws of physics should be the same for all observers.*

- **The Einstein Equivalence principle:** *WEP is valid and the outcome of any local non-gravitational experiment in a freely falling laboratory is independent of the velocity of the laboratory and its location in spacetime.*

The mathematical consequences of this first principle is that the laws of physics should be formulated in terms of frame invariant objects namely tensors. The second principle states that there is no way of distinguishing between free fall in a uniform gravitational field and uniform acceleration, and can be dissected into three parts

- **Weak equivalence principle (WEP):** *The gravitational mass equals the inertial mass.*

- **Local Lorentz Invariance (LLI):** *The outcome of any local non-gravitational experiment in a freely falling laboratory is independent of the velocity of the freely falling frame.*

- **Local Position Invariance (LPI):** *The outcome of any local non-gravitational experiment in a freely falling laboratory is independent of where and when it is performed.*

[2] Because of symmetries and it does not matter which two indexes we contract (up to a sign). The standard convention is contracting the second lower index.

The best reason to believe in these principles, at least WEP and LLI, is the solid experimental proof.

Violation of WEP will happen if some internal degree of freedom contributes differently to the inertial mass of a body than to the gravitational mass. This can be parametrized by the Eötvos parameter η which measures the difference in free fall acceleration for two bodies of different composition

$$\eta = \frac{2|a_1 - a_2|}{|a_1 + a_2|} \tag{2.28}$$

The best current bound comes from the Eöt-Wash EP-experiment [27] and reads $\eta < 10^{-13}$, which is a tight bound on any EP-violating interactions.

Any experiment that purports to test special relativity also test some aspect of LLI. The most well known experiment on this form is the Hughes-Drever experiment [28], which examined the $J = \frac{3}{2}$ ground state of the ^{7}Li nucleus in an external magnetic field and found the bound $\delta < 10^{-20}$ where δ is a parameter that measures the strength of any LLI violating interactions. Because of the remarkably small size of this parameter this experiment has been called the most precise null experiment ever performed.

The two principal tests of LPI are gravitational red-shift experiments that test the existence of spatial dependence on the outcomes of local experiments, and measurements of the constancy of the fundamental non gravitational constants. We refer to [19, Page 32-38] for a review on the experimental situation. Recently there has been some claims of a detection of a non-zero variation in the fine-structure constant and the electron-proton ratio [25]. These claims are not yet confirmed, but if they some day are then this will be evidence for physics beyond general relativity and the standard model.

Einsteins Field Equations

Einstein's field equations are the relativistic generalization of Newton's gravitational law. Einstein's vision, based on the Einstein equivalence principle, was that there was no gravitational force at all. What Newtonian theory said was a motion under the influence of the gravitational force, is according to general relativity free motion along geodesics of a curved spacetime.

To see how one can make this generalization start with the Newtonian gravitational law, which on local form can be written

$$\nabla^2\phi(r) = 4\pi G\rho(r) \tag{2.29}$$

together with

$$g(\vec{r}) = -\vec{\nabla}\phi(r) \tag{2.30}$$

where $g(\vec{r})$ is the gravitational acceleration and $\phi(r)$ the gravitational potential. The right hand side of (2.29) involves the matter density and therefore we would like to replace it with the energy-momentum tensor $T_{\mu\nu}$ which is a relativistic generalization of energy. The left hand side should, if gravity is a geometric phenomenon, be given by the geometry of space. The (second) simplest second order tensor that embodies the geometry of space is the Ricci curvature tensor $R_{\mu\nu}$ (2.27). Einstein first tried [18] $R_{\mu\nu} \propto T_{\mu\nu}$, but found that this did not work since the Ricci tensor is not always divergence free which it needs to be if we want the theory to satisfy the usual conservation of energy and momentum. After some trial and error, Einstein finally came up with the equation

$$R_{\mu\nu} - \frac{1}{2}Rg_{\mu\nu} = \kappa T_{\mu\nu} \tag{2.31}$$

where $R = g^{\mu\nu}R_{\mu\nu}$ in the Ricci-scalar and κ is a constant that is determined by requiring the correct Newtonian limit. The left hand side is called the Einstein-tensor and is divergence free, therefore making sure that $\nabla^\mu T_{\mu\nu} = 0$, which again means that energy and momentum is conserved (locally). Note that since $g_{\mu\nu}$ is a covariant constant tensor, $\nabla^\mu g_{\mu\nu} = 0$, we can also add a factor $\Lambda g_{\mu\nu}$ without spoiling this relation. Λ is the cosmological constant and with its inclusion the field equation reads

$$R_{\mu\nu} - \frac{1}{2}Rg_{\mu\nu} + \Lambda g_{\mu\nu} = \kappa T_{\mu\nu} \tag{2.32}$$

The Newtonian Limit

Since Newtonian gravity is an excellent approximation in the solar system, it is required that any new formulation of gravity agrees with the Newtonian predictions in the limit of weak gravity[3]. The motion of a free particle is given by the geodesic equation

$$\frac{d^2x^\mu}{d\tau^2} + \Gamma^\mu_{\alpha\beta}\frac{dx^\alpha}{d\tau}\frac{dx^\beta}{d\tau} = 0 \tag{2.33}$$

In the Newtonian limit, $\frac{dx^i}{d\tau} \ll 1$, this equation reduces to

$$\frac{d^2x^i}{d\tau^2} = -\Gamma^i_{00} \tag{2.34}$$

where the right hand side can be approximated as $\Gamma^i_{00} \approx \frac{1}{2}\frac{\partial g_{00}}{\partial x^i}$. Invoking the field equation (with $\Lambda = 0$), we find

$$R_{00} = \frac{1}{2}\kappa T_{00}, \quad R_{00} \approx -\frac{\partial \Gamma^i_{00}}{\partial x^i} \tag{2.35}$$

[3]By weak gravity we mean that the gravitational potential of the body is question satisfies $\Phi = \frac{GM}{R} \ll 1$ in Planck-units. Taking the earth as an example we have $\Phi_E \sim 10^{-9}$

Defining $g^i = \frac{d^2x^i}{d\tau^2}$, the gravitational acceleration, and using the perfect fluid approximation $T_{00} = \rho$ we find

$$\vec{\nabla} \cdot \vec{g} = -\frac{1}{2}\kappa\rho \tag{2.36}$$

At last, using (2.30), we recover the Newtonian gravitational law (2.29) if we set[4] $\kappa = 8\pi G$.

2.2.5 Action formulation of General Relativity

The Einstein-equation can be derived from an invariant action principle, allowing us to use the Lagrangian formalism to state general relativity (GR). The Einstein-Hilbert action [24] is defined by

$$S_{EH} = \frac{1}{16\pi G}\int \sqrt{-g}dx^4(R - 2\Lambda) \tag{2.37}$$

where g is the determinant of the metric $g_{\mu\nu}$, $R = g^{\mu\nu}R_{\mu\nu}$ is the Ricci scalar and Λ is the cosmological constant. This action describes pure gravity without any matter fields, and the interaction with matter fields follows by adding the (standard model) matter action $S_{\text{matter}}(g_{\mu\nu}, \psi_i) = -\int dx^4 \mathcal{L}_{\text{matter}}(g_{\mu\nu}, \psi_i)$, where the usual Minkowski-metric $\eta_{\mu\nu}$ have been replaced by the spacetime-metric $g_{\mu\nu}$.

The term $\sqrt{-g}$ must be included so that the action is invariant under a general coordinate transformation. Under such a transformation the the volume element, dx^4, transform as

$$dx'^4 = \left|\frac{\partial x'}{\partial x}\right| dx^4 \tag{2.38}$$

where $\left|\frac{\partial x'}{\partial x}\right|$ is the Jacobian of the transformation. The determinant of the metric g transforms as

$$g' = \left|\frac{\partial x'}{\partial x}\right|^{-2} g \tag{2.39}$$

which shows that the combination $\sqrt{-g}dx^4$ is an invariant.

A small variation in $g_{\mu\nu}$, that vanishes at infinity, leads to a variation in the total action

$$\delta S = \frac{1}{16\pi G}\int \sqrt{-g}\left[\delta R + \frac{\delta\sqrt{-g}}{\sqrt{-g}}(R - 2\Lambda)\right] + \delta S_{\text{matter}}(g_{\mu\nu}, \psi_i) \tag{2.40}$$

[4] In units where $c \neq 1$ we have $\kappa = \frac{8\pi G}{c^4}$.

The variation of the Ricci-scalar is given in [24]

$$\begin{aligned} \delta R &= g^{\mu\nu}\delta R_{\mu\nu} + R_{\mu\nu}\delta g^{\mu\nu} \\ &= R_{\mu\nu}\delta g^{\mu\nu} + \nabla_\alpha \delta\Gamma^\alpha_{\mu\nu} - \nabla_\nu \delta\Gamma^\alpha_{\mu\alpha} \end{aligned} \tag{2.41}$$

Taking the variation of $\sqrt{-g}$ yields

$$\delta\sqrt{-g} = -\frac{1}{2\sqrt{-g}}\delta g \tag{2.42}$$

Specializing to a frame where g is diagonal it is easy to see that $\delta g = g g^{\mu\nu}\delta g_{\mu\nu}$ since $g^{\mu\nu} = \frac{1}{g_{\mu\nu}}$ in this case. Since g is a tensor-density and we are dealing with a tensor-equation this equation will hold in any frame, thus

$$\delta\sqrt{-g} = \frac{1}{2}\sqrt{-g}g^{\mu\nu}\delta g_{\mu\nu} \tag{2.43}$$

The last relation we need is found from $g^{\mu\nu}g_{\mu\nu} = 4 \rightarrow g^{\mu\nu}\delta g_{\mu\nu} = -g_{\mu\nu}\delta g^{\mu\nu}$. Putting the pieces together

$$\begin{aligned} \delta S = \; & \tfrac{1}{16\pi G}\int \sqrt{-g}dx^4 \left[R_{\mu\nu} - \tfrac{1}{2}g_{\mu\nu}R + \Lambda g_{\mu\nu} + 8\pi G \tfrac{2}{\sqrt{-g}}\tfrac{\partial \mathcal{L}_{\text{matter}}}{\partial g_{\mu\nu}}\right]\delta g^{\mu\nu} \\ & + \tfrac{1}{16\pi G}\int \sqrt{-g}dx^4 \left[\nabla_\alpha \delta\Gamma^\alpha_{\mu\nu} - \nabla_\nu\delta\Gamma^\alpha_{\mu\alpha}\right] g^{\mu\nu} \end{aligned} \tag{2.44}$$

The last term is a total derivative, since $\nabla_\alpha g^{\mu\nu} = 0$, and thus by Gauss' theorem only yields a boundary term when integrated. Hence since the variation of the metric vanishes at infinity, this term does not contribute to the variation of the action. Note that in some higher dimensional theories where the spacetime has a finite boundary, for example in Brane-World models, this term does not vanish and one must modify the action (2.37) to get a consistent theory [43]. Since we require $\delta S = 0$ for any variation $\delta g^{\mu\nu}$ it follows that

$$R_{\mu\nu} - \frac{1}{2}g_{\mu\nu}R + \Lambda g_{\mu\nu} = 8\pi G\left[-\frac{2}{\sqrt{-g}}\frac{\partial \mathcal{L}_{\text{matter}}}{\partial g_{\mu\nu}}\right] \tag{2.45}$$

and we have recovered the Einsteins field equation (2.32) if we define the energy-momentum tensor as

$$T_{\mu\nu} = -\frac{2}{\sqrt{-g}}\frac{\partial \mathcal{L}_{\text{matter}}}{\partial g_{\mu\nu}} \tag{2.46}$$

This expression for $T_{\mu\nu}$ reduces to the one derived from using Noether's theorem in the cases where the EM-tensor is symmetric [45], justifying this definition. One advantage of stating GR in terms of an action is that that it becomes much easier to come up with plausible modifications, something which is very hard if working directly from the field equation. We will see an example of this when discussing $f(R)$-gravity later on.

2.2.6 Modifications of General Relativity

Einstein had a strong faith in GR and experimental verification was not a big concern for him. Famously he replied to a journalist asking him what he would do if Eddingtons experiments failed to match his theory: *Then I would feel sorry for the good lord. The theory is correct.* But it took only four years for people (Weyl 1919, Eddington 1922) to start considering modifications of the theory by including higher order invariants in its action. The GR field equation is complicated enough as it stands and there are not very many cases in which they can be solved analytically, so one should have a good reason for considering higher order terms which will complicate the equations even more. In the 1960's it was discovered that the gravitational action was not renormalizable and therefore it can not be quantized in the conventional way. It was also discovered (Utiyama and De Witt 1962) that renormalizabillity at one-loop demanded the inclusion of higher order terms in the Einstein-Hilbert action. This stimulated the interest of the scientific community in higher-order theories of gravity, i.e. to include higher-order curvature invariants with respect to the Ricci-scalar. However, the relevance of such terms in the action was thought to be relevant only in the high-energy regime that is at energy-scales close to the Planck-scale.

But in the last decades, evidence coming from cosmology and astrophysics reveals some quite interesting features. The data coming from the CMB seem to indicate that the energy budget of the universe is 73% dark energy, 22% dark matter and only 4% ordinary baryonic matter [41]. Here the term dark matter refers to some unknown form of matter that has not yet been detected in labratory experiments and the term dark energy refers to some new type of energy that has not only been detected, but which does not cluster as ordinary matter. Since this dark energy is dominating the energy budget today, the expansion of the universe seems to be accelerating, contrary to what one would expect from ordinary matter and an attractive gravitational force. In addition, one needs an early time accelerated epoch called inflation in order to solve the so-called horizon, flatness and monopole problems [48]. This period also generated the inhomogeneites acting as seeds for the formation of large scale structures.

To this day most of these observations are in perfect agreement with GR, supplemented with a scalar field which generates inflation. In this context the dark energy is described by a cosmological constant, and is the standard model of cosmology called ΛCDM. But this model does not explain the origin of inflation and is burdened with the well known cosmological constant problem: The unnatural small size of this constant.

Since GR saw the day of light back in the 1915, it has been tested extensively,

and to this day it has passed every test. For the experimental situation regarding GR the reader is referred to [19] which this section is based on. In the case that some day experiments will detect a deviation from GR there has been put forward many modifications. We will look closer at the most popular theories namely scalar-tensor theories and $f(R)$-gravity, but first we will look into some of the requirements any new gravitational theory must poses.

Basic criteria for the viability of a gravitational theory

In order to have a successful gravitational theory, the theory must at least satisfy the following principles [19, Chapter 1]:

- It must be complete: It must be possible to analyze, from 'first principles', the outcome of any experiment of interest.
- It must be self-consistent: The outcome of any experiment must be unique. If we do the calculation using two different, but equivalent, methods one must always get the same result.
- It must be relativistic: In the limit where gravity is turned off, the laws of physics must reduce to those of special relativity.
- It must have the correct Newtonian limit.

The first two criteria seems obvious, but there are many examples of gravitational models that do not satisfy this[5], but the last two criteria are based on solid experimental evidence. In order to narrow down the huge range of models that can be stated, Dicke created a framework [44] in which we can analyze experimental tests of gravity. It makes two main assumptions about the type of mathematical formalism to be used in discussing gravity:

- Spacetime is a four-dimensional manifold, with each point in the manifold corresponding to a physical event. The manifold do not a priori have either a metric or an affine connection, but the hope is that experiments will force us to conclude that it has both.
- The equations of gravity must be expressed in a covariant form, i.e. independent of the coordinates used.

With these mathematical viewpoints Dicke imposed two constraints on all acceptable theories of gravity

- Gravity must be associated with one or more fields of tensorial character (scalar, vectors, tensors etc.)

[5]For example the Milne's kinematic relativity is incomplete since it does not make any gravitational redshift prediction.

- The dynamical equations that govern gravity must be derivable from an invariant action principle.

These choices strongly confine acceptable theories. For this reason, when putting forward a new gravitational model, we should accept them only if they are fundamental to our subsequent arguments. But in fact most successful gravitational theories are those that satisfy these constraints. We are most interested in the metric theories of gravity (modifications of GR). By a metric theory we mean that it satisfies the following:

- Spacetime is endowed with a metric
- The world-lines of freely falling test-bodies are geodesics of that metric
- In local Lorentz frames (freely falling frames) the laws of physics are those of special relativity.

Some well known examples of metric theories are general relativity, Brans-Dicke and $f(R)$-gravity which we will look most closely on in the next section. The Einstein equivalence principle [19, Chapter 2] is the foundation of all metric theories of gravity, not just GR and it is possible to argue convincingly that if the EEP is true then gravity is indeed a metric theory.

Scalar-Tensor Theories

Scalar-Tensor theories are one of the most popular and well studied modifications of gravity for many reasons. First of all, they are interesting on its own. They were invented about 50 years ago by P. Jordan which introduced a term which describes a non-minimal coupling between a scalar field and gravity described by general relativity. Because of this term, the gravitational constant becomes time-dependent, and can be used to explain why this constant today is so much smaller than the coupling constants of the electro-weak theory and the theory of the strong interactions in accordance with ideas put forward by P.A.M. Dirac.

In the beginning of the 1960's C. Brans and R.H. Dicke considered a particular example of Jordan's model where the matter Lagrangian does not depend on the scalar field, making sure that the theory respected the weak-equivalence principle. This is now known as the Brans-Dicke model and will be reviewed below.

Perhaps the most compelling reason to take scalar-tensor theories seriously is that they follow naturally, as an effective 4D theory, of string and Kaluza-Klein like (multi dimensional) theories. These types of theories have also been given a serious treatment in the last couple of years, especially in connection with the Brane-World models [29]. In these models the standard

model particles are confined on a hyper-surface (a so-called brane), which is embedded in a higher-dimensional spacetime.

The Brans-Dicke Model

The Brans-Dicke theory is probably the most known competitor of Einstein's theory of general relativity. The gravitational constant $G^* = \frac{G}{\Phi}$ is not presumed to be constant but can vary is space and time. The action, in the so-called *Jordan-frame*, is given in [19]

$$S = \frac{1}{16\pi G}\int dx^4\sqrt{-\tilde{g}}\left[\tilde{R}\Phi - \omega_{BD}\frac{(\partial\Phi)^2}{\Phi}\right] + S_{\text{matter}}(\tilde{g}_{\mu\nu},\psi_i) \tag{2.47}$$

where ω_{BD} is the Brans-Dicke parameter. Introducing the field redefinitions [42] $\tilde{g}_{\mu\nu} \to g_{\mu\nu}\Phi$ and $\phi = -M_p\sqrt{3/2+\omega_{BD}}\log\Phi$ the action transforms into the so-called *Einstein frame* where the coefficient of the Einstein-Hilbert term is constant

$$S = \frac{1}{16\pi G}\int dx^4\sqrt{-g}\left[R - (\partial\phi)^2\right] + S_{\text{matter}}(e^{\frac{2\beta}{M_p}}g_{\mu\nu},\psi_i) \tag{2.48}$$

with $\beta = \frac{1}{\sqrt{6+4\omega_{BD}}}$. In this formulation, gravity is described by general relativity supplemented by a ϕ mediated fifth-force. Test masses will follow geodesics of the Jordan-frame metric $e^{\frac{2\beta\phi}{M_p}}g_{\mu\nu}$, and from the geodesic equation stated in the Jordan-frame we find that this fifth-force force is given by[6]

$$\vec{F}_\phi = -\frac{\beta}{M_p}\vec{\nabla}\phi \tag{2.49}$$

in the non-relativistic limit. The field equation for ϕ follows from the variation of the (2.48) and the result is[7]

$$\Box\phi = \frac{\beta\rho}{M_p}e^{\frac{\beta\phi}{M_p}} \tag{2.50}$$

When $\beta\phi \ll M_p$, the solution in a static spherical symmetric metric reads[8]

$$\phi = 2\beta M_p U(r) \quad \to \quad F_\phi = 2\beta^2 F_{\text{gravity}} \tag{2.51}$$

where U is the gravitational potential. This shows that the fifth-force, in the weak gravitational limit, is gravitational with strength $\alpha = 2\beta^2 = \frac{1}{3+2\omega}$. The best current bounds on the BD parameter is $4\cdot 10^4 \lesssim \omega_{BD}$ and comes from the Cassini-experiment [21]. The need for this large value of the parameter makes the model less natural, but there exist modifications where ω_{BD} is

[6] A derivation of this result is given in the chapter 'Review of the Chameleon model'.
[7] The field equation is derived in the chapter 'Review of the Chameleon model'.
[8] This result is derived in the appendix.

made into a function of ϕ so its value today can be explained through its cosmological evolution providing an explanation for this apparent fine-tuning problem. Nevertheless, it has remained a paradigm for the introduction of scalar fields into gravitational theory, and as such has enjoyed a renaissance in connection with theories of higher dimensional space-time.

The reason we bring this model up is that when looking at the chameleon model later on we will be able to treat that model as an effective BD model in the solar system. Since several experimental bounds have already been calculated for BD we will be able to find experimental bounds for the chameleon rather easily.

$f(R)$ Gravity

The Einstein-Hilbert action governing the dynamics of GR is given by (2.37)

$$S = \frac{1}{16\pi G}\int dx^4\sqrt{-g}R + S_{\text{matter}}(g_{\mu\nu},\psi_i) \tag{2.52}$$

where R is the Ricci-scalar, $g = \det g_{\mu\nu}$, and $\mathcal{L}_m$ is the standard model Lagrangian describing the different matter fields. Variation of the above action with respect to the metric $g_{\mu\nu}$ gives the GR field equation

$$R_{\mu\nu} - \frac{1}{2}g_{\mu\nu}R = 8\pi G\ T_{\mu\nu} \tag{2.53}$$

where $T_{\mu\nu} = -\frac{2}{\sqrt{-g}}\frac{\delta\mathcal{L}_{\text{matter}}}{\delta g_{\mu\nu}}$ is the energy-momentum tensor. The action (2.52) is the simplest one created out of the geometrical Lorentz-scalars R, $R_{\mu\nu}R^{\mu\nu}$ and $R_{\mu\nu\alpha\beta}R^{\mu\nu\alpha\beta}$. It is reasonable to think that (2.52) is only a low energy approximation describing gravity. A more general theory can be constructed by letting the Ricci scalar be replaced by some function $f(R)$ of the Ricci-scalar. We therefore consider the action

$$S = \frac{1}{16\pi G}\int dx^4\sqrt{-g}f(R) + S_{\text{matter}}(g_{\mu\nu},\psi_i) \tag{2.54}$$

The resulting field equation is given in [22] and reads

$$\frac{df(R)}{dR}R_{\mu\nu} - \frac{1}{2}f(R)g_{\mu\nu} = \nabla_\mu\nabla_\nu\frac{df(R)}{dR} + g_{\mu\nu}\Box\frac{df(R)}{dR} + 8\pi G\ T_{\mu\nu} \tag{2.55}$$

The reason $f(R)$-models are interesting for us is that they can be shown to be mathematically equivalent to a scalar-tensor theory as shown in the next section.

Equivalence between $f(R)$-gravity and scalar-tensor theories

The equivalence of $f(R)$-gravity and scalar-tensor theories is well known, but authors usually just state this equivalence without giving a rigorous proof and we will therefore provide one here. Staring with the field-equation (2.55)

$$f'(R)R_{\mu\nu} - \frac{1}{2}f(R)g_{\mu\nu} = \nabla_\mu\nabla_\nu f'(R) + g_{\mu\nu}\Box f'(R) + 8\pi G\, T_{\mu\nu} \tag{2.56}$$

we introduce a new scalar-field ϕ via

$$f'(R) = e^{-\frac{2\beta\phi}{M_p}} \tag{2.57}$$

where $\beta = \frac{1}{\sqrt{6}}$. We define the Einstein frame metric $\tilde{g}_{\mu\nu}$ by a conformal transformation

$$\tilde{g}_{\mu\nu} = e^{-\frac{2\beta\phi}{M_p}} g_{\mu\nu} \tag{2.58}$$

and let $\tilde{R}$ be the Ricci-scalar of $\tilde{g}_{\mu\nu}$. The Christoffel symbols for the Einstein frame metric are calculated using (2.58) and (2.22) with the result

$$\tilde{\Gamma}^\alpha_{\sigma\gamma} = \Gamma^\alpha_{\sigma\gamma} - \frac{\beta}{M_p}\left(\phi_{,\gamma}\,\delta^\alpha_\sigma + \phi_{,\sigma}\,\delta^\alpha_\gamma - g_{\sigma\gamma}\phi^{,\alpha}\right) \tag{2.59}$$

Computing the Ricci-tensor

$$\tilde{R}_{\mu\nu} = \tilde{\Gamma}^\alpha_{\mu\nu,\alpha} - \tilde{\Gamma}^\alpha_{\mu\alpha,\nu} + \tilde{\Gamma}^\alpha_{\mu\nu}\tilde{\Gamma}^\lambda_{\lambda\alpha} - \tilde{\Gamma}^\alpha_{\mu\lambda}\tilde{\Gamma}^\lambda_{\alpha\nu} \tag{2.60}$$

we find

$$\tilde{R}_{\mu\nu} = R_{\mu\nu} + \frac{\beta}{M_p}\left(2\nabla_\mu\nabla_\nu\phi + g_{\mu\nu}\Box\phi\right) + \frac{2\beta^2}{M_p^2}\left(\nabla_\mu\phi\nabla_\nu\phi - g_{\mu\nu}(\nabla\phi)^2\right) \tag{2.61}$$

Note that $\Box$ is written in terms of the Jordan-frame metric g. Further we find that the Ricci-scalar, $\tilde{R} \equiv \tilde{g}^{\mu\nu}\tilde{R}_{\mu\nu}$, is given by

$$\tilde{R} = e^{\frac{2\beta\phi}{M_p}}\left(R + \frac{6\beta^2}{M_p}\Box\phi - \frac{6\beta^2}{M_p^2}(\nabla\phi)^2\right) \tag{2.62}$$

If we now go back to the field equation and rewrite it in terms of the Einstein-frame metric using the relations above we find

$$\tilde{R}_{\mu\nu} - \frac{1}{2}\tilde{R}\tilde{g}_{\mu\nu} = 8\pi G\, T_{\mu\nu}e^{\frac{2\beta\phi}{M_p}} + 8\pi G\left[\tilde{\nabla}_\mu\phi\tilde{\nabla}_\nu\phi - g_{\mu\nu}\left(\frac{1}{2}(\tilde{\nabla}\phi)^2 + V(\phi)\right)\right] \tag{2.63}$$

where

$$V(\phi) = M_p^2\frac{Rf'(R) - f(R)}{2f'(R)^2} \tag{2.64}$$

The last term in (2.63) corresponds to the energy-momentum tensor, $T^{\phi}_{\mu\nu}$, of a minimal coupled scalar field and the matter-fields are seen to couple to ϕ universally. This coupling can be found by letting the matter-species 'feel' the conformal transformed metric $\tilde{g}$. The action giving the field equation (2.63) is given by

$$S = \int dx^4 \sqrt{-\tilde{g}} \left[\frac{\tilde{R}}{16\pi G} - \frac{1}{2}\tilde{g}^{\mu\nu}\nabla_\mu\phi\nabla_\nu\phi - V(\phi) \right] + S_{\text{matter}} \left(e^{\frac{2\beta\phi}{M_P}} \tilde{g}_{\mu\nu}, \psi_i \right) \tag{2.65}$$

The Einstein-frame action (2.65) is the action of a scalar-tensor theory showing the claimed equivalence. Note that the two actions (2.54) and (2.65) are equivalent only for $\beta = \frac{1}{\sqrt{6}}$. Starting from (2.65) and allowing different matter-species to couple with different strength to ϕ then the model cannot be transformed to the $f(R)$ since the EP would then be violated in the Einstein-frame, but not in the Jordan-frame.

Jordan-frame and Einstein-frame formulation

An $f(R)$-model and a scalar-tensor model are related by a conformal transformation, and are thus mathematically equivalent.[9] The first is stated in the Jordan-frame where gravity is modified and test-particles moves on geodesics of the physical metric. The second is stated in the Einstein-frame where gravity is described by general relativity supplemented by a scalar field which give rise to a fifth-force and the test-particles move on the geodesics of the conformal transformed metric. But even though the two formulations are mathematically equivalent it does not automatically mean that they are physically equivalent. By choosing a frame, which means certain conventions and units of time etc., only one frame can be physically correct. However, if we consider any arbitrary conventions for adjustable, not fixed, then the two mathematically equivalent theories can also be physically equivalent [23].

Despite the fact that these frames have been around for along time there is still debate about whether either, both, or neither frame is a 'physical' frame which can be compared to observations and experiment. Due to the simplicity in working in the Einstein-frame makes it the 'natural' frame to work with in many cases, and when working with $f(R)$-gravity it can in save a lot of time to work in the other frame [12].

[9] This is only true when all matter-fields couple to ϕ with the same strength. If we consider the Einstein-frame to be fundamental then, in general, this will not be true since loop-corrections to the coupling-function will alter the coupling-parameters. We will consider our potentials and couplings as 'already effective' in order to avoid this problem.

2.2.7 The Parametrized Post Newtonian Formalism

Newtonian gravity is a very good approximation in the solar system, and the GR corrections are usually well below the 1% level. Gravity experiments have yet to reveal any correction to GR, and this means that the corrections to GR (if any) can be treated perturbative. Since any new gravitational theory must give the correct Newtonian limit the lowest order corrections can first kick in at the next order in the perturbations which are called the post-newtonian corrections. Gravitational theoriest have developed a variety of mathematical tools to analyze the result of new high precision experiments, and one of the most developed tool is the parametrized post-newtonian formalism (PPN). In this formalism there is a general method for determining the post-newtonian metric for any new (metric) gravitational theory. The formalism is explained thouroughy in [19], and a cook-book recipe for calculating PPN metric is stated. But the calculations have many details involved which are not explained, so we will use the Brans-Dicke model as an example on how to do the (long) calculation to obtain the PPN parameters. This result will also come in handy when looking at the chameleon model later on since in the solar system the chameleon is approximatly a Brans-Dicke field. We will start with a short introduction to the PPN formalism.

PPN bookkeeping methods

The PPN formalism is a way of stating a consistent perturbation theory for gravitational theories, but in any perturbation theory we need the knowledge of what terms to keep and what terms to trow away. The formalism therefore contains a set of bookkeeping rules to keep track of small quantities.

The gravitational potential satisfies $|U| \ll 1$ (in $M_p = 1$ units) in most familiar situations. In fact $|U| < 10^{-5}$ everywhere in the solar system and is thus a small quantity. Planetary velocities are related to U by the viral relation $|U| \sim v^2$, and the pressure inside the sun and the planets are generally less than the gravitational energy density[10] $p \lesssim \rho|U|$. The internal energy Π (energy density to rest mass density) is also typically less than or similar to the gravitational potential. These quantities are assigned a order of magnitude in the PPN formalism,

$$U \sim v^2 \sim \frac{p}{\rho} \sim \Pi \sim \mathcal{O}(2) \tag{2.66}$$

Single terms of v are $\mathcal{O}(1)$, U^2 is $\mathcal{O}(4)$ and so on. In the equation of motion we have both gradients and time-derivatives, and from the Euler-equation describing fluid flow we have $\frac{\partial}{\partial t} \sim v \cdot \nabla$ justifying the last rule $\frac{\partial}{\partial t} / \frac{\partial}{\partial x} \sim \mathcal{O}(1)$,

[10] This can be seen by looking at Newtonian equilibrium between pressure and gravity inside a planet which gives $p = \frac{\rho|U|}{2}$ at the center.

i.e. a time derivative is one order higher than a position derivative. With these book-keeping tools we can now analyze the post-Newtonian metric. The Lagrangian describing the dynamics for a test-particle in a given metric $g_{\mu\nu}$ is given by

$$L = (-g_{\mu\nu}\frac{dx^\mu}{d\tau}\frac{dx^\nu}{d\tau})^{\frac{1}{2}} = \left(-g_{00} - 2g_{0j}v^j - g_{ij}v^iv^j\right)^{1/2} \tag{2.67}$$

In the Newtonian limit this reduces to

$$L = (1 - 2U - v^2)^{1/2} \tag{2.68}$$

Using our bookkeeping tools we see that Newtonian effects corresponds to an accuracy in L to $\mathcal{O}(2)$. To get post-Newtonian effects we must therefore go two step up to $\mathcal{O}(4)$ since terms of order $\mathcal{O}(3)$ are not allowed in order to have conservation of energy in the Newtonian limit [19, Page 90]. Expanding the Lagrangian to $\mathcal{O}(4)$

$$L = \left(1 - 2U - v^2 - g_{00}[\mathcal{O}(4)] - 2g_{0j}[\mathcal{O}(3)]v^j - g_{ij}[\mathcal{O}(2)]v^iv^j\right)^{1/2} \tag{2.69}$$

we see that in order to find the post-Newtonian limit of any metric theory we need the knowledge of

$$\begin{array}{lll} g_{00} & \text{to} & \mathcal{O}(4) \\ g_{0j} & \text{to} & \mathcal{O}(3) \\ g_{ij} & \text{to} & \mathcal{O}(2) \end{array} \tag{2.70}$$

Application of the PPN formalism

Now that we have the rules to keep track of the small quantities we can proceed to discuss the application of the PPN formalism. When given a new model we must first identify the variables. In the case of GR we have only the metric $g_{\mu\nu}$, in Brans-Dicke we have an additional scalar field ϕ, in other models a vector field A_μ and so on.

Then we set the cosmological boundary conditions, assuming a flat and isotropic cosmology. With isentropic coordinates in the rest frame of the universe (the CMB frame), we have

$$\begin{array}{lll} g_{\mu\nu} & \rightarrow & g^{(0)}_{\mu\nu} = (-c_0, c_1, c_1, c_1) \\ \phi & \rightarrow & \phi_0 \\ A_\mu & \rightarrow & (A, 0, 0, 0) \end{array} \tag{2.71}$$

Because the asymptotic values may affect the post-Newtonian metric, we must in some cases require a full cosmological solution.

We expand the variables in a post-Newtonian series about the asymptotic values:

$$\begin{array}{lcl} g_{\mu\nu} & = & g^{(0)}_{\mu\nu} + h_{\mu\nu} \\ \phi & = & \phi_0 + \psi \\ A_\mu & = & (A + a_0, a_1, a_2, a_3) \end{array} \tag{2.72}$$

Generally, the post-Newtonian order of these perturbations are given by

$$\begin{array}{lcl} h_{00} & \sim & \mathcal{O}(2) + \mathcal{O}(4) \\ h_{ij} & \sim & \mathcal{O}(2) \\ h_{0j} & \sim & \mathcal{O}(3) \\ \psi & \sim & \mathcal{O}(2) + \mathcal{O}(4) \\ a_0 & \sim & \mathcal{O}(2) + \mathcal{O}(4) \\ a_i & \sim & \mathcal{O}(3) \end{array} \tag{2.73}$$

We substitute these forms into the field equations, keeping only terms that are necessary to obtain a final, consistent post-Newtonian solution for $h_{\mu\nu}$. To solve the resulting field equations, it is convenient to introduce the following potentials, which are defined more properly in [19, Page 95]:

$$\begin{array}{lll} \nabla^2 U = -4\pi\rho & \nabla^2(\Phi_W + 2U^2 - 3\Phi_2) = 2\chi_{,ij}\, U_{,ij} & V_{j,j} = -U_{,0} \\ \nabla^2 V_j = -4\pi\rho v_j & \nabla^2\chi = -2U & W_{j,j} = U_{,0} \\ \nabla^2\Phi_1 = -4\pi\rho v^2 & \nabla^2\Phi_3 = -4\pi\rho\Pi & \chi_{,0j} = V_j - W_j \\ \nabla^2\Phi_4 = -4\pi p & \chi_{,00} = \mathcal{A} + \mathcal{B} - \Phi_1 & \nabla^2\Phi_2 = -4\pi\rho U \end{array} \tag{2.74}$$

Note that ∇^2 is the usual three-space Laplacian.[11] The Ricci-tensor $R_{\mu\nu}$, in terms of the metric $h_{\mu\nu}$ to order $\mathcal{O}(4)$, is given by [19, Page 121]

$$\begin{array}{lll} R_{00} = & -\frac{1}{2}\nabla^2 h_{00} - \frac{1}{2}(h_{jj,00} - 2h_{j0,j0}) + \frac{1}{2}h_{00,j}(h_{jk,k} - \frac{1}{2}h_{kk,j}) \\ & -\frac{1}{4}|\nabla h_{00}|^2 + \frac{1}{2}h_{jk}h_{00,jk} \\ R_{0j} = & -\frac{1}{2}(\nabla^2 h_{0j} - h_{k0,jk} + h_{kk,0j} - h_{kj,0k}) \\ R_{ij} = & -\frac{1}{2}(\nabla^2 h_{ij} - h_{00,ij} + h_{kk,ij} - h_{ki,kj} - h_{kj,ki}) \end{array} \tag{2.75}$$

The last ingredient is the relations for the contra-variant components of the energy momentum tensor which, in the perfect fluid approximation, is given by

$$\begin{array}{l} T^{00} = \rho(1 + \Pi + 2U + v^2 + \mathcal{O}(4)) \\ T^{0j} = \rho(v^j + \mathcal{O}(3)) \\ T^{ij} = \rho(v^i v^j + \mathcal{O}(4)) + p\delta^{ij} \end{array} \tag{2.76}$$

We mention again that Π is the internal energy (energy density to rest mass density) of the system in question, U the gravitational potential, p the pressure and v^i the coordinate velocity. The relations above is in most cases all

[11] The reason we don't need to consider the retarded potentials, as GR predicts, is due to the choice of gauge when solving the field equations.

we need in order to solve the field equations, and the first step is solving for h_{00} to $\mathcal{O}(2)$. Assuming that $h_{00} \to 0$ far from the system, one obtains

$$h_{00} = 2\alpha U \tag{2.77}$$

where U is the Newtonian gravitational potential and α is a function of the cosmological matching parameters plus coupling constants that may appear in the field equations. The metric to lowest order, $\mathcal{O}(2)$, now have the form

$$g_{00} = -c_0 + 2\alpha U, \quad g_{ij} = c_1\delta_{ij}, \quad g_{0i} = 0 \tag{2.78}$$

To put the metric in the standard Newtonian and post-Newtonian form, we can make a change of coordinates

$$x^{\hat{0}} = \sqrt{c_0}x^0 \tag{2.79}$$

$$x^{\hat{i}} = \sqrt{c_1}x^i \tag{2.80}$$

and a change of units $G_{\text{today}} = \frac{\alpha}{c_0 c_1} \equiv 1$ to get

$$g_{\hat{0}\hat{0}} = -1 + 2\hat{U}, \quad g_{\hat{i}\hat{j}} = \delta_{ij}, \quad g_{\hat{0}\hat{i}} = 0 \tag{2.81}$$

This we recognize as the Newtonian limit of the metric. We now continue to solve h_{ij} to $\mathcal{O}(2)$ and h_{0i} to $\mathcal{O}(3)$. The solutions can be extracted using the expressions in (2.75). Once this is done comes the hardest part: To solve h_{00} to $\mathcal{O}(4)$ using the previous calculated solutions for h_{ij}, h_{0j} and h_{00} except in terms $A(h_{00})$ where $\mathcal{O}(A(h_{00})) < \mathcal{O}(4)$ like for example $\nabla^2 h_{00}$. The last part consists of making a gauge-transformation to the standard post-Newtonian gauge described in [19, Page 96].

When all this is done, the result will be on the form

$$\begin{aligned}
g_{00} = \;& -1 + 2U - 2\beta U^2 - 2\xi\Phi_W + (2\gamma + 2\alpha_3 + \zeta_1 - 2\xi)\Phi_1 \\
& +2(3\gamma - 2\beta + 1\zeta_2 + \xi)\Phi_2 + 2(1 + \zeta_3)\Phi_3 \\
& +2(3\gamma + 3\zeta_4 - 2\xi)\Phi_4 - (\zeta_1 - 2\xi)\mathcal{A} \\
g_{0j} = \;& -\tfrac{1}{2}(4\gamma + 3 + \alpha_1 - \alpha_2 + \zeta_1 - 2\xi)V_j - \tfrac{1}{2}(1 + \alpha_2 - \zeta_1 + 2\xi)W_j \\
g_{ij} = \;& (1 + 2\gamma U)\delta_{ij}
\end{aligned} \tag{2.82}$$

where $\gamma, \beta, \xi, \zeta_i, \alpha_i$ are the 10 post-Newtonian parameters. The result is not pretty, but the point is this: Every (metric) gravitational theory will give a unique set of post-Newtonian parameters which can easily be compared with experiments. This allows one to check a particular model up against many different gravitational experiments, in which the result often are given in terms of the PPN parameters, with only one single (but long) calculation.

The different parameters have different interpretations

γ :	How much space curvature g_{ij} is produced by unit rest mass
β :	How much nonlinearity is there in the superposition law for gravity
α_i :	The extent of preferred frame effects
ζ_i :	The failure of conservation of energy, momentum and angular momentum

In all models discussed in this thesis we have $\alpha_i = \zeta_i = 0$ leaving us with only γ, β and ξ to be determined.

GR has only two non-zero parameters: $\gamma = \beta = 1$, and experimental bounds [19] are in very good agreement with these values. To show how to calculate the PPN parameters, we have included a calculation for the Brans-Dicke theory below. The result and the steps on how to calculate them is given in [19, Page 123], but there is no detailed calculations so we will give one here.

Note that the PPN formalism has constant parameters and therefore cannot accommodate Yukawa-like modifications with a finite range. But these cases can be incorporated into the framework by working with effective parameters that may have both a scale and time dependence [42].

PPN parameters for the Brans-Dicke model

We start with the action (2.47) of a the Brans-Dicke model:

$$S = \frac{1}{16\pi G}\int dx^4\sqrt{-g}\left[R - \frac{\omega}{\phi}(\partial\phi)^2\right] + S_{matter}(g_{\mu\nu},\psi_i) \tag{2.83}$$

Variation of the action above with respect to $g_{\mu\nu}$ and ϕ gives us the two field equations [19, Page 123]

$$\begin{aligned} &R_{\mu\nu} - \tfrac{1}{2}g_{\mu\nu}R = \tfrac{8\pi T_{\mu\nu}}{\phi} + \tfrac{\omega}{\phi^2}\left(\phi_{,\mu}\,\phi_{,\nu} - \tfrac{1}{2}g_{\mu\nu}\phi_{,\alpha}\,\phi^{,\alpha}\right) + \tfrac{1}{\phi}\left(\phi_{;\mu\nu} - g_{\mu\nu}\Box\phi\right) \\ &\Box\phi = \tfrac{8\pi T}{3+2\omega} \end{aligned} \tag{2.84}$$

By contracting the indices in the first equation and using this to rewrite the equation without R we get the more convenient form

$$R_{\mu\nu} = \frac{8\pi}{\phi}(T_{\mu\nu} - \frac{1}{2}g_{\mu\nu}T) + \frac{\omega}{\phi^2}\phi_{,\mu}\,\phi_{,\nu} + \frac{1}{\phi}(\phi_{;\mu\nu} + \frac{1}{2}g_{\mu\nu}\Box\phi) \tag{2.85}$$

The variables in the theory are the metric $g_{\mu\nu}$, the scalar field ϕ, the Brans-Dicke parameter ω and the cosmological field-value ϕ_0. We choose local

quasi-Cartesian coordinates in which $g_{\mu\nu}$ is asymptotically Minkowski and expand the metric and ϕ around these asymptotically values

$$\begin{array}{l} g_{\mu\nu} = \eta_{\mu\nu} + h_{\mu\nu} \\ \phi = \phi_0 + \psi \end{array} \tag{2.86}$$

First step is to calculate h_{00} to $\mathcal{O}(2)$. Since $\psi \sim \mathcal{O}(2)$, to the required order we find

$$\begin{array}{l} g_{00} = -1, \quad T_{00} = -T = \rho \\ R_{00} = -\frac{1}{2}\nabla^2 h_{00} \\ \nabla^2\psi = -\frac{8\pi\rho}{3+2\omega} \rightarrow \psi = \frac{2U}{2+3\omega} \end{array} \tag{2.87}$$

where we have used $\Box\psi = \nabla^2\psi$ since $\psi_{,00}$ is $\mathcal{O}(4)$. Inserting these expressions in (2.85):

$$R_{00} = -\frac{1}{2}\nabla^2 h_{00} = 4\pi\rho\frac{4+2\omega}{3+2\omega}\frac{1}{\phi_0} \tag{2.88}$$

which has the solution $h_{00} = 2G_{today}U$ with $G_{today} = \frac{4+2\omega}{3+2\omega}\frac{1}{\phi_0}$ being the gravitational constant measured in the cosmological background today. We impose units in which $G_{today} = 1$ and with these units $\phi_0 = \frac{4+2\omega}{3+2\omega}$ which can be used to remove this (in principle unknown) parameter from our equations. Now, $h_{00} = 2U$, which is on the correct PPN form. Next step is to calculate h_{ij} to $\mathcal{O}(2)$. To simplify the analysis we impose the gauge conditions

$$h^{\mu}_{i,\,\mu} - \frac{1}{2}h^{\mu}_{\mu,i} = 0 \tag{2.89}$$

where $h^{\mu}_{\alpha} \equiv \eta^{\mu\beta}h_{\beta\alpha}$ to $\mathcal{O}(2)$. This gives us

$$\begin{array}{l} g_{ij} = \delta_{ij}, \quad T_{ij} = 0, \quad T = -\rho \\ R_{ij} = -\frac{1}{2}\nabla^2 h_{ij} \end{array} \tag{2.90}$$

The solution $\psi = \frac{2U}{2+3\omega}$ found above is still valid to this order. We insert these results in (2.85)

$$R_{ij} = -\frac{1}{2}\nabla^2 h_{ij} = \frac{4\pi\rho\delta_{ij}}{\phi_0} + \frac{\psi_{,ij}}{\phi_0} - \frac{4\pi\rho\delta_{ij}}{\phi_0(3+2\omega)} \tag{2.91}$$

which has the solution

$$h_{ij} = 2\frac{1+\omega}{2+\omega}U\delta_{ij} + \frac{1}{2+\omega}\chi_{,ij} \tag{2.92}$$

We must now calculate h_{0j} to $\mathcal{O}(3)$. Imposing another gauge condition (which is still allowed since we have fixed only 3 gauge-degrees of freedom above)

$$h^{\mu}_{0,\mu} - \frac{1}{2}h^{\mu}_{\mu,0} = -\frac{1}{2}h_{00,0} \tag{2.93}$$

we find

$$\begin{aligned} &g_{0j} = 0, \quad T_{0j} = -T^{0j} = -\rho v_j, \quad T = -\rho \\ &R_{0j} = -\tfrac{1}{2}(\nabla^2 h_{0j} + U_{,0j}\,) \\ &\psi = \tfrac{2U}{2+3\omega} \end{aligned} \tag{2.94}$$

Note the way the EM-tensor is calculated: We must use the lower order solutions $h_{\mu\nu}$ already calculated in order to get the covariant components to the correct order.

$$\begin{aligned} T_{0j} = g_{0\mu}g_{\nu j}T^{\mu\nu} &= g_{00}g_{0j}T^{00} + g_{0i}g_{0j}T^{0i} + g_{00}g_{ij}T^{0i} \\ &= \mathcal{O}(0+3+2) + \mathcal{O}(3+3+3) + \mathcal{O}(0+0+3) \end{aligned} \tag{2.95}$$

where only the last term has the correct order. This term is given by

$$T_{0j} = g_{00}g_{ij}T^{i0} = (-1+2U)\delta_{ij}T^{0i} = -T^{0j} + 2UT^{0j} \tag{2.96}$$

and since the last term is of order $\mathcal{O}(5)$ it can be discarded. Here the result is the same as using the Minkowski metric to lower the indices, but in general this will not be true so extreme care must be taken when raising and lowering indices.

Inserting (2.94) into (2.85) we get the equation determining h_{0j}:

$$R_{0j} = -\frac{1}{2}(\nabla^2 h_{0j} + U_{,0j}\,) = -\frac{8\pi\rho v_j}{\phi_0} - \frac{4U_{,0j}}{\phi_0(3+2\omega)} \tag{2.97}$$

which has the solution

$$h_{0j} = -\frac{1}{2}\left(\frac{10+7\omega}{2+\omega}\right)V_j - \frac{1}{2}W_j + \frac{1}{2+\omega}\chi_{,0j} \tag{2.98}$$

We now have $h_{\mu\nu}$ to the desired order and can attack the hardest part, which is calculating h_{00} to $\mathcal{O}(4)$. In doing so we use the lower order solutions for $h_{\mu\nu}$ in the field equation (2.85). The covariant components of the energy-momentum tensor to $\mathcal{O}(4)$ becomes

$$\begin{aligned} &T_{00} = g_{\mu 0}g_{\nu 0}T^{\mu\nu} = (\eta_{00} + h_{00})T^{00} = \rho(1 + \Pi - 2U + v^2) \\ &T = g_{00}T^{00} + g_{ij}T^{ij} = -\rho(1 + \Pi - 3\tfrac{p}{\rho}) \end{aligned} \tag{2.99}$$

Using the gauge conditions defined above to simplify the expressions we get

$$R_{00} = -\frac{1}{2}\nabla^2(h_{00} + 2U^2 - 8\Phi_2 - \frac{1}{2+\omega}(\Phi_W + 2U^2 - 3\Phi_3)) \tag{2.100}$$

and where the different relations between the potential (2.74) have been used. For ψ we only need the solution to $\mathcal{O}(2)$ derived above, and the field equation (2.85) reads

$$\begin{aligned} R_{00} =& 4\pi\rho\left[1 + \Pi - U\left(\frac{5+2\omega}{2+\omega}\right)\right] + 8\pi\rho v^2\left(\frac{3+2\omega}{4+2\omega}\right) \\ &+ 12\pi\left(\frac{1+\omega}{2+\omega}\right)p - \frac{\nabla^2\chi_{,00}}{4+2\omega} \end{aligned} \tag{2.101}$$

By again using the definition of the different potentials (2.74) we can write this equation in the more convenient form

$$\begin{aligned} R_{00} = &- \nabla^2 \left[U + \Phi_3 - \Phi_2 \left(\frac{5+2\omega}{2+\omega} \right) \right] - \frac{3+2\omega}{2+\omega} \nabla^2 \Phi_1 \\ &- 3\frac{1+\omega}{2+\omega} \nabla^2 \Phi_4 - \frac{1}{4+2\omega} \nabla^2 \chi_{,00} \end{aligned} \tag{2.102}$$

The solution for h_{00} is now found by simply equating (2.102) to (2.100). The result is

$$h_{00} = 2U - 2U^2 + 4 \left(\frac{3+2\omega}{4+2\omega} \right) \Phi_1 + 4 \left(\frac{1+2\omega}{4+2\omega} \right) \Phi_2 + 2\Phi_3 \tag{2.103}$$

$$+ 6 \left(\frac{1+\omega}{2+\omega} \right) \Phi_4 + \frac{1}{2+\omega} (\Phi_W - 2U^2 - 3\Phi_3) + \tag{2.104}$$

To summarize our findings:

$$\begin{array}{l} h_{00} = 2U - 2U^2 + 4 \left(\frac{3+2\omega}{4+2\omega} \right) \Phi_1 + 4 \left(\frac{1+2\omega}{4+2\omega} \right) \Phi_2 + 2\Phi_3 \\ +6 \left(\frac{1+\omega}{2+\omega} \right) \Phi_4 + \frac{1}{2+\omega} (\Phi_W - 2U^2 - 3\Phi_3) + \frac{1}{2+\omega} (\mathcal{A} + \mathcal{B} - \Phi_1) \\ h_{0j} = -\frac{1}{2} \frac{10+7\omega}{2+\omega} V_j - \frac{1}{2} W_j + \frac{1}{2+\omega} \chi_{,0j} \\ h_{ij} = 2\frac{1+\omega}{2+\omega} U \delta_{ij} + \frac{1}{2+\omega} \chi_{,ij} \end{array} \tag{2.105}$$

This is the post-Newtonian metric, but in order to read off the PPN parameters we must make a gauge-transformation to get the metric on the standard post-Newtonian form. This transformation is found by the requirement that any gauge-transformation $x^{\hat{\mu}} = x^\mu + \zeta^\mu$ allowed (this choice have been made for simplicity) has to be a simple functional that goes as $|\zeta^\mu|/|x^\mu| \to 0$ far from the system. The only simple functional that has this form is $\zeta_0 = \lambda_1 \chi_{,\mu}$, $\zeta_j = \lambda_2 \chi_{,j}$. Under a gauge transformation the metric changes as

$$\hat{g}_{\hat{\mu}\hat{\nu}} = g_{\mu\nu} - \zeta_{\mu;\nu} - \zeta_{\nu;\mu} \tag{2.106}$$

The allowed gauge transformations reads

$$\begin{array}{l} \hat{g}_{00} = g_{00} - \lambda_1 \chi_{,00} + 2\lambda_2 \Gamma^j_{00} \chi_{,j} \\ \hat{g}_{0j} = g_{0j} - (\lambda_1 + \lambda_2) \chi_{,0j} \\ \hat{g}_{ij} = g_{ij} - \lambda_2 \chi_{,ij} \end{array} \tag{2.107}$$

where the Christoffel-symbol to the required order is the same as in the Newtonian-limit $\Gamma^j_{00} = -U_{,j}$. This gauge-transformation will change the invariant volume element $\sqrt{-g} dx^3 u^0$, and thereby the gravitational potential $U_{,j}$ in the expression above which complicates things. The reader is referred to [19, Page 97] for a proper derivation. Using the identities for χ we find that the allowed gauge-transformations can be written

$$\begin{array}{l} \hat{g}_{00} = g_{00} - 2\lambda_1 (\mathcal{A} + \mathcal{B} - \Phi_1) - 2\lambda_2 (U^2 + \Phi_W - \Phi_2) \\ \hat{g}_{0j} = g_{0j} - (\lambda_1 + \lambda_2) \chi_{,0j} \\ \hat{g}_{ij} = g_{ij} - 2\lambda_2 \chi_{,ij} \end{array} \tag{2.108}$$

The standard post-Newtonian gauge is defined as the gauge which is diagonal and isotropic and in which g_{00} contains no term $\mathcal{B}$. That means we must choose λ_1 and λ_2 so that $\chi_{,ij}$ and $\mathcal{B}$ disappears from the equations. Note that this uniquely defines the PPN parameters leaving no ambiguity in the final answer. From (2.105) this is seen to require $\lambda_1 = \lambda_2 = \frac{1}{4+2\omega}$. After this gauge-transformation the metric reads

$$\begin{aligned} g_{00} &= -1 + 2U - 2U^2 + 2\left(\tfrac{3+2\omega}{2+\omega}\right)\Phi_1 + 2\left(\tfrac{1+2\omega}{2+\omega}\right)\Phi_2 + 2\Phi_3 + 6\left(\tfrac{1+\omega}{1+2\omega}\right)\Phi_4 \\ g_{0j} &= -\tfrac{1}{2}\left(\tfrac{10+7\omega}{2+\omega}\right)V_j - \tfrac{1}{2}W_j \\ g_{ij} &= \left[1 + 2\left(\tfrac{1+\omega}{1+2\omega}\right)U\right]\delta_{ij} \end{aligned} \tag{2.109}$$

Comparing the formulas above with the definition of the PPN parameters (2.82) we see that $\gamma = \frac{1+\omega}{2+\omega}$, $\beta = 1$ and the rest of the parameters are zero. The current bound on the Eddington-parameter γ is $\gamma - 1 = (2.1 \pm 2.3) \cdot 10^{-5}$ [21] shows the need for $\omega_{BD} > 10^5$ in order for the model to be in agreement with experiments.

2.3 Cosmology

2.3.1 Introduction

One of the most successful applications of GR is within the field of cosmology. Where Newtons gravitational theory fails to describe the evolution of the universe, general relativity is able to make predictions for the universe which agrees very well with observations. Observations also shows that the matter (on large scales) seems to be evenly distributed in space. As GR is built on the principle of relativity, we have a similar principle that is used when dealing with universe models. This is the *cosmological principle* which states that

- There is no special point in the universe, the galaxies are evenly distributed in space at large scales.
- There is no special spatial direction in the universe, the galaxies are evenly distributed in different angular directions at large scales.

Or more compact: At large scales the universe is both homogeneous and isotropic. This principle provides us with the simplest cosmological models for the evolution of the universe and one can show that it forces [24, Page 269] the metric to take the Friedmann-Lemaître-Robertson-Walker (FLRW) form

$$ds^2 = -dt^2 + a(t)^2 \left(\frac{dr^2}{1 - kr^2} + r^2 d\theta^2 + r^2 \sin^2 \theta d\phi^2 \right) \tag{2.110}$$

This is an exact solution to the Einstein field equations where the only free parameter k describes different types of geometry and $a(t)$ is determined through the matter distribution via the Friedmann equations. For $k > 0$ the universe is said to be closed and the spatial space has a shape that is topologically equivalent to a 3-sphere. For $k = 0$ the spatial space is the well known Euclidean geometry, and we say that the universe is flat even though it will generally have a curved spacetime. The last case is $k < 0$, in which the universe is said to be open and the geometry is called hyperbolic. See fig(2.1) for 2D analogies for the different geometries parameterized by k.

2.3.2 The Friedmann equations

Under the assumption that our universe is homogeneous and isotropic, the energy-momentum tensor of a perfect fluid can be written [24, Page 187]

$$T_{\mu\nu} = (\rho + p) u_\mu u_\nu + p g_{\mu\nu} \tag{2.111}$$

Here ρ is the proper energy (or mass) density of the fluid, p its pressure and u_μ the four-velocity of the fluid which can only have a time-component in

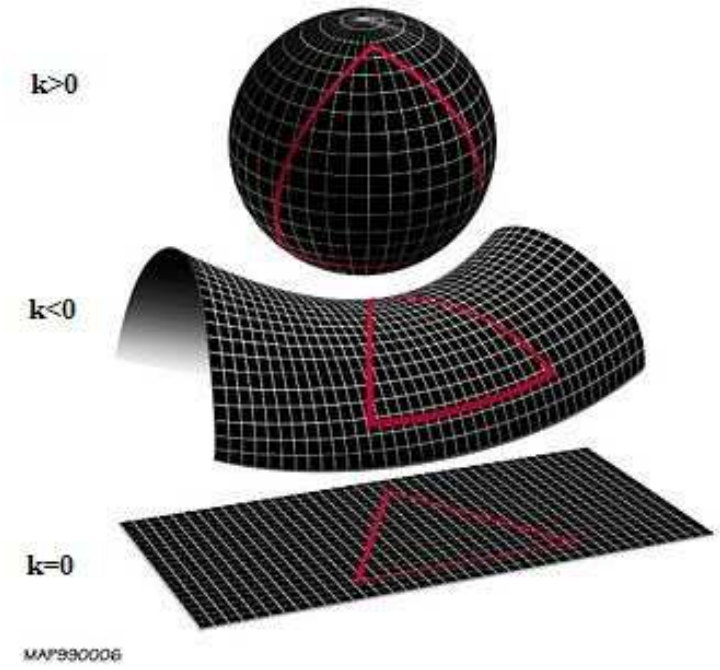

Figure 2.1: 2D analogies of the 3-space geometry corresponding to the three different values of k. Figure taken from [41].

order to satisfy the assumption of spatial isotropy. This makes the energy-momentum tensor diagonal in the coordinate system (2.110) and by solving the Einstein equations we find the Friedmann equations [24, Page 272]:

$$H^2 \equiv \left(\frac{\dot{a}}{a}\right)^2 = \frac{8\pi G}{3}\rho - \frac{k}{a^2} \tag{2.112}$$

$$\frac{\ddot{a}}{a} = -\frac{4\pi G}{3(\rho + 3p)} \tag{2.113}$$

In the case where we have several different fluids one replaces ρ (and p) with the sum of this quantity over the different fluids. Conservation of the energy-momentum tensor, $\nabla_\mu T^{\mu\nu} = 0$ which follows from the Einstein equations, gives the continuity equation[12]

$$\dot{\rho} + 3H(\rho + p) = 0 \tag{2.114}$$

For a fluid with an equation of state $p = \omega\rho$, where ω is a constant, this equation has the solution

$$\rho = \rho_0 \left(\frac{a_0}{a}\right)^{3(\omega+1)} \tag{2.115}$$

Non-relativistic matter has an equation of state $\omega = 0$, while radiation (and relativistic matter) has $\omega = \frac{1}{3}$. Looking more closely on the first equation in (2.112), it tells us that the effective gravitational energy is $\rho + 3p$ meaning that pressure has a gravitational effect and in order to have an accelerated expanding universe, $\ddot{a} > 0$, the dominating fluid must satisfy $p < -\frac{\rho}{3} < 0$. We say it must have a negative pressure or equivalent the equation of state needs to satisfy $\omega < -\frac{1}{3}$. In order to work with these equations it is convenient to introduce the density parameters

$$\Omega_i = \frac{\rho_i}{3H^2 M_p^2} \tag{2.116}$$

for the fluids and

$$\Omega_k = -\frac{k}{a^2 H^2} \tag{2.117}$$

for the curvature. With these definitions the Friedman's first equation goes over to

$$\sum_i \Omega_i + \Omega_k = 1 \tag{2.118}$$

This allows us to interpret Ω_i as the energy-density in ρ_i relative to the total energy density of the universe.

[12]Note that this equation assumes that there are no interactions between the different fluids so that each energy-momentum tensor is separately conserved. On cosmological scales this is a good approximation.

2.3.3 The ΛCDM-model

Consider a universe model with matter and a cosmological constant. We could (should) also include radiation, but since radiation contributes very little to the energy budget today it can be neglected in the late universe (at the background level). The Friedmann equations (2.112) reads

$$H^2 = \frac{8\pi G}{3}(\rho_m + \Lambda) \tag{2.119}$$

$$\ddot{a} = -\frac{4\pi G}{3}(\rho_m - \Lambda) \tag{2.120}$$

Since Λ is a constant and ρ_m is decreasing with increasing a we will eventually reach a point where $\Lambda > \rho_m$. When this happens the universe will go into a phase of accelerated expansion. This model is called the ΛCDM and is the standard model of cosmology today since its the simplest model that is in agreement with experiments. The matter density ρ_m is composed of ordinary baryonic matter (atoms) and a new component *dark matter* which do not interact with ordinary matter. One of the reasons behind this lies in the structure formation: If there was only ordinary matter then the structures we observe today should not have had time enough to form. The best fit for the density parameters, taken from the WMAP 7 year data [41], is

$$\begin{array}{lcl} \Omega_{\text{dark matter}} & = & 0.222 \pm 0.026 \\ \Omega_{\text{baryonic matter}} & = & 0.0449 \pm 0.0028 \\ \Omega_\Lambda & = & 0.734 \pm 0.029 \end{array} \tag{2.121}$$

The best fit for the Hubble parameter today is $H_0 = 100h\frac{km}{s\ Mpc}$ with $h = 0.710 \pm 0.025$. Using $\Omega_\Lambda = \frac{\Lambda}{3M_p^2 H_0^2}$ we can estimate the size of the cosmological constant

$$\Lambda = 3H^2 M_p^2 \Omega_\Lambda \sim 10^{-120} M_p^4 \tag{2.122}$$

2.3.4 Dark Energy

Dark energy is a hypothetical form of energy that permeates all of space and tends to increase the rate of expansion of the universe. It is the most popular way to explain observations that the universe appears to be expanding at an accelerating rate.

The standard explanation for dark energy is a cosmological constant, but there exist a lot of other models that are in agreement with observations. The most popular generalizations of a cosmological constant are scalar fields such as quintessence, dynamic quantities whose energy density can vary in time and space. Scalar fields which do change in spacetime can be difficult to distinguish from a cosmological constant (in the late universe) because

the change may be extremely slow. Nevertheless, the fine-tuning of the dark energy can in some cases be explained by the cosmological evolution of the quintessence-field.

High-precision measurements of the expansion of the universe are required to understand how the expansion rate changes over time. In general relativity, the evolution of the expansion rate is parameterized by the cosmological equation of state. Measuring the equation of state of dark energy is a big effort in observational cosmology today. As discussed in the introduction of this thesis if an equation of state $\omega \neq -1$ is ever observed then the cosmological constant is not the correct description of dark energy. So even though a cosmological constant is in agreement with experiments today, it is nonetheless useful to consider more complicated models in case some day observations will tell us otherwise. We can have two cases here, either is the late time acceleration of the universe due to some new dynamical degrees of freedom or it can be due to some breakdown of general relativity on cosmic scales. We will in this thesis focus on the cases where dark energy can be described as a scalar field.

Cosmological Constant

In ΛCDM, dark energy currently accounts for 73% of the total mass-energy of the universe and is described by a cosmological constant. The cosmological constant is physically equivalent to vacuum energy since it can be rewritten as an energy-momentum tensor, $T_{\mu\nu} = -\frac{\Lambda}{8\pi G} g_{\mu\nu}$, in the Einstein-equations. The size of the vaccum energy is predicted by quantum field theories and reads $\Lambda \sim M_p^4$. This conclusion follows from dimensional analysis and effective field theory: If the universe is described by an effective local quantum field theory down to the Planck scale, then we would expect a cosmological constant of the order of $M_p^4 = 1$ (in Planck-units). From (2.122) we see that this prediction is about 120 orders of magnitude larger than the observed cosmological constant. This discrepancy has been termed 'the worst theoretical prediction in the history of physics'. There is no known natural way to derive the tiny cosmological constant used in cosmology from particle physics and this is a motivation for looking at other dark energy models.

Quintessence

We start with the Einstein-Hilbert action (2.37) describing gravity and add a minimal coupled scalar field with the Lagrangian

$$\mathcal{L}_\Phi = -\sqrt{-g}\left[\frac{1}{2}(\partial\Phi)^2 + V(\Phi)\right] \tag{2.123}$$

Minimal coupled means that it couples to ordinary matter only through the metric $g_{\mu\nu}$. Since observations suggest that dark energy is smoothly dis-

tributed in our universe we can assume that the scalar field is homogeneous. With this assumption the Lagrangian reduces to

$$\mathcal{L}_\Phi = \sqrt{-g}\left[\frac{1}{2}\dot{\Phi}^2 - V(\Phi)\right] \tag{2.124}$$

on cosmological scales. The energy-momentum tensor of the field is given by (2.46)

$$T_{\mu\nu} = -\frac{2}{\sqrt{-g}}\frac{\partial \mathcal{L}_\phi}{\partial g_{\mu\nu}} \tag{2.125}$$

In the perfect fluid approximation (2.111) we find

$$\rho_\phi = \frac{1}{2}\dot{\Phi}^2 + V(\Phi) \tag{2.126}$$

and

$$p_\phi = \frac{1}{2}\dot{\Phi}^2 - V(\Phi) \tag{2.127}$$

The equation of state, $\omega = \frac{p}{\rho}$, is thus

$$\omega_\Phi = \frac{\frac{1}{2}\dot{\Phi}^2 - V(\Phi)}{\frac{1}{2}\dot{\Phi}^2 + V(\Phi)} \tag{2.128}$$

The observed cosmic acceleration today indicates that $\omega_\Phi \approx -1$ which again means that we must require that our field is slowrolling in the sense that $\frac{\dot{\Phi}^2}{2V(\Phi)} \ll 1$. The equation of motion for Φ is derived in the appendix and reads

$$\Box\Phi - \frac{dV}{d\Phi} = 0 \tag{2.129}$$

In a flat FLRW background metric it reduces to

$$\ddot{\Phi} + 3H\dot{\Phi} + \frac{dV}{d\Phi} = 0 \tag{2.130}$$

This equation is analogous to a particle with position $\Phi(t)$ rolling down a potential $V(\Phi)$. The term $3H\dot{\Phi}$ acts as a friction force on the particle. If the potential is too steep in the sense that $m_\Phi = \sqrt{V_{,\Phi\Phi}}$ today is larger than the friction term $H \lesssim m_\Phi$, the field rolls to fast and the equation of state will not resemble a cosmological constant. Today this means that m_Φ, which we can interpret as the mass of the Φ-particles have to be lower than $H_0 \sim 10^{-33}eV$. Compared to the mass of the electron, $m_e \sim 10^6$eV, this is extremely small. This is one of the reasons we don't consider a coupling to matter: If the Φ-field couples to matter, and the strength of this coupling is not to small, it should have been detected in particle accelerators by now. A coupling to matter would also result in a long-range $\lambda = \frac{1}{m_\Phi}$ fifth-force, and

again this should have been detected by now if the coupling is not too small. Of course this argument only applies when the field equation is linear: if the coupling to matter results in a non-linear field-equation this is not generally the case as we will see when looking at chameleon fields later on.

Most quintessence models require a fine-tuning in the initial conditions in order to give the desired dynamics, but there exist potential which give rise to attractor solutions where the field will reach the attractor for a large range of initial conditions. One such potential is the Ratra-Peebles potential

$$V(\Phi) = \frac{M^{n+4}}{\Phi^n} \tag{2.131}$$

Here M is a parameter with dimension of mass and $n > 0$. For a thorough review of quintessence the reader is referred to [26] which this section is based on.

2.3.5 Perturbations

On large scales the universe is homogeneous and isotropic today, and it looks to have been this way all the way since the beginning. But a homogeneous and isotropic universe should not have any structures. This problem is solved by assuming that after inflation there was some small perturbations in the matter density

$$\delta_m(\vec{x}, t) = \frac{\rho(\vec{x}, t) - \rho(t)}{\rho(t)} \tag{2.132}$$

where $\rho(t)$ is the average matter density. These perturbations can either grow with time to form structure of be diluted depending on how fast the universe expands. The equations governing the growth of the perturbations comes from perturbing the metric and solving the Einstein equations to first order (trowing away all higher order terms). The perturbations are usually studied in Fourier-space, where one set

$$\delta_m(\vec{x}, t) = \sum_{\vec{k}} \delta_m(\vec{k}, t) e^{i\vec{k}\cdot\vec{x}} \tag{2.133}$$

To linear order the different modes, $\delta_m \equiv \delta_m(\vec{k}, t)$, do not mix and the equation describing the perturbations, see [47], is

$$\ddot{\delta}_m + 2H\dot{\delta}_m = \frac{3}{2}\Omega_m H^2 \delta_m \tag{2.134}$$

in the co-moving gauge. In the matter era this leads to the growing solution $\delta_m \sim a$. But ordinary matter cannot cluster until the time of recombination since photons are in to great a number with an average energy large enough

to rip electrons away from the protons. This is a problem since then the perturbation has not had enough time to grow to give the observed large scale structure of the universe. And if they are tuned to give the desired effect, then the perturbations in the cosmic microwave background will be much larger than what is allowed by observations. The solution is by introducing dark matter, matter that does not interact with photons and other particles and can thus start to cluster much earlier providing a driving term for the clustering of ordinary matter. See [47], [48] for a through discussion. A modified gravitational theory can significantly change the equations governing the growth of the linear perturbations, as we will see when discussing the chameleon later on.

Chapter 3

Review of the Chameleon Model

3.1 Introduction

The simplest modifications of gravity leads to the introduction of a scalar field which couple to matter in a non-minimal way, as we have seen some examples of in the previous section. Scalar fields have a long history in physics, but none have been detected so far, even though the whole basis of particle physics is (at least within the standard framework today) based on the existence of the Higgs scalar-field. In cosmology, there is growing evidence for the existence of nearly massless scalar fields in our Universe. This evidence consists of a host of observations, from supernovae luminosity-distance measurements [2] to the cosmic microwave background anisotropy [3], which suggests that 73% of the current energy budget consists of a dark energy fluid with negative pressure. To the present time, the observations are consistent with a non-zero cosmological constant, but the dark energy is more generally modeled as quintessence: a scalar field rolling down a flat potential [26]. In order for the quintessence field to be evolving on cosmological time scales today, its mass must be of order of the present Hubble parameter H_0. Massless scalar fields or moduli are abundant in string and supergravity theories. Compactifications of string theory result in a plethora of massless scalars in the low-energy, fourdimensional effective theory. However, these massless fields generally couple directly to matter with gravitational strength, and therefore lead to unacceptably large violations of the EP. Therefore, if the culprit for quintessence is one of the moduli of string theory, some mechanism must effectively suppress its effective matter coupling which leads to the EP-violation.

The chameleon model, first proposed by Khoury and Weltman [1], provides this mechanism by having a coupling that gives the scalar field a mass that depends upon the local matter density. In regions of high density such as the Earth the field will have a large mass, but in the interstellar space where the density is very low the field will have a small mass. This leads to an exponentially suppressed EP violating effect in any experiment performed in a high density environment (e.g. on the earth) in agreement with experiments, but in an experiment performed in space it may produce EP violating greater than the current bounds derived from laboratory experiments such as the Eöt-Wash EP-experiment [27]. In the solar system, where the density is much lower than on earth, the moduli are essentially free, with a Compton wavelength (inverse mass) that can be much larger than the size of the solar system. On cosmological scales, where the density is very low, the mass can be of the order of the present Hubble parameter, making the field a potential candidate for causing the late time acceleration of the universe.

Density dependent mass terms have been studied before [31, 32, 33, 34, 35], but the novelty in the chameleon model is that the scalar-field can couple

to matter with gravitational strength and still be in agreement with experiments. This is because we live in a very dense environment and as long as the chameleon mass is large enough on earth we will be able to evade the current EP and fifth force bounds through what is called the thin-shell mechanism. As long as the mass of the chameleon inside the earth is large enough the field will be frozen at the minimum of its effective potential, which consist of a self-interaction term $V(\phi)$ and a term coming from the conformal coupling to matter $\rho A(\phi)$, and thus only a thin-shell near the surface will contribute to the field outside the body. We refer to the model as a chameleon, since its physical properties, such as its mass, depend sensitively on the environment. Moreover, in regions of high density, the chameleon will tend to blend with its environment and becomes essentially invisible to searches for EP violation and fifth force. One exciting result from this mechanism is that it can be possible to detect violations of the EP in upcoming satellite experiments such as STEP, MICROSCOPE and GG [4, 5, 6] that are much stronger than the current bounds derived from earth based experiments. A detection of this type will be a strong evidence for the existence of chameleons.

The satelitte experiments named above, will test the universality of free-fall in orbit with expected accuracy of $10^{-15} - 10^{-18}$. If SEE does measure an effective Newton's constant different from that on Earth, or if STEP observes an EP violating signal larger than permitted by the Eöt-Wash experiment, this will strongly indicate that a chameleon mechanism is realized in Nature. For otherwise it would be hard to explain the discrepancies between measurements in the laboratory and those in orbit.

3.2 The Chameleon Action

The action describing the chameleon model is, $S = S_{EH} + S_\phi + S_{\text{matter}}$,

$$S = \int dx^4\sqrt{-g}\left[\frac{RM_p^2}{2}\right] - \int dx^4\sqrt{-g}\left[\frac{1}{2}(\partial\phi)^2 + V(\phi)\right] + S_{\text{matter}}(\tilde{g}^{(i)}_{\mu\nu}, \psi_i) \tag{3.1}$$

where g is the determinant of the metric $g_{\mu\nu}$, R the Ricci-scalar, $M_p = \frac{1}{8\pi G}$ and ψ_i the different matter-fields. The metric g is called the Einstein-frame metric and $\tilde{g}$ the Jordan-frame metric. The matter fields couple to ϕ via a conformal rescaling on the form

$$\tilde{g}^{(i)}_{\mu\nu} = e^{\frac{2\beta_i\phi}{M_p}} g^{(i)}_{\mu\nu} \tag{3.2}$$

Here β_i are dimensionless coupling constants, in principle one for each matter field. Variation of (3.1) with respect to ϕ allows us to find the equation of

motion for ϕ:

$$\begin{aligned}\delta S &= \int dx^4\sqrt{-g}\left[-\nabla_\mu\phi\nabla^\mu\delta\phi - V_{,\phi}\,\delta\phi - \frac{1}{\sqrt{-g}}\frac{\partial\mathcal{L}_{\rm matter}}{\partial\phi}\right] \\ &= \int dx^4\sqrt{-g}\left[(\nabla_\mu\nabla^\mu\phi) - V_{,\phi} - \frac{1}{\sqrt{-g}}\sum_i \frac{\partial\mathcal{L}_{\rm matter}}{\partial\tilde{g}^{(i)}_{\mu\nu}}\frac{\partial\tilde{g}^{(i)}_{\mu\nu}}{\partial\phi}\right]\delta\phi \\ &= \int dx^4\sqrt{-g}\left[\Box\phi - V_{,\phi} - \sum_i \frac{2\beta_i}{M_p}e^{\frac{4\beta_i\phi}{M_p}}\frac{1}{\sqrt{-\tilde{g}}}\frac{\partial\mathcal{L}_{\rm matter}}{\partial\tilde{g}^{(i)}_{\mu\nu}}\tilde{g}^{(i)}_{\mu\nu}\right]\delta\phi\end{aligned} \tag{3.3}$$

On the first line we have used the commutativity of differentiation and variation, on the next line an integration by parts to rewrite the kinetic term and on the last line the relation $\sqrt{-g_i} = e^{-\frac{4\beta_i\phi}{M_p}}\sqrt{-\tilde{g}_i}$ which follows from (3.2). Requiring $\delta S = 0$ gives the field equation

$$\Box\phi = V_{,\phi} + \sum_i \frac{2\beta_i}{M_p}e^{\frac{4\beta_i\phi}{M_p}}\frac{1}{\sqrt{-\tilde{g}}}\frac{\partial\mathcal{L}_{\rm matter}}{\partial\tilde{g}^{(i)}_{\mu\nu}}\tilde{g}^{(i)}_{\mu\nu} \tag{3.4}$$

This last term represents the trace of the energy-momentum tensor, $\tilde{T}_i = -\tilde{\rho}_i$, in the Jordan-frame. The matter-density $\tilde{\rho}_i$, on cosmological scales will not satisfy the conservation equation (2.114). In order to write the equations on the standard form where all the ϕ-dependence is explicit it is standard practice to write the equation in terms of the Einstein-frame matter density which satisfy the usual continuity equation $\dot{\rho} + 3H\rho = 0$.

3.3 The matter-density in the Einstein-frame

In the Jordan-frame, and assuming that the matter fields ψ_i do not interact with each other, each energy-momentum tensor

$$\tilde{T}^{\mu\nu}_{(i)} = -\frac{2}{\sqrt{-\tilde{g}}}\frac{\partial\mathcal{L}_{\rm matter}}{\partial\tilde{g}^{(i)}_{\mu\nu}} \tag{3.5}$$

is conserved: $\tilde{\nabla}_\mu\tilde{T}^{\mu\nu}_{(i)} = 0$ [15]. Under the assumption that the matter-field (i) can be described as a perfect isentropic fluid with equation of state $\tilde{\rho}_i = \omega_i\tilde{p}_i$ we have

$$\tilde{T}^{\mu\nu}_{(i)}\tilde{g}^{(i)}_{\mu\nu} = -\tilde{\rho}_i(1 - 3\omega_i) \tag{3.6}$$

So far this is the standard picture. In going over to the Einstein-frame we impose, without loss of generality, a flat FLRW background metric

$$ds^2 = -dt^2 + a(t)^2(dx^2 + dy^2 + dz^2) \tag{3.7}$$

The corresponding metric in the Jordan-frame reads

$$ds^2 = -e^{\frac{2\beta\phi}{M_p}}dt^2 + \tilde{a}(t)^2(dx^2 + dy^2 + dz^2) \tag{3.8}$$

where $\tilde{a} \equiv ae^{\frac{\beta\phi}{M_p}}$. Computing the Christoffel symbols in the Jordan-frame, suppressing the subscript (i) for now,

$$\tilde{\Gamma}^{\mu}_{\alpha\nu} = \Gamma^{\mu}_{\alpha\nu} + \frac{\beta}{M_p}\left(\delta^{\mu}_{\nu}\phi_{,\alpha} + \delta^{\mu}_{\alpha}\phi_{,\nu} - g_{\nu\alpha}\phi^{,\mu}\right) \tag{3.9}$$

we find

$$\tilde{\nabla}_{\mu}\tilde{T}^{\mu\nu}_{(i)} = (a^{3(1+\omega_i)}\rho_i)_{,0} = 0 \tag{3.10}$$

where $\rho_i = \tilde{\rho}_i e^{3(1+\omega_i)\frac{\beta_i\phi}{M_p}}$ and is the Einstein-frame density since it satisfies the usual continuity relation $\rho_i \propto a^{-3(1+\omega_i)}$.

With this definition we can write

$$\frac{2}{\sqrt{-g}}\frac{\partial\mathcal{L}_{\text{matter}}}{\partial\tilde{g}^{(i)}_{\mu\nu}}\tilde{g}^{(i)}_{\mu\nu} = \rho_i(1-3\omega_i)e^{(1-3\omega_i)\frac{\beta_i\phi}{M_p}} \tag{3.11}$$

Substituting this result in (3.4) we obtain the field-equation in which all of the ϕ-dependence is explicit

$$\Box\phi = \frac{\partial}{\partial\phi}\left(V(\phi) + \sum_i \rho_i e^{(1-3\omega_i)\frac{\beta_i\phi}{M_p}}\right) \tag{3.12}$$

We may thus write the field-equation in terms of a single effective potential

$$\Box\phi = V_{\text{eff},\phi} \tag{3.13}$$

$$V_{\text{eff}}(\phi) = V(\phi) + \sum_i \rho_i e^{(1-3\omega_i)\frac{\beta_i\phi}{M_p}} \tag{3.14}$$

We will for simplicity assume that all matter species couple to ϕ with the same β_i and that the matter in study is non-relativistic, i.e. $\omega_i \approx 0$. With these assumptions, the effective potential reduces to

$$V_{\text{eff}}(\phi) = V(\phi) + \rho e^{\frac{\beta\phi}{M_p}} \tag{3.15}$$

For the purpose of this paper we will not be interested in the strong gravity regime (black holes, neutron stars etc.), and it will suffice to approximate the geometry of spacetime as Minkowski-space $g_{\mu\nu} \approx \eta_{\mu\nu}$. This is valid as long as the Newtonian potential is small everywhere and the back-reaction on the metric due to the energy density in ϕ is negligible[1]. See fig(3.1) for a plot of the effective potential, and fig(3.2) for a plot of the effective potential in a high density environment relative to a low density environment.

Since the matter fields couple to the Jordan-frame metric $\tilde{g}_{\mu\nu}$ the geodesics of test bodies will be the geodesics of this metric. Note that this means that a measurement of matter-fields will be a measurement in terms of the Jordan-frame metric and in this sense $\tilde{\rho}$ is the physical density. But as it turns out, experimental bounds require $\frac{\beta\phi}{M_p} \ll 1$ and therefore $\rho \approx \tilde{\rho}$.

[1] As long as $\beta\phi \ll M_p$ this will be true.

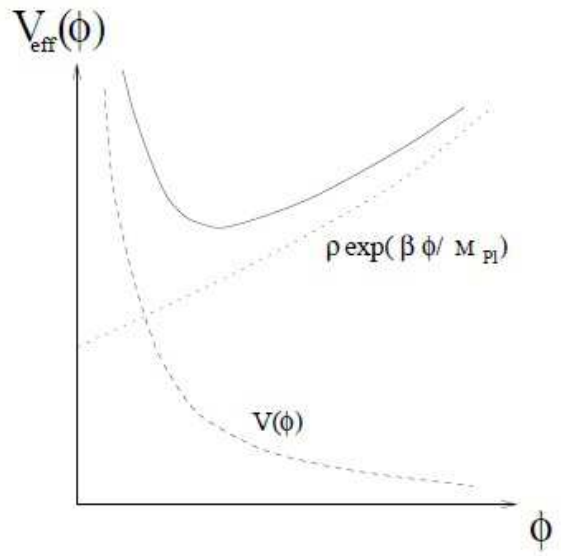

Figure 3.1: The Chameleon effective potential V_{eff} (solid curve) is the sum of two contributions: one from the actual potential $V(\phi)$ (dashed curve), and the other from its coupling to the matter density ρ (dotted curve). Figure taken from [1]

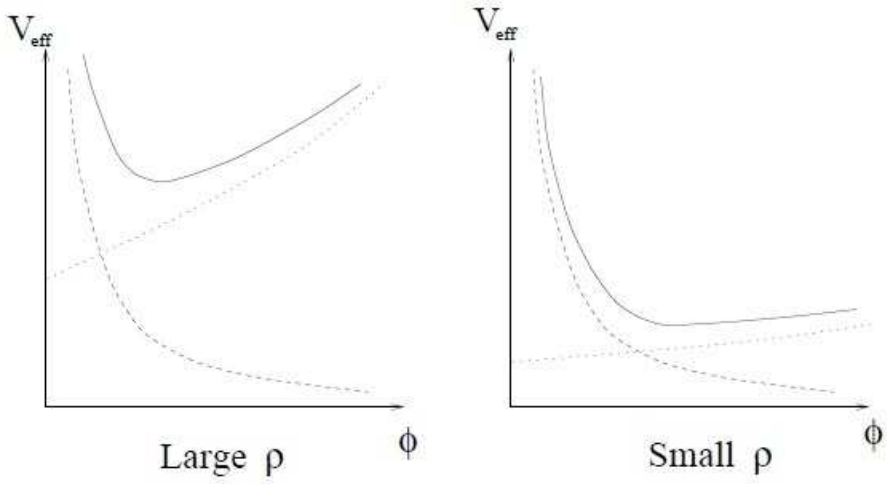

Figure 3.2: The Chameleon effective potential for large and small ρ, respectively. This illustrates that, as ρ decreases, the minimum shifts to larger values of ϕ and the mass of small fluctuations (the curvature of the potential) decreases. Figure taken from [1].

3.4 The Chameleon Potential

There are many potentials that give rise to a chameleon mechanism, but in the original formulation of the model [1] the potential $V(\phi)$ was assumed to be of the runaway form, meaning that it is monotonically decreasing and satisfies

$$\lim_{\phi\to\infty}\frac{V_{,\phi}}{V}=0, \quad \lim_{\phi\to\infty}\frac{V_{,\phi\phi}}{V_{,\phi}}=0,... \tag{3.16}$$

$$\lim_{\phi\to 0}\left|\frac{V_{,\phi}}{V}\right|=\infty, \quad \lim_{\phi\to 0}\left|\frac{V_{,\phi\phi}}{V_{,\phi}}\right|=\infty,... \tag{3.17}$$

This requirement was made to have the model agreeing with expectations from string-theory and super gravity, but also guarantees that there will be a chameleon mechanism in the model. If we don't consider 'requirements' like these, the single most important ingredient in a chameleon model is having an effective potential which has a minimum which depends on the local matter density, and we will look at the Ratra-Peebles potentials

$$V(\phi)=M^4\left(\frac{M}{\phi}\right)^n \tag{3.18}$$

where M has units of mass and n is a positive constant. This potential can give rise to the late time cosmic acceleration of the universe via the slow-roll mechanism and which is an example of a potential which often arise in string theory and super-gravity [36, 37, 38].

The minimum $\phi_{\min}$ of the effective potential is given by the equation

$$V_{,\phi}+\frac{\beta\rho}{M_p}e^{\frac{\beta\phi}{M_p}}=0 \tag{3.19}$$

In the following we will assume $\beta\phi \ll M_p$, and we will show[2] that this condition is satisfied when the model is in agreement with experiments. With this approximation the solution reads

$$\phi_{\min}=\left(\frac{\beta\rho}{nM^3M_p}\right)^{-\frac{1}{n+1}}M \tag{3.20}$$

The mass associated with the field is given by the second derivative of the effective potential. For small fluctuations about a minimum, $\phi_{\min}$, we find

$$m^2_{\min}\equiv V_{,\phi\phi}(\phi_{\min})=\frac{(n+1)\beta\rho}{M_p\phi_{\min}} \tag{3.21}$$

[2]See for example the section 'BBN bounds'

3.5 The Chameleon Force

In the Jordan-frame a freely falling test-particle will move on a geodesic of the Jordan frame metric. The geodesic equation reads

$$\ddot{x}^\mu + \tilde{\Gamma}^\mu_{\alpha\nu}\dot{x}^\alpha\dot{x}^\nu = 0 \tag{3.22}$$

Transforming to the Einstein-frame using (3.9) we find

$$\ddot{x}^\mu + \Gamma^\mu_{\alpha\nu}\dot{x}^\alpha\dot{x}^\nu + \frac{\beta}{M_p}\left(\phi_{,\alpha}\dot{x}^\alpha\dot{x}^\mu + \phi_{,\nu}\dot{x}^\nu\dot{x}^\mu - \dot{x}^\nu\dot{x}_\nu\phi^{,\mu}\right) = 0 \tag{3.23}$$

In the non-relativistic limit a test-particle of mass m will experience a chameleon fifth-force given by

$$\frac{\vec{F}_\phi}{m} = -\frac{\beta}{M_p}\vec{\nabla}\phi \tag{3.24}$$

From this relation its clear that the weak equivalence principle is violated, at a particle level, if and only if different matter-species couple to ϕ with a different β. When dealing with a macroscopic body the force is found by integrating (3.24) over the individual test-particles making up the body.

3.6 Spherical Solutions to the Field Equation

In order to study the observable consequences of the Chameleon model we must first understand the profile ϕ acquires on Earth and in the solar system. We will therefore look for solutions to the field equation inside and outside a spherical body with homogeneous density ρ_c in a background of homogeneous density ρ_b. This can for example be a ball in the atmosphere, where $\rho_b = \rho_{atm}$, or a planet in which ρ_b is the average matterdensity in the universe/solar system.

The field-equation (3.4) is the one-particle field equation. In macroscopic bodies the density is strongly peaked near the nuclei of the individual atoms from which it is formed and these atoms are separated from each other by distances much greater than their radii. Rather than explicitly considering the microscopic structure of a body, it is standard practice to define an 'averaged' field theory that is valid over scales comparable to the body's size. If our field theory were linear, then the averaged equations would be the same as the microscopic ones. It is important to note, though, that this is very much a property of linear theories and is not in general true of non-linear ones. However, it was showed in [10] that the averaged or coarse-grained field equation is the same as the microscopic field equation in most cases. The effect of the non-linearities is to place an upper limit on the mass of the

chameleon inside the body. For this review we will ignore this effect.

In a static spherical symmetric metric with weak gravity $\Box = \frac{d^2}{dr^2} + \frac{2}{r}\frac{d}{dr}$ and the field equation reduces to[3]

$$\frac{d^2\phi}{dr^2} + \frac{2}{r}\frac{d\phi}{dr} = -\frac{nM^{n+4}}{\phi^{n+1}} + \frac{\beta\rho(r)}{M_p} \tag{3.25}$$

where

$$\rho = \begin{cases} \rho_c \text{ for } r < R \\ \rho_b \text{ for } r > R \end{cases} \tag{3.26}$$

Throughout the analysis a subscript $_c$ is used when talking about quantities defined for the body and subscript $_b$ is used when referring to quantities defined for the background. ϕ_c is the minimum of the effective potential inside the body where $\rho = \rho_c$, ϕ_b is the minimum in the background where $\rho = \rho_b$ and m_c (m_b) is the mass of small fluctuations around ϕ_c (ϕ_b). We impose the boundary conditions

$$\begin{aligned} \left.\frac{d\phi}{dr}\right|_{r=0} &= 0 \\ \left.\frac{d\phi}{dr}\right|_{r=\infty} &= 0 \\ \phi(r \to \infty) &= \phi_b \end{aligned} \tag{3.27}$$

The first condition follows from the symmetry around $r = 0$, and the others follows from the physical requirement that the ϕ-force between a body and a test-particle vanishes when the distance between them becomes infinite.

In the center of the body we can have two cases depending on how far off the field sits relative to the minimum.

3.6.1 Thick-shell regime: $\phi_i \gg \phi_c$

In the thick-shell regime the field starts off sufficiently displaced from ϕ_c, and it will begin to roll down the effective potential as soon as it is released at $r = 0$. In this limit $|V_{,\phi}| \ll \frac{\beta\rho_c}{M_p}$ and we can neglect the term $V_{,\phi}$. The field equation then reads

$$\frac{d^2\phi}{dr^2} + \frac{2}{r}\frac{d\phi}{dr} = \frac{\beta\rho_c}{M_p} \tag{3.28}$$

with the solution

$$\phi = \phi_i + \frac{\beta\rho_c r^2}{6M_p} \quad \text{for} \quad 0 < r < R \tag{3.29}$$

[3]We have used the approximation $\frac{\beta\phi}{M_p} \ll 1$ in which the exponential can be neglected.

which will be valid all the way to $r = R$ since the field is increasing making the approximation $|V_{,\phi}| \ll \frac{\beta\rho_c}{M_p}$ better and better as we approach $r = R$. For $r > R$ we can Taylor-expand the effective potential around ϕ_b:

$$V_{\text{eff}} = V_{\text{eff}}|_b + V_{\text{eff},\phi\phi}|_b (\phi - \phi_b) + ... \tag{3.30}$$

$$= m_b^2(\phi - \phi_b) + \mathcal{O}[(\phi - \phi_b)^2] \tag{3.31}$$

Since the field-value at $r = R$ satisfies $\left|\frac{\phi(R)-\phi_b}{\phi_b}\right| < 1$ the linear term will dominate over the higher order terms in the Taylor expansion. This allows us to approximate

$$\frac{d^2\phi}{dr^2} + \frac{2}{r}\frac{d\phi}{dr} = m_b^2(\phi - \phi_b) \quad \text{for} \quad r > R \tag{3.32}$$

The solution that obeys the boundary conditions (3.27) is given by

$$\phi = \phi_b - \frac{ARe^{m_b(R-r)}}{r} \tag{3.33}$$

and is on the well known Yukawa form which is often found in scalar-field models. The mass-term m_b gives the chameleon a finite range, and its existence is contributed to the potential. A linear or quadratic potential will lead to a constant mass, but any other choices will make the mass-term density dependent. Matching the two solutions for $r < R$ and $R < r$ by demanding that the profile must be smooth[4] at $r = R$ gives

$$A = \frac{\beta\rho_b R^2}{3M_p} \tag{3.34}$$

$$\phi_i = \phi_b - \frac{\beta\rho_c R^2}{2M_p} \tag{3.35}$$

We have assumed $m_b R \ll 1$ in writing down this solution, an assumption which is justified since $m_b \ll m_c$ and as we will show later: $m_c R$ is typically of order 1 or smaller in the thick-shell regime. The full solution can be summarized as

$$\begin{aligned} \phi &= \phi_b - \tfrac{\beta\rho_c R^2}{2M_p} + \tfrac{\beta\rho_c r^2}{6M_p} \quad \text{for} \quad r < R \\ \phi &= \phi_b - \tfrac{\beta}{4\pi M_p}\tfrac{M_1 e^{-m_b r}}{r} \quad \text{for} \quad r > R \end{aligned} \tag{3.36}$$

The chameleon force on a test-mass outside the body is found by using (3.24), and the result after restoring $G = \frac{1}{8\pi M_p^2}$ is

$$F_\phi(r) = -m\frac{\beta}{M_p}\frac{d\phi}{dr} = -2\beta^2\frac{GmM}{r^2}(1 + m_b r)e^{-m_b r} \tag{3.37}$$

[4]By smooth at $r = R$ we mean that the function value and the first derivative matches, but place no restrictions on the second derivative.

which for separations $r < m_b^{-1}$ reduces to

$$F_\phi(r) = 2\beta^2 F_{\text{gravity}}(r) \tag{3.38}$$

This shows that close to the body ϕ will manifest itself as a correction to the Newtonian gravitational constant: $G_{\text{eff}} = G(1 + 2\beta^2)$, a correction that vanishes as we move further away than $r \sim m_b^{-1}$ from the body.

3.6.2 Thin-shell regime: $\phi_c \approx \phi_i$

When $\phi_i \approx \phi_c$ the driving term satisfy $V_{\text{eff},\phi} \approx 0$, and after releasing the field at $r = 0$ it will initially be frozen. It will remain at ϕ_c until the friction term $\frac{1}{r}\frac{d\phi}{dr}$ becomes small enough for the field to start rolling down the potential. Thus,

$$\phi \approx \phi_c \quad \text{for} \quad 0 < r < R_r \tag{3.39}$$

for some $0 < R_r < R$. In the region $R_r < r < R$ the field will increase rapidly and the approximation $|V_{,\phi}| \ll \frac{\beta\phi}{M_p}$ will quickly become valid. This allows us to approximate the field-equation by

$$\frac{d^2\phi}{dr^2} + \frac{2}{r}\frac{d\phi}{dr} = \frac{\beta\rho_c}{M_p} \quad \text{for} \quad R_r < r < R \tag{3.40}$$

with the solution

$$\phi = \phi_c + \frac{\beta\rho_c R_{roll}^2}{6}\left(\frac{r^2}{R_{roll}^2} + \frac{2R_{roll}}{r} - 3\right) \quad \text{for} \quad R_r < r < R \tag{3.41}$$

Outside the body the Yukawa-profile (3.33) will be valid. Matching the field value and first derivative at $r = R$ determines A,

$$A \approx \phi_b - \phi_c \tag{3.42}$$

and the thin-shell factor

$$\frac{\Delta R}{R} \equiv \frac{\phi_b - \phi_c}{\frac{\beta\rho_c}{M_p}R^2} \approx \frac{R - R_r}{R} \tag{3.43}$$

Where we have used that $\phi_b \gg \phi_c$, $m_c R \gg 1$ and assumed $m_b R < 1$ since we are interested in the case where the chameleon has a long-range. The thin-shell factor can be written, using (3.20) and (3.21),

$$\frac{\Delta R}{R} = \frac{\phi_b}{\phi_c}\frac{(n+1)}{(m_c R)^2} = \left(\frac{\rho_c}{\rho_b}\right)^{\frac{1}{n+1}}\frac{n+1}{(m_c R)^2} \tag{3.44}$$

and the condition $\frac{\Delta R}{R} \ll 1$ will be satisfied when

$$(m_c R)^2 \gg (n+1)\left(\frac{\rho_c}{\rho_b}\right)^{\frac{1}{n+1}} \gg 1 \tag{3.45}$$

In the following we refer to $\frac{\Delta R}{R} \ll 1$ as the thin-shell condition[5]. We can now express the chameleon force on a test-mass outside the body[6]

$$F_\phi(r) = 2\beta^2 \frac{3\Delta R}{R} F_{\text{gravity}}(r) \quad \text{for} \quad r < m_b^{-1} \tag{3.46}$$

and we see that the force is suppressed by the thin-shell factor $\frac{\Delta R}{R} \ll 1$ relative to the thick-shell case described above. In other words: $\frac{\Delta R}{R}$ describes how much of the mass of the body that contributes to the fifth-force. The existence of this factor is contributed to the non-linearities of the field equation since in the linear case the superposition principle holds. This relationship can also be found from physical reasoning: When the mass of the chameleon is large its interaction dies off within a distance $\Delta R \sim m_c^{-1}$ from the surface and the field outside the body will be shielded from the core. The condition on $m_c R$ (3.45) can also be turned around so that if $m_c R$ does not satisfy this condition we will also have $\frac{\Delta R}{R} > 1$ and the thick-shell solution derived above is valid. The full solution can therefore be summarized as

$$\begin{aligned} \phi(r) &= -\tfrac{\beta}{4\pi M_p} \tfrac{M_c e^{-m_b r}}{r} + \phi_b \qquad \text{when} \quad \tfrac{\Delta R}{R} > 1 \\ \phi(r) &= -\tfrac{\beta}{4\pi M_p} \tfrac{3\Delta R}{R} \tfrac{M_c r^{-m_b r}}{r} + \phi_b \quad \text{when} \quad \tfrac{\Delta R}{R} \ll 1 \end{aligned} \tag{3.47}$$

with $\frac{\Delta R}{R}$ defined by (3.43). Compared with numerical simulations the expressions derived above are usually good to within 10%, but more accurate solutions can be found in [20].

3.7 Experimental Bounds

We will go through some typical experiments that bounds the chameleon such as EP-violation and fifth-force experiments, and show how the thin-shell mechanism works to evade even very tight experimental constraints. Experimental bounds have been derived in several papers [1, 10, 13, 61], to mention some. We will only go through some basic properties to show the thin-shell mechanism in action and refer the reader to the references for a more thorough discussion. When looking at the generalized chameleon coupling later on, the experimental bounds will be worked out in a more detailed manner.

3.7.1 Fifth-Force and EP violation searches

The potential energy associated with a fifth-force can be parameterized as a Yukawa potential

$$\mathcal{V}(r) = \alpha \frac{GM}{r} e^{-r/\lambda} \tag{3.48}$$

[5] A more detailed derivation gives that $\epsilon = \frac{\Delta R}{R} + \frac{1}{m_c R}$ is a more accurate expression for the thin-shell factor, see [20] .

[6] The force behavior is more thoroughly discussed in the section 'Chameleon with a Field-dependent coupling'

where α is the strength of the force and λ the range. Fifth force searches and EP experiments are usually performed in a vacuum, but the non zero pressure p in these 'vacuums' will correspond to a non-zero density[7] ρ_b. When test-particles inside the vacuum chamber have a thick-shell, the strength of the interaction relative to gravity can be read off from (3.37):

$$\alpha = 2\beta^2 \tag{3.49}$$

Inside a vacuum chamber the field will sit at a field-value $\phi_{\rm vac}$ where its mass satisfy $m^2_{\rm vac} = V_{,\phi\phi}(\phi_{\rm vac}) \approx 1/R^2_{\rm vac}$ and $R_{\rm vac}$ is the size of the chamber, see [1]. Note that in the extreme cases where $m_{\rm min}R_{\rm vac} > 1$ the field will sit at the minimum inside the vacuum chamber, but this is not a very interesting regime since the chameleon force will be exponentially suppressed. When the test-particles have a thin-shell then from (3.46) we see that the strength of the interactions are now

$$\alpha = 2\beta^2 \left(\frac{3\Delta R}{R}\right)^2 \tag{3.50}$$

For ranges $\lambda \approx 10cm - 1m$, the tightest bound on α from laboratory experiment comes from the experiment of Hoskins et. al. [40]

$$\alpha < 10^{-3} \tag{3.51}$$

The experiment used test-particles with $M_{\rm test} \approx 40g$ and $R_{\rm test} \approx 1cm$. When the test-particles have a thick-shell the experiments constraints $\beta \lesssim 0.01$. Lets see what happens when the test-particles have a thin-shell. Since the chameleon-mass inside the chamber satisfies

$$m^2_{\rm vac} = M^2 n(n+1)\left(\frac{M}{\phi_{\rm vac}}\right)^{n+2} = \frac{1}{R_{\rm vac}} \tag{3.52}$$

we find

$$\phi_{\rm vac} \approx (MR_{\rm vac})^{\frac{2}{n+2}} M \tag{3.53}$$

Using the thin-shell condition (3.43), with $\phi_{\rm vac} = \phi_b$ and assuming $\phi_{\rm vac} \gg \phi_c$, we find that the experimental constraint can be written as a bound on M:

$$M \lesssim 10^{\frac{3n}{4+n}} (1mm)^{-1} \tag{3.54}$$

There is also a constraint on β since we implicitly have assumed that we have a thin-shell, but this is a very weak constraint and a quick calculation using $M \sim (1mm)^{-1}$ shows that the test-particles have a thin-shell for all $\mathcal{O}(1) \lesssim \beta$ given that $4 \lesssim n$. Having a large β leads to a small thin-shell

[7] This density can be estimated by using the ideal gas law $\rho = \frac{p}{R_{\rm air}T}$.

factor and we are left with the counter-intuitive effect that a stronger matter-coupling leads to less restrictive bounds. This is the chameleon mechanism in a nut-shell!

Thus, experiments of this type cannot detect a very strongly coupled chameleon, but as we shall see below there exists other experiments that are more sensitive to a large coupling (for example BBN and PPN). The bound on the mass-scale M coincides with the dark energy scale, and its quite a coincident that it is derived from local experiments.[8] The natural scale[9] for the potential is the Planck-scale M_p, and since $M \ll M_p$ this model suffers from fine-tuning. This fine-tuning is however no better or worse than a cosmological constant.

3.7.2 EP violation

EP-violation experiments measure the difference in free fall acceleration between two test-bodies towards an attractor. Deviations from the equivalence principle are parametrized by the Eötvos-parameter η

$$\eta \equiv \frac{2|a_1 - a_2|}{|a_1 + a_2|} \approx |\alpha_1 - \alpha_2| \tag{3.55}$$

where α_i is the ratio of the free fall acceleration of body i relative to the Newtonian prediction. The best bound on η comes from the Eöt-Wash EP-experiment and reads $\eta < 10^{-13}$ [27]. To proceed we assume that different bodies couple to ϕ with a β_i which are all of the same order β. If the two test-masses and the attractor (with coupling β_A) have a thick-shell the bound reads $\eta = 2\beta_A|\beta_1 - \beta_2| < 10^{-13}$ which is a very tight constraint on the coupling constants[10]. If the attractor have a thin-shell, but the test-bodies don't, the bound becomes

$$2\beta^2 \frac{3\Delta R}{R} < 10^{-13} \tag{3.56}$$

For the test-particles used in the Eöt-Wash experiment, the resulting bound becomes weaker than the fifth-force bound discussed above. This allows $\mathcal{O}(1) \lesssim \beta$ and shows how the thin-shell condition provides a way of evading the tight experimental bound. Even though there might be a violation of WEP on a particle level this need not manifest itself for macroscopic bodies.

[8] The full analysis shows that this is not only the case for this experiment, see [1].

[9] The energy-scale where gravity must be treated quantum-mechanical.

[10] One might be tempted to just assume that all matter field couple to ϕ with the same strength. But quantum corrections will in general induce a change in the couplings which are different for different matter fields.

3.7.3 PPN corrections

When β is of order unity we generally have $m_b^{-1} \gg 1Au$ and the chameleon will essentially be a free field in the solar system. The field profile outside a thin-shelled sun reads

$$\phi = \phi_b - \frac{\beta}{4\pi M_p}\frac{3\Delta R}{R}\frac{M_s e^{-m_b r}}{r} \tag{3.57}$$

For ranges $r < m_b^{-1}$ we can neglect the exponential factor and the field-profile is that of a massless scalar-field with matter coupling $\beta_{\text{eff}} = \beta\frac{3\Delta R}{R}$. This allows us to treat our model as an effective Brans-Dicke model with a Brans-Dicke parameter given by[11]:

$$\frac{1}{3+2\omega_{BD}} = 2\beta_{\text{eff}}^2 = 18\beta^2\left(\frac{\Delta R}{R}\right)^2 \tag{3.58}$$

The tightest constraints on the Brans-Dicke parameter in the solar system comes from the Cassini-experiment and reads $\omega_{BD} > 2.4 \cdot 10^5$ [21], and is easily satisfied as long as the solar system bodies (the sun, planets etc.) have thin-shells. The thin-shell factor is proportional to R^{-2} and because planets have a large radii, the thin-shell condition is usually satisfied even for very small β's. For this reason, PPN bounds do not give rise to very good constraints on the parameters.

3.7.4 BBN bounds

If the standard model particles have a larger/smaller mass today than at the time of big bang nucleosynthesis (BBN) it would have meant that the nucleosyntesis would have started at a different time. Measurements constraint any variation of this type to be less than 10% since BBN. Since out chameleon couple to matter via a conformaly transformed metric, the standard model particles will aquire a ϕ-dependence on the form

$$m = m_0 e^{\frac{\beta\phi}{M_p}} \approx m_0\left(1 + \frac{\beta\phi}{M_p}\right) \tag{3.59}$$

A variation in ϕ leads to a variation

$$\frac{\Delta m}{m} = \frac{\beta\Delta\phi}{M_p} \tag{3.60}$$

in m. Assuming that the chameleon follows the minimum as the universe evolves, then ϕ is an increasing function of time and the bound reduces to

$$\frac{\beta\phi_{\text{today}}}{M_p} \lesssim 0.1 \tag{3.61}$$

[11] See the definition below (2.48)

with ϕ_{today} being the field value in the cosmological background today ($\rho_b \sim \rho_{critical}$). Using (3.20) and taking $M \sim M_{\text{dark energy}}$ ($M^4 \sim \rho_b$) we find the bound

$$\frac{\beta M}{M_p}\left(\frac{\beta\rho}{nM^3M_p}\right)^{-\frac{1}{n+1}} \lesssim 0.1 \tag{3.62}$$

$$\beta \lesssim \frac{M_p}{10M} \sim 10^{29} \tag{3.63}$$

and we see that BBN constraints only the highest coupled models.

3.7.5 Combined bounds

In the sections above we have only looked at the phenomenological effects the chameleon have in different types of experiments. The full analysis, using the potential

$$V(\phi) = \sigma M^4\left(\frac{M}{\phi}\right)^n \tag{3.64}$$

where σ is a dimensionless constant for the case $n = -4$, is found in [10]. The resulting bounds are shown in figure (3.3). Note that for low β the bounds does not depends on the value of M. This is because when we have a small β the chameleon will in most experiments act as a linear scalar field, it is in the thick-shell regime, and thus the potential is negligible. For larger β the bounds does only depend on the value of M. This is due to the coupling-strength $2\beta^2\left(\frac{3\Delta R}{R}\right)^2$ being almost β independent (it depends on β only implicitly through ϕ_b).

3.8 Cosmology

The chameleon scalar field can act as a dark energy fluid and be responsible for the late time acceleration of the universe. Since the chameleon can couple to matter with gravitational strength it could potentially produce strong cosmological signatures. The cosmology of the chameleon model using an inverse exponential potential

$$V(\phi) = M^4\exp\left(\frac{M}{\phi}\right)^n \tag{3.65}$$

was studied in [14] and we will just re-state some basic properties here. First off all this potential was chosen over (3.18) since in the limit $\phi \to \infty$ we get $V(\phi) \to M^4$: a cosmological constant. The potential scale M must therefore be fine-tuned in the same manner as the cosmological constant, thus not providing a solution to the fine-tuning problem. But as discussed above, this is also required by local experiments. In the following we take

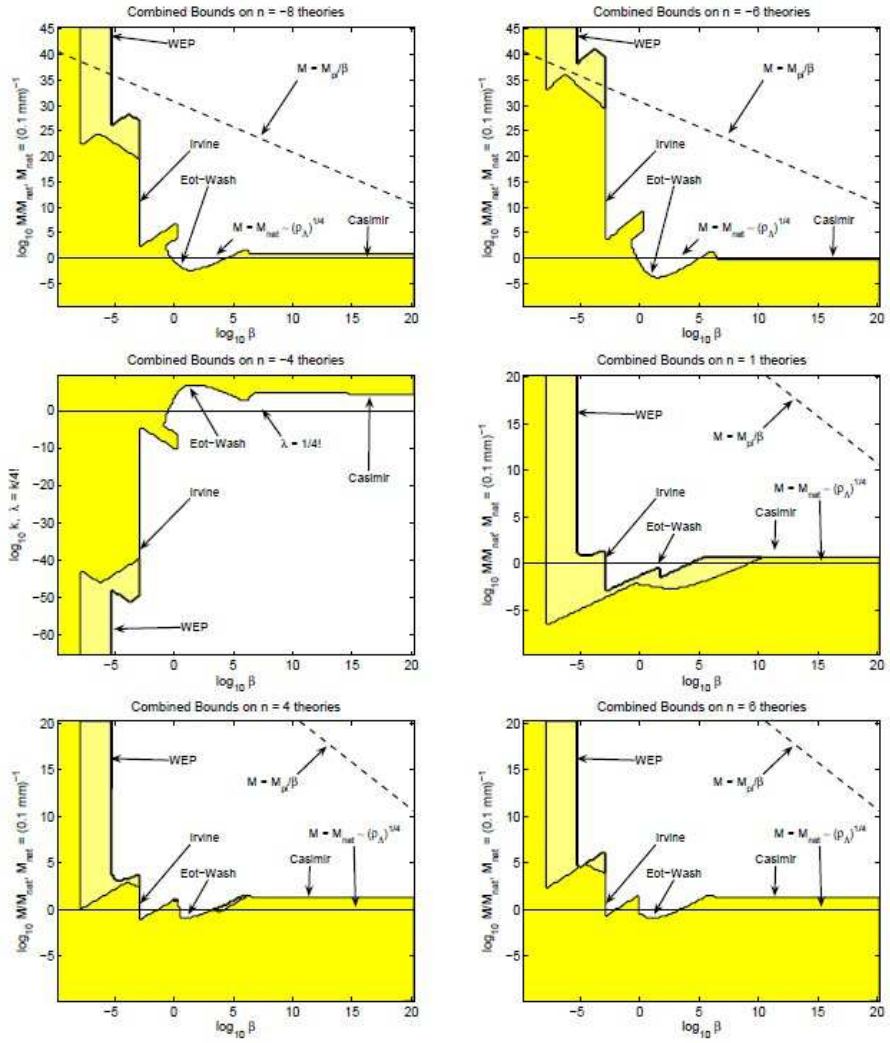

Figure 3.3: Combined constraints on chameleon theories. The whole of shaded area shows the regions of parameter space that are allowed by the current data. Future space-based tests could detect the more lightly shaded region. The solid black lines indicate the cases where M and σ take 'natural values'. For $n \neq -4$, a natural value for M is required if the chameleon is to be dark energy. The dotted-black line indicates when $M = M_p/\beta$ i.e. when the mass scale of the potential is the same as that of the matter coupling. The amount of allowed parameter space increases with $|n|$.

$M = M_{\text{dark energy}} \sim 10^{-3}\text{eV}$.

The cosmological field equation in a flat FLRW background[12] is given by

$$\ddot{\phi} + 3H\dot{\phi} + V_{\text{eff},\phi} = 0 \tag{3.66}$$

When the field is close to the minimum we can simplify this equation by linearizing around ϕ_{min}:

$$\ddot{\phi} + 3H\dot{\phi} + m^2_{\text{min}}(\phi - \phi_{\text{min}}) \approx 0 \tag{3.67}$$

For $\mathcal{O}(1) \lesssim \beta$ and $\mathcal{O}(1) \lesssim n$ the field will satisfy $\frac{m^2_{\text{min}}}{H^2} \gg 1$ since the Planck-time and (3.67) will be under damped. This will make sure that the chameleon settles at the minimum eventually. It was shown in [14] that for a large span of initial condition the field will converge to the attractor $\phi = \phi_{\text{min}}$ and follow this at least until the present era.

When the field follows the attractor we can calculate the equation of state directly from $\dot{\rho_\phi}/\rho_\phi = -3H(1+\omega_{\text{eff}})$, where $\rho_\phi = \frac{1}{2}\dot{\phi}^2 + V$ for a homogeneous scalar-field. This yields

$$\omega_{\text{eff}} = -1 + \frac{1}{\Gamma} \tag{3.68}$$

with $\Gamma = \frac{VV_{,\phi\phi}}{V^2_{,\phi}}$. When the field follows the minimum, using (3.20), Γ can be written

$$\Gamma = 1 + \frac{n+1}{n}\left(\frac{\phi_{\text{min}}}{M}\right)^n \tag{3.69}$$

and it is clear that $\Gamma \gg 1$ for $\phi_{\text{min}} \gg M$ which means that $\omega_{\text{eff}} \approx -1$ today. The chameleon can produce the same energy density and equation of state as the cosmological constant and can thus be responsible for the late time acceleration of our universe. Note that the equation of state is not given by the usual expression for a minimal coupled scalar field $\omega_{usual} = \frac{\dot{\phi}^2 - 2V}{\dot{\phi}^2 + 2V}$ since ϕ is non-minimally coupled. Along the attractor $V_{\text{eff},\phi} = 0$. Taking the time-derivative yields

$$\dot{\phi}_{\text{min}} = -\frac{3H\rho_m V_{,\phi}}{V_{,\phi\phi}} > 0 \tag{3.70}$$

where the ϕ-dependent functions on the r.h.s is to be evaluated at $\phi = \phi_{\text{min}}$. This result can be used to show that the field will be slow-rolling along the attractor:

$$\frac{\dot{\phi}^2_{\text{min}}}{2V(\phi_{\text{min}})} \approx \frac{9}{2}\frac{H^2}{m_{\text{min}^2}}\frac{1}{\Gamma} \ll 1 \tag{3.71}$$

[12]This equation is derived in the appendix for a minimal-coupled scalar-field. The equation in our case follows by replacing the potential with the effective potential.

The difference from ΛCDM, in the background evolution, is usually much less than 1% when the field is following the attractor. This makes it hard to discriminate between this model and ΛCDM using only the background evolution. In order to find interesting cosmological effects we must look at the perturbations.

3.8.1 Perturbations

The linear matter perturbations[13] in the co-moving gauge $v = 0$ is derived in [14]. When the chameleon follows the minimum, the Fourier-modes δ_m of the linear matter perturbations $\frac{\rho(x,t)-\rho(t)}{\rho(t)}$ satisfy

$$\ddot{\delta}_m + 2H\dot{\delta}_m = \frac{3}{2}\Omega_m H^2 G \left(1 + \frac{2\beta^2}{1 + \frac{a^2 V_{,\phi\phi}}{k^2}}\right) \tag{3.72}$$

This equation is similar to equation (2.134) for ΛCDM with the difference that the perturbations will now feel a different gravitational constant for length scales smaller than $\lambda = 2\pi V_{,\phi\phi}^{-1/2}$. For typical $\mathcal{O}(1)$ values of n and β we find $\lambda \lesssim 100pc$ which is a rather small cosmological length scale. This means that the chameleon in general only affects the non-linear clustering of matter, see [49] for a discussion on the small scale structure formation within chameleon models. By considering a lower n we can increase this length scale, leading to some interesting signatures like dispersion in the matter perturbation relevant to the galaxy power spectrum. This can provide a way of using observations of the large scale structure in the universe to discriminating the chameleon from ΛCDM and is the subject of our first original production [39].

3.9 Detecting Chameleons

The thin-shell mechanism is what allows the chameleon to couple to matter with gravitational strength and still be in agreement with observations, but it also what makes it hard to detect the field in any experiment. We will look at some experiments / observations that might provide a way of detecting the field.

3.9.1 Weakly coupled chameleons

The three satelitte experiments MICROSCOPE, STEP and GG [4, 5, 6] mentioned in the introduction is probably the best card in detecting a chameleon. Typically test-masses in the above satellite experiments don't necesarilly

[13] In the section 'Cosmology of chameleons with field-dependent couplings' we will generalize this derivation to a general Chameleon model

have a thin-shell and therefore the fifth-force due to the scalar field will be of the same order as gravity. This means that MICROSCOPE, STEP and GG could measure violations of EP stronger than currently allowed by laboratory experiments. Furthermore the SEE-project could measure an effective gravitational constant $G_{\text{eff}} = G(1 + 2\beta^2)$ that differs by $\mathcal{O}(1)$ from the value measured on earth. Such an outcome of the experiment would constitute strong evidence for the existence of chameleons in our universe.

3.9.2 Strongly coupled chameleons

In [77] the chameleon pressure between two parallel plates in the presence of an intervening medium was investigated. When the background density varies so does the mass of the chameleon. The background gas in a vacuum chamber weakens the chameleon interaction mechanism with a screening effect that increases with the plate separation and with the density of the intervening medium. This phenomenon might open up new directions in the search of chameleon particles with future long range Casimir force experiments.

3.9.3 Chameleons as dark energy

The background evolution of any viable chameleon model is typically indistinguishable from ΛCDM, leaving little hope of finding effects in e.g. the deceleration parameter or the statefinder parameters. In order to discriminate between different dark energy models it can be useful to use both the perturbations and the background expansion by looking at the late time growth of the matter perturbations. Most dark energy models inside GR yield a quasi constant growth factor. But as we shall see in the next chapter, chameleon models can give rise to a more rapid growth and dispersion on different scales. This can allow to detect the chameleon via observations of the late time growth of the linear matter perturbations. However any detection which does not agree with ΛCDM does not directly confirm the existence of a chameleon since there are many other dark energy models which can produce this effect.

3.9.4 A coupling to photons

The chameleon model, as stated in this thesis, does not lead to a coupling to photons since the electromagnetic action is conformal invariant [76]. We can however generalize the model by considering a photon-coupling $e^{\frac{\beta_\gamma \phi}{M_p}} F^{\mu\nu} F_{\mu\nu}$ where $F^{\mu\nu}$ is the electromagnetic field-strength. A coupling of this type can lead to some interesting effects. It was showed in [75] that a coupling between chameleon-like scalar fields and photons induces linear and circular

polarization in the light from astrophysical sources. Thus the chameleon can be detected via observations of starlight polarization in our galaxy.

Also, if chameleons couple strongly to photons, then they are ideally suited to probes of the afterglow phenomenon, the first of which was the GammeV experiment at Fermilab [79]. The experiment used a closed, evacuated cylindrical chamber, with glass windows at the ends and a magnetic field in the interior. When streaming photons through the windows they will occasionally oscillate into chameleon particles in the background magnetic field [59, 78]. If the mass of one of these chameleons in the walls of the chamber is greater than its total energy inside the chamber, then it will reflect from the wall; such a chameleon will be trapped in the chamber. After the photon source has been turned off, any remaining chameleons will oscillate back into photons in the magnetic field, producing an observable 'afterglow' of photons. The GammeV experiment have looked for this effect, but found no effect so far.

Chapter 4

On the growth of matter perturbations in the Chameleon Model

4.1 Introduction

We consider the growth of matter perturbations on low redshifts in a specific chameleon dark energy (DE) model. In the chameleon model reviewed in the last section, the growth of the linear matter perturbations are usually not affected by the modifications of gravity since the range of the field is to small for natural values of the parameters. This can however change if we consider $n < 1$, n being the slope of the Ratra-Peebles potential, or look at other potentials.

This section is part of a larger article which is a collaboration with Radouane Gannouji, Bruno Moraes, David F. Mota, David Polarski and Shinji Tsujikawa. The work shown here is mainly the part I have been involved in and are the preliminary results.

4.1.1 The Model

We consider a universe where gravity and the matter content of the universe are described by the following action

$$S = \int d^4x\sqrt{-g}\left(\frac{R}{16\pi G} - \frac{1}{2}g^{\mu\nu}\partial_\mu\phi\ \partial_\nu\phi - V(\phi)\right) + S_m\left[A^2(\phi)\ g_{\mu\nu}, \psi_i\right] \tag{4.1}$$

where ψ_i stands for any matter field, however it will be enough for our purposes to consider only dust-like matter (baryons and cold dark matter). We see that matter fields are universally coupled to the metric $A^2(\phi)\ g_{\mu\nu} \equiv \tilde{g}_{\mu\nu}$ (the metric in the Jordan frame) and not to $g_{\mu\nu}$ (the metric in the Einstein frame (EF)). We can extend this to arbitrary functions $A_i(\phi)$ for each component ρ_i. We concentrate on spatially flat Friedman-Lemaître-Robertson-Walker (FLRW) universes with a time-dependent scale factor $a(t)$ and a metric

$$ds^2 = g_{\mu\nu}\ dx^\mu\ dx^\nu = -dt^2 + a^2(t)\ d\mathbf{x}^2 \tag{4.2}$$

The corresponding background equations are given by

$$3H^2 = 8\pi G\left(\rho_m^* + \frac{1}{2}\dot{\phi}^2 + V\right) \tag{4.3}$$

$$\dot{H} = -4\pi G\left(\rho_m^* + \dot{\phi}^2\right) \tag{4.4}$$

The quantity ρ_m^* is the energy density of dust-like matter in the Jordan frame and we have kept the star to avoid any confusion. It is important to realize

that ρ_m^* evolves according to

$$\rho_m^* \propto A(\phi)\ a^{-3} \tag{4.5}$$

Hence one can formally define the Einstein-frame density $\rho_m \equiv A^{-1}\ \rho_m^*$ which scales like a^{-3}. However when ϕ is quasi-static, ρ_m^* will evolve like usual dust. The reason we choose to write out equations this way is to simplify the derivation of the perturbations later on. We have further

$$\ddot{\phi} + 3H\dot{\phi} = -V_{,\phi} - \alpha(\phi)\ \rho_m^* \equiv -V_{\mathrm{eff},\phi} \tag{4.6}$$

where $\alpha(\phi) = \frac{d\log\phi}{d\phi}$ and dust-like matter obeys the equation

$$\dot{\rho}_m^* + 3H\rho_m^* = \frac{\dot{A}}{A}\ \rho_m^* \tag{4.7}$$

Note that we have

$$\frac{\dot{A}}{A} = \frac{d\ln A}{d\phi}\ \dot{\phi} \equiv \alpha(\phi)\ \dot{\phi} \tag{4.8}$$

For the particular case

$$A^2 = e^{2\beta\phi/\mathrm{M_p}} \tag{4.9}$$

${\mathrm{M_p}}^{-2} \equiv 8\pi G$, we have obviously $\alpha = \beta/\mathrm{M_p}$ a constant. We note that neither dust, nor the scalar field ϕ obeys the conservation equation $\dot{\rho}_i = -3H(\rho_i + p_i)$. They satisfy instead

$$\dot{\rho}_m^* + 3H\rho_m^* = \frac{d\ln A}{dt}\ \rho_m^* \tag{4.10}$$

$$\dot{\rho}_\phi + 3H(\rho_\phi + p_\phi) = -\frac{d\ln A}{dt}\ \rho_m^* \tag{4.11}$$

In (4.11) we have defined

$$p_\phi \equiv \frac{1}{2}\dot{\phi}^2 - V \tag{4.12}$$

the usual pressure of a minimally coupled scalar field. We can introduce the following relative densities in the standard way

$$\Omega_i = \frac{8\pi G\rho_i}{3H^2} \tag{4.13}$$

and we have in particular

$$\Omega_m^* = \frac{8\pi G\rho_m^*}{3H^2} = \Omega_{m,0}^*\ (1+z)^3\ \frac{A}{A_0} \tag{4.14}$$

4.1.2 The Perturbations

In the following section we will consider the particular case (4.9). As the metric, we consider the FLRW spacetime with the scalar perturbations.

$$ds^2 = -(1+2\alpha)dt^2 - 2aB_{,i}dtdx^i + a^2\left((1+2\psi)\delta_{ij} + 2\gamma_{,i;j}\right)dx^i dx^j \quad (4.15)$$

In the gauge-ready formulation[1] [16], the scalar perturbations equations are (we consider $\mathrm{M_p} \equiv 1$)

$$\begin{aligned}
\dot{\chi} + H\chi - \alpha - \psi &= 0 \quad (4.16)\\
\kappa + \frac{\Delta}{a^2}\chi - \frac{3}{2}(\rho_m^* v + \dot{\phi}\delta\phi) &= 0 \quad (4.17)\\
\ddot{\delta\phi} + 3H\dot{\delta\phi} + (V_{,\phi\phi} - \frac{\Delta}{a^2})\delta\phi + & \\
\beta(2\alpha\rho_m^* + \delta\rho_m^*) + 2\alpha V_{,\phi} - \dot{\phi}(\dot{\alpha} - 3H\alpha + \kappa) &= 0 \quad (4.18)\\
\dot{v} - \alpha + \beta(\dot{\phi}v - \delta\phi) &= 0 \quad (4.19)\\
\dot{\delta\rho_m^*} + 3H\delta\rho_m^* - \rho_m^*\left(\kappa - 3H\alpha + \frac{\Delta}{a^2}v\right) - \beta(\rho_m^*\dot{\delta\phi} + \delta\rho_m^*\dot{\phi}) &= 0 \quad (4.20)\\
H\kappa + \frac{\Delta}{a^2}\psi - \left(-\delta\rho_m^* + \alpha\dot{\phi}^2 - \dot{\phi}\dot{\delta\phi} - V_{,\phi}\delta\phi\right)/2 &= 0 \quad (4.21)\\
\dot{\kappa} + 2H\kappa + 3\alpha\dot{H} + \frac{\Delta}{a^2}\alpha - \left(\delta\rho_m^* - 4\alpha\dot{\phi}^2 + 4\dot{\phi}\dot{\delta\phi} - 2V_{,\phi}\delta\phi\right)/2 &= 0 \quad (4.22)
\end{aligned}$$

with

$$\chi = a(B + a\dot{\gamma}) \quad (4.23)$$

$$\kappa = 3(-\dot{\psi} + H\alpha) - \frac{\Delta}{a^2}\chi \quad (4.24)$$

The choice of a gauge will simplify the system. We will work in the so-called co-moving gauge ($v = 0$) where we can close the system for the two variables $(\delta\phi, \delta_m^*)$

$\delta\phi$ is the perturbation of the chameleon field and δ_m^* is the matter density perturbations in the Einstein frame defined by

$$\delta_m^* \equiv \frac{\delta\rho_m^*}{\rho_m^*} - \frac{\dot{\rho}_m^*}{\rho_m^*}v \equiv \frac{\delta\rho_m^*}{\rho_m^*} \quad \text{in the co-moving gauge,} \quad (4.25)$$

[1] In this article the equations governing the matter perturbations have been derived for a large class of scalar-field models and after som short calculations we can just read off the equations for our specific model.

In the following part of the article we will omit the *. In Fourier space, we have

$$\ddot{\delta}_m + 2H\dot{\delta}_m - \frac{1}{2}\rho_m\delta_m + \delta\phi\left(V_{,\phi} - \beta[6H^2 + 6\dot{H} - \frac{k^2}{a^2} + 2\dot{\phi}^2]\right) - \delta\dot{\phi}\left(5\beta H + 2\dot{\phi}\right) - \beta\delta\ddot{\phi} = 0 \quad (4.26)$$

$$\delta\ddot{\phi} + (3H + 2\beta\dot{\phi})\delta\dot{\phi} + \left(m_\phi^2 + \frac{k^2}{a^2} - 2\beta^2\rho_m - 2\beta V_{,\phi}\right)\delta\phi + \beta\rho_m\delta_m - \dot{\phi}\dot{\delta}_m = 0 \quad (4.27)$$

where k is a co moving wavenumber and $m_\phi = \sqrt{V_{,\phi\phi}}$ is the mass of the chameleon field.

The perturbation of the chameleon field exhibits an oscillating term that we can derived by a (J)WKB approximation [58]

$$\delta\phi_{osc} \propto a^{-3/2}(m_\phi^2 + \frac{k^2}{a^2})^{-1/4}\ \cos\left(\int\sqrt{m_\phi^2 + \frac{k^2}{a^2}}dt\right) \quad (4.28)$$

During the matter phase, we can approximate this oscillating term. We have in all cases $m_\phi \gg k/a$ in the early universe, but during the matter phase we can have a transition two an other regime $m_\phi \ll k/a$.

In the regime where the mass of the scalaron is large compared to the scale term (k^2/a^2) and for the Ratra-Peebles potential (3.18)

$$\phi = \frac{n+1}{\beta}W(\mathrm{C}^{\mathrm{ste}}t^{\frac{2}{n+1}}) \quad (4.29)$$

where $W(.)$ is the Lambert W-function defined by $W(x)e^{W(x)} = x$.

The oscillating term of the perturbation of the scalar field is then in the early matter phase.

$$\delta\phi_{\mathrm{osc}} \propto t^{-\frac{n}{2(1+n)}}\ \cos\left(\mathrm{C}^{\mathrm{ste}}t^{-\frac{1}{1+n}}\right) \quad (4.30)$$

In some cases, during the matter phase, we can have a transition from the regime dominated by the mass of the chameleon to the regime dominated by the scale term. The transition is characterized by $m_\phi \simeq k/a$. In this case, the oscillating term is

$$\delta\phi_{\mathrm{osc}} \propto \frac{\cos(\mathrm{C}^{\mathrm{ste}}kt^{1/3})}{\sqrt{k}t^{2/3}} \quad (4.31)$$

We can see that in all cases, the oscillating term is time-decreasing during the matter phase and this term can be chosen small in the past because

of the initial condition and because of the finite value of the mass of the chameleon. This is a very important difference with $f(R)$-gravity models where the oscillating term can be infinite because of the mass of the scalaron which is not bounded above. The divergence of this mass in $f(R)$-gravity can be get round by adding a UV-term [57].

In the Newtonian regime and when the chameleon is slowrolling along its attractor, all the terms (except the mass of the chameleon $V_{,\phi\phi}$) are negligible relative to the term k^2/a^2. Then eq(4.26,4.27) reduces to

$$\begin{array}{rcl} \ddot{\delta}_m + 2H\dot{\delta}_m - \frac{1}{2}\rho\delta_m + \beta\frac{k^2}{a^2}\delta\phi &=& 0 \\ (m_\phi^2 + \frac{k^2}{a^2})\delta\phi + \beta\rho\delta_m &=& 0 \end{array} \tag{4.32}$$

Which can be written

$$\ddot{\delta}_m + 2H\dot{\delta}_m - 4\pi G_{\rm eff}\rho_m\delta_m = 0 \tag{4.33}$$

where the effective gravitational constant is given by

$$G_{\rm eff} = G\left(1 + 2\frac{\beta^2}{1 + a^2 m_\phi^2/k^2}\right) \tag{4.34}$$

We see that in chameleon models $G_{\rm eff}$ is a scale-dependent quantity. We recognize here the gravitational potential per unit mass in real space of the type

$$V(r) = -\frac{G}{r}\ \left(1 + 2\beta^2\ e^{-m_\phi r}\right)\ . \tag{4.35}$$

The range L of the fifth force satisfies

$$L \sim (V_{,\phi\phi})^{-\frac{1}{2}} = m_\phi^{-1}\ . \tag{4.36}$$

It is clear from eq.(4.34) that the scale-dependent driving force induces in turn a scale dependence in the growth of matter perturbations with two asymptotic regimes,

$$G_{\rm eff} = G(1 + 2\ \beta^2) \qquad k \gg a\ (V_{,\phi\phi})^{\frac{1}{2}}\ , \tag{4.37}$$

$$= G \qquad k \ll a\ (V_{,\phi\phi})^{\frac{1}{2}}\ . \tag{4.38}$$

We can introduce the characteristic scale λ_c

$$\lambda_c = \frac{2\pi}{(V_{,\phi\phi})^{\frac{1}{2}}}\ . \tag{4.39}$$

which for the potential $V(\phi) = M^4 \left(\frac{M}{\phi}\right)^n$ with $M = M_{\text{dark energy}}$ can be written

$$\frac{\lambda_c}{1pc} \sim 10^{-5+\frac{15}{n+1}} \beta^{-\frac{(n+2)}{2(n+1)}} \tag{4.40}$$

The two asymptotic regimes (4.37,4.38) corresponds to the following scales

$$G_{\text{eff}} = G(1 + 2\ \beta^2) \qquad \lambda \ll \lambda_c\ , \tag{4.41}$$

$$= G \qquad \lambda \gg \lambda_c\ . \tag{4.42}$$

On scales $\lambda \gg \lambda_c$ matter perturbations do not feel the fifth force during their growth. On the contrary, on scales much smaller than λ_c they do feel its presence. The question is now what is the order of magnitude of the scale λ_c in viable chameleon models. From (4.40) we see that λ_c can be of order of the galactic size for small n. But if $\beta \ll 1$ then even small cosmological scales will not feel the chameleon's presence. We need $n < 1$ and $\mathcal{O}(1) \lesssim \beta$ in order to have a modified growth-rate.

To find the evolution of δ_m for arbitrary r.h.s. of eq.(4.33) with high accuracy requires numerical calculations. It is possible however to find analytical expressions in the two asymptotic regimes (4.37,4.38) during the matter stage when $\Omega_m^* \approx 1$, a regime still valid until low redshifts. In this way we obtain

$$\delta_m \propto a^{\frac{1}{4}\left(-1+\sqrt{1+24(1+2\beta^2)}\right)} \qquad k \gg a(V_{,\phi\phi})^{\frac{1}{2}}\ , \tag{4.43}$$

$$\delta_m \propto a \qquad k \ll a(V_{,\phi\phi})^{\frac{1}{2}}\ . \tag{4.44}$$

As expected the two regimes are similar for very small β values. At large redshifts during the matter era the interesting cosmic scales are (deep) in the regime $k \ll a(V_{,\phi\phi})^{\frac{1}{2}}$, and deep inside the Hubble radius as well.

Provided the chameleon mass is not too large there are relevant sub horizon scales that go from the second into the first regime. When this is so we get a scale-dependent increase in the growth of matter perturbations on small cosmic scales. For $n = 1$ the chameleon mass is very large, this increase takes place on very small scales $\sim$ 100pc and the presence of the chameleon field is not felt on larger cosmic scales.

One way to describe the growth of perturbations is by introducing the function $\gamma(z)$ as follows

$$f = \Omega_m(z)^{\gamma(z)}\ . \tag{4.45}$$

This is exactly in the spirit of using both the perturbations and the background expansion in order to discriminate between various DE models. The

interesting point is whether the chameleon models we are considering here exhibit a characteristic signature which allows to discriminate them from DE models inside GR and in particular from ΛCDM. It is known that a large class of DE models inside GR yield a quasi-constant γ with values close to that of ΛCDM.

We will first start by looking at the local gravity bounds for the potential $V(\phi) = M^4 e^{\left(\frac{M}{\phi}\right)^n}$. This potential reduces to the Ratra-Peebles potential $M^4\left(\frac{M}{\phi}\right)^n$ when $\phi \gg M$, which will typically be the case in the time after BBN. This means the two potentials produce the same late time cosmological evolution, but the local gravity bounds can be different since we typically have $M \lesssim \phi$ in a high density environment.

4.2 Local Gravity Bounds on the Inverse power exponential

Local gravity bounds for chameleon models have been calculated in several papers. Most of them have focused on the Ratra-Peebles potential

$$V(\phi) = M^4\left[1 + \left(\frac{M}{\phi}\right)^n\right] \tag{4.46}$$

See e.g. [10] for experimental bounds on the coupling β as function of M and n. It was found that for $n = 1, 4, 6$ the region $\beta \sim 10^{-2} - 10^4$ is excluded by the Eöt-Wash experiment[2]. It was also found that the region of allowed parameter space grows with increasing n, implying that the case $n < 1$ is also excluded. This effect is because the potential gets steeper for bigger n and the thin-shell condition is more easily satisfied.

We will calculate the bounds for the inverse power exponential potential

$$V(\phi) = M^4 \exp\left[\left(\frac{M}{\phi}\right)^n\right] \tag{4.47}$$

for the (cosmologically) interesting region $(n, \beta) = 0.01 - 10$. When $\phi \gg M$ this potential reduces to (4.46) which will be the case in the cosmological background today. We must therefore choose $M = \Lambda^{\frac{1}{4}} \approx 2.4 \cdot 10^{-3}$eV to get the correct dark energy density today.

Experimental bounds on the inverse power exponential have been calculated for the Casimir effect. In [13] it was found that for $M \sim 10^{-3}$eV our potential satisfy the current Casimir bounds for $(n, \beta) = \mathcal{O}(1)$.

[2]The experimental bounds are shown in the chapter 'Review of the Chameleon model'.

4.2.1 Fifth Force Searches

The potential energy associated with the chameleon fifth force can be parameterized by a Yukawa-potential

$$V = \alpha \frac{GM_1M_2}{r^2} e^{-r/\lambda} \tag{4.48}$$

where α is the strength and λ is the range. When two test-masses have a thin-shell $\alpha = 2\beta^2 \left(\frac{3\Delta R}{R}\right)^2$, where $\frac{\Delta R}{R}$ is the thin-shell factor. If the test masses don't have a thin-shell the chameleon acts as a minimal coupled scalar field with $\alpha = 2\beta^2$.

Fifth force searches and EP-violation experiments are often performed in a vacuum. When test-particles have a thin-shell the thin-shell factor is given by

$$\frac{\Delta R}{R} = \frac{\phi_v - \phi_c}{6\beta\Phi_c M_p} \tag{4.49}$$

where ϕ_v is the field-value in the vacuum chamber, ϕ_c is the field-value deep inside the body and Φ_c the Newtonian potential of the test-particles. Khoury and Weltman [1] found the following about the chameleon in a vacuum chamber.

Chameleon in a vacuum chamber

Deep inside the vacuum chamber (VC) the field-value is such that the chameleon-mass is equal to the inverse radius R_v of the VC

$$V_{,\phi\phi}(\phi_v) = \frac{1}{R_v^2} \tag{4.50}$$

Throughout the chamber the field varies slowly with

$$\left|\frac{d\phi}{dr}\right| \lesssim \frac{\phi_v}{R_v} \tag{4.51}$$

Outside the chamber the field falls off to the field-value in the atmosphere within a radius m_{atm}^{-1} of the walls. We would normally expect that the range of the chameleon force should be less that the size of the chamber. If this is the case, our approach will provide an upper bound for the mass and since our potential is on a runaway-form we will have $\phi_v^{actual} \geq \phi_v$. The thin-shell factor then shows that we will find a lower bound on α.

4.2.2 The Hoskins Experiment

The experiment of Hoskins et. al. [40] (whose bounds probably have been improved since 1985, but which is good enough for our purposes) found the

bound $\alpha < 10^{-3}$ for ranges $\lambda = m_v^{-1} \approx 10cm - 1m$. When $n \lesssim 2$ the test-masses used in the experiment do not have thin-shells so the chameleon acts as a standard scalar field with matter coupling β and constant mass m. The experiment then bounds $2\beta^2 \lesssim 10^{-3}$ or $\beta \lesssim 0.01$. For $n > 3$ the test-masses do have thin-shells and the parameter space in interest $0.01 \lesssim \beta \lesssim 10$ is allowed by this experiment.

Given our assumptions and that we are underestimating the strength, we have that the parameter space $3 \lesssim n$ for all β or $\beta < 0.03$ for all n satisfy the experimental bound.

4.2.3 The Eöt-Wash Experiment

The 2006 Eöt-Wash experiment [53] searched for deviations from the $1/r^2$ force law of gravity. The experiment uses two plates, the detector and attractor, which are separated by a distance d and the attractor is rotating with a angular velocity ω. The detector has 42 4.767mm diameter holes bored into it with a 21-fold azimuthal symmetry. The attractor is similar only the holes have diameter 3.178mm and it is mounted on top of a thicker tantalum plate with 42 6.352mm holes. This thicker plate is designed as to cancel any torque on the detector due to any $1/r^2$ force. Both plates are made of molybdenum with density $\rho_c = 10.2\text{g/cm}^3$, radius $R_p = 3.5\text{cm}$ and thickness $t = 0.997\text{mm}$. The plates are in a vacuum of pressure 10^{-6}torr which corresponds to a background density $\rho_b = 1.6 \cdot 10^{-6}\text{g/cm}^3$. In between the plates there is a $d_{shield} = 10\mu\text{m}$ BeCu-sheet whose purpose to shield the detector from electrostatic forces.

In [10] it was shown that for very high values of β this sheet may develop a thin-shell which in turn will shield the chameleon force/torque by a factor $\exp(-m_{shield}d_{shield})$. But in our case $0.01 < \beta < 10$ this sheet will not have a significant effect on the experiment.

The Chameleon Force between two plates

The force on one plate due to another plate lying parallel to it from a chameleon scalar field ϕ, was derived in [10, 12, 13]. Both plates are assumed to satisfy the thin-shell conditions and we treat the plates as being infinite, flat slabs and take plate one to occupy the region $z < -d/2$ and body two to occupy the region $d/2 < z$. The value of the field at $z = 0$ will be referred to as ϕ_0, the value of ϕ deep inside the plate as ϕ_c, the value at the surface as ϕ_s and in the background as ϕ_b. With the above definitions, ϕ obeys

$$\frac{d^2\phi}{dz^2} = V' - V'_c \tag{4.52}$$

in $z < \frac{d}{2}$ and

$$\frac{d^2\phi}{dz^2} = V' - V_b' \tag{4.53}$$

in $-d/2 < z < d/2$. Integrating these equations we find

$$\frac{1}{2}\left(\frac{d\phi}{dz}\right)^2 = V - V_c - V_c'(\phi - \phi_c) \tag{4.54}$$

in $z < -d/2$ and

$$\frac{1}{2}\left(\frac{d\phi}{dz}\right)^2 = V - V_0 - V_b'(\phi - \phi_0) \tag{4.55}$$

in $-d/2 < z < d/2$. Matching at $z = -d/2$ determines ϕ_s:

$$\phi_s = \frac{V_c - V_0 + V_b'\phi_0 - V_c'\phi_c}{V_b' - V_c'} \tag{4.56}$$

If the second plate where not present then $V_0 = V_b$ and $\phi_s = \bar{\phi}_s$ where

$$\bar{\phi}_s = \frac{V_c - V_b + V_b'\phi_b - V_c'\phi_c}{V_b' - V_c'} \tag{4.57}$$

The attractive force per unit area of plate one due to plate two is therefore

$$\frac{F_\phi}{A} = \int_{d/2}^{d/2+t} \beta\rho_c \frac{d\delta\phi}{dx} dx \approx \beta\rho_c(\bar{\phi}_s - \phi_s) = V_0 - V_b - V_b'(\phi_0 - \phi_b) \tag{4.58}$$

where t is the thickness of the plates. We have neglected the contribution from the surface at $x = d/2 + t$ since the perturbation in ϕ deep inside the plate will be exponentially suppressed when $m_c R_p \gg 1$. To find ϕ_0 we integrate equation (4.55) in the region $-d/2 < z < 0$ and find

$$\frac{d}{\sqrt{2}} = \int_{\phi_s}^{\phi_0} \frac{d\phi}{\sqrt{V - V_0 - V_b'(\phi - \phi_0)}} \tag{4.59}$$

In the case $V(\phi) = M^4\left(\frac{M}{\phi}\right)^n$ we find

$$\frac{Md}{\sqrt{2}} = \int_{y_s}^{y_0} \frac{y^{n/2}dy}{\sqrt{1 - (y^n/y_0)^n + \frac{\beta\rho_b}{M_p M^3}(y - y_0)y^n}} \tag{4.60}$$

where $y = \phi/M$. In the case $V(\phi) = M^4 e^{\left(\frac{M}{\phi}\right)^n}$ we find

$$\frac{nMd}{\sqrt{2}} = \int_{x_0}^{x_s} \frac{x^{-(n+1)/n}dx}{\sqrt{\exp x - \exp x_0 + \frac{\beta\rho_b}{M_p M^3}(x^{-1/n} - x_0^{-1/n})}} \tag{4.61}$$

where $x = (M/\phi)^n$. Its hard to evaluate the integral above analytically, except in the two limits: $d \ll m_c^{-1}$ gives a constant forcelaw $\frac{F_\phi}{A} \approx V(\phi_c)$. $d \gg m_b^{-1}$ leads to an exponential suppressed force. In $m_c^{-1} \ll d \ll m_b^{-1}$ the force was found numerically to have an inverse powerlaw behavior similar to what has been found previously for the Ratra-Peebles potential, see [13]. When the plates have a thin-shell we have that the potential energy for the two plates due to the chameleon force is given by

$$\mathcal{V}(d) = A \int_d^\infty \frac{F_\phi(z)}{A} dz \tag{4.62}$$

In the Eöt-Wash experiment the two plates are rotated relative to each other. Since there are missing holes in the plates this rotation will change the surface area of one plate facing the other which will induce a torque on the detector. This torque is given by the rate of change of the potential with the rotated angle

$$T_\phi \approx \frac{dA}{d\theta} e^{-m_{shield} d_{shield}} \int_d^\infty \frac{F_\phi(z)}{A} dz \tag{4.63}$$

where we have included the effect of the electrostatic shield. The factor $\frac{dA}{d\theta}$ depends only on the experimental setup and in the Eöt-Wash experiment its value is given by $\left\langle \frac{dA}{d\theta} \right\rangle = 3.0 \cdot 10^{-3} m^2$ [12]. When doing the numerics we used a cutoff in the integration at $z \approx R_h$ where $R_h = \mathcal{O}(2mm)$ being the size of the holes in the plates. In doing this we are underestimating the torque since we are neglecting contributions from $z > R_h$. The derivation above is adopted from *Brax et. al.* [12]. Note that in this derivation we have assumed that the chameleon in this experiment does lie at the minimum of its effective potential inside the vacuum chamber. When the chamber is small and the density low enough the field will not sit at this minimum, but instead take on a value where $m^2 \sim 1/R^2$ with R being the size of the chamber as stated above. For our parameter space this will not affect the bounds and can be ignored.

Eöt-Wash Bounds

The Eöt-Wash experiment with plate-separation $d = 55\mu m$ gave the bound $T_\phi < 0.87 \cdot 10^{-17} Nm$. The thin-shell factor for the plates is given by

$$\frac{\Delta R}{R} = \frac{\phi_b}{6\beta M_p \Phi_c} \tag{4.64}$$

where Φ_c is the gravitational potential of the plates which can be approximated as $\Phi_c = \mathcal{O}\left(\frac{\rho_c R_p R_{thickness}}{8 M_{pl}^2}\right)$. We don't need to know its precise value, but only the order of magnitude in order to see where we can use the above analysis. When the plates don't have a thin-shell the chameleon will act as a

linear scalar field with matter coupling β and constant mass $m \sim R_{chamber}^{-1}$. The bound found in the Eöt-Wash experiment is $2\beta^2 < 2.5 \cdot 10^{-3}$, $\beta < 0.04$ for $1/m = 0.4 - 0.8mm$. See fig(4.1) for a plot of the thin-shell factors for the inverse power law and the exponential inverse power potential (being the same). We see that its only for $n \geq 4$ that we have possible thin-shells. A more detailed analysis shows that the numerical results are also good for $n \sim 3$. We found that for $2 \lesssim n$ with $0.01 \lesssim \beta \lesssim 10$ the torque on the detector due to the chameleon is bigger than what is allowed by the experiment. When $1/m \gg 1mm$ as is the case when $n \lesssim 3$ the chameleon force will fall off as $1/r^2$ and the experiment will not be able to detect the chameleon. For $n \lesssim 3$ we can bound the chameleon by experiments looking for Yukawa-forces with longer ranges.

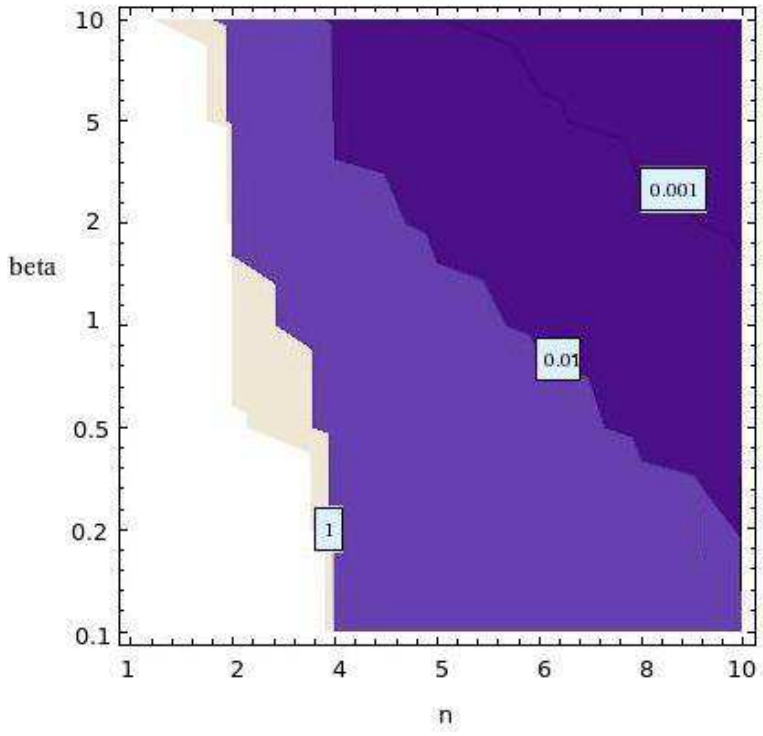

Figure 4.1: Thin-shell factor for the plates used in the Eöt-Wash experiment for both the inverse power- and the exponential-potential.

4.2.4 Lunar Laser Ranging bounds

Measurements of the difference in free-fall acceleration of the Moon and the Earth towards the Sun constraints this to be less than one part in 10^{13} [54],

that is

$$\frac{|a_{moon} - a_{earth}|}{a_N} \lesssim 10^{-13} \tag{4.65}$$

where a_N is the Newtonian acceleration. When the Moon has a thin-shell (which implies that the Sun and the Earth also has a thin-shell), we find

$$\frac{|a_{moon} - a_{earth}|}{a_N} \approx 18\beta^2 \left(\frac{\Delta R}{R}\right)_{sun} \left[\left(\frac{\Delta R}{R}\right)_{moon} - \left(\frac{\Delta R}{R}\right)_{earth}\right] \tag{4.66}$$

Calculating the thin-shell factors numerically we found that $0.01 \lesssim \beta \lesssim 10$ is allowed for $0.5 \lesssim n$, see fig(4.2). We also did the same analysis for the inverse power potential, and because $\phi \gg M$ in the background today the results are identical to the bounds shown in fig(4.2).

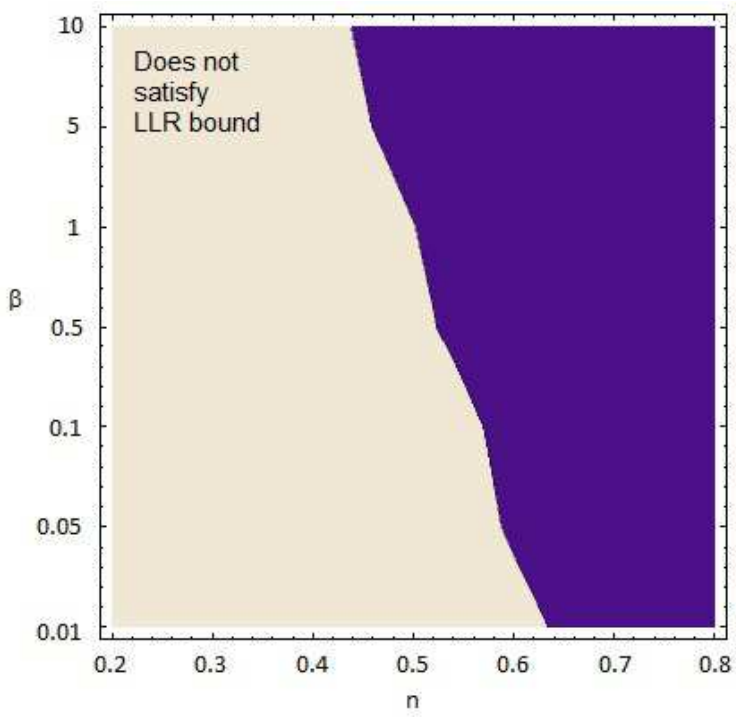

Figure 4.2: LLR bounds for the inverse exponential potential (and the inverse power potential for the given range). For $n > 0.8$ the bound is satisfied and for $0.01 < n < 0.2$ the bound is not satisfied for the given β-range.

4.2.5 PPN bounds

As long as planets in the solar system satisfy the thin-shell condition, then Post-Newtonian bounds are easily satisfied [1]. This can be seen from looking

at the profile outside the thin-shelled earth

$$\phi \approx \phi_b - 6\beta \frac{\Delta R_E}{R_E} \frac{GM_E}{r} e^{-m_b r} \tag{4.67}$$

Since $m_b r \ll 1$ in most cases, this corresponds to a massless scalar field whose effective matter coupling is given by $\beta_{\text{eff}} = 3\beta \frac{\Delta R_E}{R_E}$. Treating our theory as Brans-Dicke which is a good approximation in the solar-system since the chameleon is essentially a free field. The Brans-Dicke parameter can be read off as $3 + 2\omega_{BD} = \frac{1}{2\beta^2_{eff}}$ which gives

$$\frac{1}{\omega_{BD}} \approx 36\beta^2 \left[\frac{\Delta R_E}{R_E}\right]^2 \tag{4.68}$$

We find that the currently strongest bound $\omega_{BD} > 10^5$ [21] is satisfied as long as the LLR bound above is satisfied.

4.2.6 Combined Local Gravity Bounds

Combining the above bounds we have that the parameter space $0.03 \lesssim n \lesssim 10$ for $0.1 \lesssim \beta \lesssim 10$ is ruled out. This is mainly because of the Eöt-Wash experiment, since solar system experiments do allow $n \sim 1$. Bigger values of n makes the thin-shell condition more easily satisfied and the bounds will be weaker.

For the allowed range of parameters, we found that the background and linear perturbation cosmology of these models is identical to that of ΛCDM. This is not the case, however, if we choose to couple the chameleon field only to dark matter instead of all matter. In this case, local constraints are avoided, and we can see that cosmological constraints become the most important.

4.3 The Perturbations in the inverse power exponential potential model

Let us consider now the specific model with

$$V(\phi) = M^4 \, e^{\left(\frac{M}{\phi}\right)^n} \, . \tag{4.69}$$

The rationale behind chameleon models is that gravitational interactions generically arise from string theory with $\beta \sim \mathcal{O}(1)$ ands further that only one energy scale appears in the scalar field potential, here the scale M. This fact is crucial when one is looking for a consistent background evolution. Indeed it is clear that if the chameleon field is to play the role of DE then

it energy density today must be of the order of $\rho_{cr,0}$. Hence we must have $M \sim 10^{-12}$ GeV. We will assume that the field ϕ has reached the minimum of the effective potential $V_{\rm eff}$ already in the very early universe before BBN. The crucial point is that this typically corresponds to $\frac{M}{\phi} \ll 1$ from the early universe on until today. Though there is some significant evolution of ϕ at low redshifts as the minimum of $V_{\rm eff}$ moves to higher values of ϕ, still $\frac{M}{\phi}$ remains exceedingly small. In our model we have $A = 1$ in excellent approximation from very high redshifts on whenever $\beta\frac{\phi}{M_p} \ll 1$.

As a result there is a self-consistent solution for which the potential V remains quasi-constant to very high accuracy from the early stages of its evolution on (after it has reached the minimum of $V_{\rm eff}$ though) until today. The corresponding background evolution is therefore identical to that of a universe with a cosmological constant Λ. As the potential V should dominate the present-day energy density, we must have $M^4 \sim 10^{-47}$ GeV. This is also the scale we need to choose to evade local gravity bounds.

In what follows we explain briefly how the various model parameters enter in the growth of matter perturbations. If we assume that the (chameleon) field ϕ sits in the minimum of the effective potential from the early stages of the universe on, then we have $\frac{\phi}{M_{Pl}} \ll 1$ during the subsequent evolution until today. As a result the background evolution is nothing else than that of ΛCDM. Note that the conformal factor $A(\phi) \equiv e^{\beta\phi/M_p}$, with $M_p^{-2} \equiv 8\pi G$, satisfies $A = 1$ to very high accuracy, so it will disappear from equations and does not have to be considered here. In our fiducial model we have $m^2 \equiv V_{,\phi\phi}$ so it is possible to change the mass scale m by varying the parameters of the potential (here n). Hence the parameter n can be used in order to tune the critical scale λ_c (λ_c depends also marginally on β, see (4.40)).

In such models with $n = 1$ we have $\lambda_c \sim 10^2$ kpc today, in other words this scale is not only very deep inside the Hubble radius but also on scales that have gone strongly non-linear today. However, it is possible to have $\lambda_c \sim$ a few Mpc for $n < 1$ while at the same time the background expansion remains very nearly that of λCDM.

Actually three possibilities can arise: the model is indistinguishable from ΛCDM; the model is distinguishable from ΛCDM but shows no dispersion and finally it is distinguishable from ΛCDM and it shows dispersion.

Models with $n \geq 1$ belong to the first class, they are typically indistinguishable from ΛCDM, the same (slowly varying) function $\gamma(z)$ is obtained as in ΛCDM. In other words the growth of matter perturbations does not allow to distinguish these models from ΛCDM.

Interesting cases can arise for $n < 1$ that belong to all three classes. As mentioned earlier we have then $\lambda_c \sim$ a few Mpc and significant departures from ΛCDM can be obtained, sometimes together with a strong dispersion. We can consider 3 regimes for γ_0.

- **(i)** The phase space (n, β) for which $\gamma_0 > 0.53$ for all scales, this is the GR regime.
- **(ii)** The phase space for which at all scales $\gamma_0 < 0.43$, this is the scalar regime.
- **(iii)** The phase space for which γ_0 is dispersed between $[0.43, 0.53]$.

For $n = 0.1$ no dispersion is obtained, the model with $\beta = 0.1$ shows a departure of about 2% from ΛCDM while the model with $\beta = 0.5$ shows a large departure, without dispersion though. Actually some very small dispersion can be obtained at $z \sim 0.5$ for larger β values.

As a representative interesting case, let us consider the model with $n = 0.4$. For $\beta = 0.1$, the model shows very little dispersion with a departure from ΛCDM of about 1%, see Figure (4.3). So this model is essentially indistinguishable from ΛCDM. For $\beta \geq 0.5$ one obtains for scales larger than $\lambda \geq 5h^{-1}$Mpc $\gamma(z)$ values close to that of ΛCDM with some restricted dispersion, see Figure (4.3). However very interestingly, there is a strong dispersion on smaller scales and a significant gap is found between $1h^{-1}$Mpc and $5h^{-1}$Mpc, this gap increases for increasing β as we can see on Figure (4.3). We have checked that for very large β values, for example $\beta = 50$, the background evolution is like that of ΛCDM while a very large gap is obtained between the functions $\gamma(z)$ for $1h^{-1}$Mpc and $5h^{-1}$Mpc.

4.4 Conclusions

We have derived the equations determining the linear matter perturbations in the standard chameleon model, and studied the effect on the growth factor γ. It was found that for small values of n, the parameter determining the slope of the potential, the growth of the linear perturbations can be significantly larger than in ΛCDM while the background evolution was found to agree with ΛCDM to an accuracy of $1-2\%$ for most interesting cases. This effect is due to the fifth force acting on the growth of matter perturbations on cosmic scales. However, it must be emphasized that gravity constraints force us to have a gravitational coupling of the chameleon field to dark matter only in order to have these ΛCDM deviating effects.

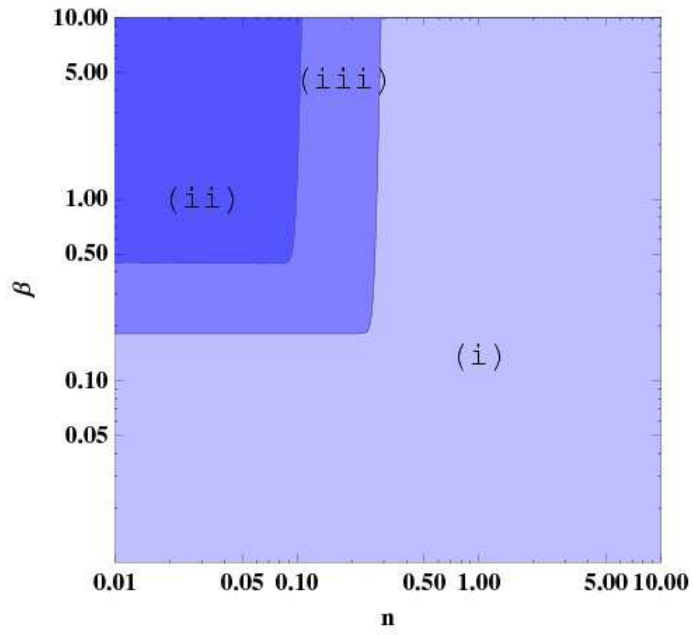

Figure 4.3: We summarized the three regimes for γ_0

If future observations will measure the growth function $\gamma(z,k)$ with high accuracy and find significant deviations from ΛCDM, for which $\gamma \approx 0.55$, is quasi-constant and scale independent, then our model can account for this.

In the full article, to appear, we will investigate the evolution of $\gamma(z,k)$ with several different potentials together with the local bounds.

Chapter 5

Chameleons with a Field-dependent Coupling

5.1 Introduction

Modern cosmological observations strongly suggest that visible matter contributes only a few percent to the total energy budget. The rest is made of dark matter and dark energy. While dark matter is very well motivated within particle physics, dark energy is harder to explain within particle physics models. Scalar fields are natural candidates for dark energy, but the dark energy scalar field should be very light to explain the accelerated expansion. In addition, its coupling to matter should be very small. Alternatively, dark energy (and dark matter) might signal a breakdown of General Relativity on large scales.

In the last three decades, scalar fields have played an important role in both cosmology and particle physics (see e.g. [69, 70] and references therein). The best motivated particle physics candidate for a scalar field is the Higgs boson, part of the standard model of particle physics, which itself has yet to be observed. Even though no scalar fields have ever been observed directly yet, they are a general feature of high energy physics beyond the standard model and are often related to the presence of extra-dimensions. Scalar fields have been postulated as means to explain the early and late time acceleration of the Universe. However, it is almost always the case that such fields interact with matter: either due to a direct Lagrangian coupling or indirectly through a coupling to the Ricci scalar or as the result of quantum loop corrections. Both for inflation in the early universe and for dark energy, such couplings can lead to problems. In inflation, for example, couplings might destroy the flatness of the potential needed to drive a period of inflation. If there are scalar fields which permeate the universe today and have non-zero couplings to matter, then they would induce an additional force in nature. If the scalar field self-interactions are negligible, then the experimental bounds on such a field are very strong: either the couplings to matter are much smaller than gravity, or the scalar fields are very heavy, so that they are short-ranged.

However, a certain class of theories have been proposed, in which the scalar field(s) properties depend on the environment: These are the class of chameleon field theories, proposed by Khoury and Weltman [1], that employed a combination of self-interaction and couplings to matter of the scalar-field to avoid the most restrictive of the current bounds. In the models that they proposed, which from now on will be referred to as the standard chameleon model (SCM), a scalar field couples to matter with gravitational strength, in harmony with general expectations from string theory, whilst, at the same time, remaining relatively light on cosmological scales. They also showed that local gravity constraints were (roughly) satisfied as long as the mass-scale of the potential satisfied $M \lesssim (1mm)^{-1}$. This coincides with the scale associated with the late time acceleration of the universe, and it is surprising that it should come from local gravity experiments. We will, in this paper, show that this result carries over to other classes of

chameleon models in which the coupling becomes field dependent and hence is environment-dependent.

The chameleon with a constant coupling has been subject to many studies [13, 14, 49, 61, 62, 63] to mention some. Most relevant experimental bounds have been calculated for the two fiducial potentials introduced by Khoury and Weltman. There have been very few studies on the different types of couplings [1]. However, it would be important to investigate whether the chameleon mechanism is present in more general classes of models and therefore we will go one step further and generalize the chameleon mechanism to the inverse power law coupling. In doing so the coupling to matter, similar to β in the SCM, becomes dynamical and will for everyday objects typically be much smaller than the matter coupling which is felt by small particles in the vacuum of space. When objects become big (in density and size) in a way defined later we will also have an additional suppression of the fifth-force by a thin-shell effect very similar to what has been found for the SCM. We derive the far field of thin-shell bodies and show that the same effect as found in [10] for the SCM follows: The far field of a thin-shelled body is independent of the composition of the body.

This paper is divided into roughly three parts: in the first section we study the behaviour of the scalar field inside and outside a spherical body. We find that the theory exhibits the chameleon mechanism and find the thin-shell solution. This allows us to make predictions for the chameleon behaviour on earth and in the solar system. In the second section we derive expressions for the chameleon force law between different objects and ranges, which can be succinctly stated by introducing the effective coupling. And in the last section we calculate the bounds on our parameters from the Eöt-Wash experiment, fifth-force searches, post-newtonian corrections and Casimir experiments.

We will show that the model allows for a very large local matter coupling, $|\beta,_{\phi_c}|M_p$, to be compatible with all the available data. This is entirely due to the thin-shell effect. We will also show how non-linear effects ensure that the field value taken by the chameleon far away from a body with a thin-shell is independent of λ, the parameter that describes the strength of the coupling in the Lagrangian.

5.1.1 Notation and conventions

We will always work in units of $c \equiv 1$ and $\hbar \equiv 1$, the metric is given the signature $(-,+,+,+)$ and we will use the convention $M_p \equiv \frac{1}{\sqrt{8\pi G}}$ for the Planck-mass. The frame referring to g will be called the Einstein frame, and the frame referring to $\tilde{g}$ the Jordan frame. When speaking about the chameleon mass $m_\phi^2 \equiv V_{eff,\phi\phi}$ we refer to the mass of oscillations about a

[1] See [11] for a brief note on the power law coupling $\beta(\phi) = \left(\frac{\lambda\phi}{M_p}\right)^n$.

minimum of the effective potential. In looking at the field inside and outside a body the quantities of that body are referred to with a subscript $_c$ and the background with a subscript $_b$. For example the minimum of the effective potential inside a body is denoted by ϕ_c. When speaking about quantities such as $\beta_{,\phi}(\phi_b)$ we will sometimes simply write $\beta_{,\phi_b}$.

5.1.2 The Chameleon Action

The action governing the dynamics a general scalar-tensor theory is given by

$$S = \int dx^4\sqrt{-g}\left[\frac{RM_p^2}{2} - \frac{1}{2}(\partial\phi)^2 - V(\phi) - \mathcal{L}_m(\tilde{g}_{\mu\nu}, \psi_i)\right] \tag{5.1}$$

where g is the determinant of the metric $g_{\mu\nu}$, R is the Ricci-scalar and ψ_i are the different matter fields. The matter fields couple to $\tilde{g}_{\mu\nu}$ which is related to $g_{\mu\nu}$ via a conformal rescaling of the form

$$\tilde{g}_{\mu\nu} = A(\phi)^2 g_{\mu\nu} \tag{5.2}$$

The SCM corresponds to the choice $A(\phi) = e^{\frac{\beta\phi}{M_p}}$ where β is a constant together with $V(\phi) = M^4\left(1 + \frac{M^n}{\phi^n}\right)$. Cosmological and local gravity experiments impose $\frac{\beta\phi}{M_p} \ll 1$ at least since the time of Big Bang Nucleosynthesis (BBN) so that in most applications of this model we can without loss of generality set $A = 1 + \frac{\beta\phi}{M_p}$. This model have been found to be in agreement with experiments even for $\beta \gg 1$ providing a little fine-tuning of the potential no worse than a cosmological constant. This is different from a minimally coupled scalar field for which fifth-force and equivalence principle experiments require a coupling strength much smaller than unity. In this work, we will study an inverse power coupling

$$\log A(\phi) \equiv \beta(\phi) = \left(\lambda\frac{M_\beta}{\phi}\right)^k \tag{5.3}$$

where M_β is a mass-scale and λ a dimensionless parameter. We will refer to this model as a chameleon due to similarities with the SCM, even though we do not know a priori whether this model will produce a chameleon thin-shell suppression effect.

5.1.3 The Chameleon Potential

The most important ingredient in a chameleon field theory is that the effective potential that has a minimum which depends on the local matter density. The simplest type of potential, for our coupling (5.3), having this property is the power law potential

$$V(\phi) = \sigma M^4\left(\frac{\phi}{M}\right)^n \tag{5.4}$$

where M is a mass scale and σ a dimensionless parameter for the case $n = 4$. This potential gives rise to an effective potential, defined below, of the same type as in the SCM. Here M can be any mass-scale, but in order for the chameleon to act as a dark-energy candidate we need $V(\phi_{today}) \sim \Lambda$ together with an equation of state $\omega \approx -1$. It is therefore convenient to set $M = M_{DE} = \Lambda^{\frac{1}{4}}$ and have the cosmological constant as part of the potential. In this case we can think of the potential as a Taylor expansion of a more complicated potential such as $V = M^4 \exp(\phi^n/M^n)$, for $\phi \ll M$.

5.1.4 The Field equation

Variation of the action (5.1) with respect to ϕ yields the field-equation

$$\Box\phi = V_{,\phi} + \sum_i \frac{2}{\sqrt{g}} \frac{\partial \mathcal{L}_m}{\partial g^{(i)}_{\mu\nu}} g^{(i)}_{\mu\nu} \beta^{(i)}_{,\phi} \tag{5.5}$$

where the sum is over the different matter-species and we have allowed for different couplings to different species. Assuming that the matter fields ψ^i do not interact with each other, each energy-momentum tensor (suppressing the (i) for now)

$$\tilde{T}^{\mu\nu} = -\frac{2}{\sqrt{\tilde{g}}} \frac{\partial \mathcal{L}_m}{\partial \tilde{g}_{\mu\nu}} \tag{5.6}$$

is conserved in the Jordan-frame [15]

$$\tilde{\nabla}_\nu \tilde{T}^{\mu\nu} = 0 \tag{5.7}$$

where $\tilde{\nabla}$ is the Levi-Civita connection corresponding to the metric $\tilde{g}$. In the perfect fluid approximation where each matter species behaves as a perfect isentropic fluid with equation of state $\tilde{p} = \omega_i \tilde{\rho}$ we have

$$\tilde{T}^{\mu\nu}\tilde{g}_{\mu\nu} = -\tilde{\rho} + 3\tilde{p} = -\tilde{\rho}(1 - 3\omega_i) \tag{5.8}$$

Going to the Einstein frame we choose, without loss of generality, a FLRW background metric. The energy density ρ in the Einstein-frame is the one that obeys the usual continuity equation $\rho \propto a^{-3(1+\omega_i)}$. Computing the Christoffel-symbol

$$\tilde{\Gamma}^\mu_{\alpha\nu} = \Gamma^\mu_{\alpha\nu} + \frac{d \ln A}{d\phi} \left(\delta^\mu_\alpha \phi_{,\nu} + \delta^\mu_\nu \phi_{,\alpha} - g_{\alpha\nu}\phi^{,\mu}\right) \tag{5.9}$$

and using (5.7) we find that

$$\frac{d}{dt}\left(\rho_i a^{3(1+3\omega_i)}\right) = 0 \tag{5.10}$$

where

$$\rho_i = A_i^{3(1+\omega_i)}(\phi)\tilde{\rho}_i \tag{5.11}$$

is the Einstein-frame density satisfying the usual continuity equation $\dot{\rho_i} + 3H\rho_i = 0$. Using this, the equation of motion in the Einstein-frame is

$$\Box\phi = V_{,\phi} + \sum_i \rho_i(1-3\omega_i)A_{i,\phi}A_i^{(1-3\omega_i)} \tag{5.12}$$

and we see that the dynamics of ϕ is not solely determined by V, but by an effective potential given by

$$V_{\rm eff}(\phi) = V(\phi) + \sum_i \rho_i A_i^{(1-3\omega_i)}(\phi) \tag{5.13}$$

To simplify things we will assume that all the different matter species couple to ϕ with the same $A(\phi)$ and we will only look at non-relativistic matter so $\omega_i \approx 0$ and the field equation becomes $\Box\phi = V_{\rm eff,\phi}$ with

$$V_{\rm eff}(\phi) = V(\phi) + \rho A(\phi) \tag{5.14}$$

Note that since the matter fields couple to $\tilde{g}$ and the geodesics of a test-particle are the geodesics of this metric, $\tilde{\rho}$ is the physical density. But we do not need to be too careful about this since, as we will show, in all practical applications we will have $A(\phi) \approx 1$ and the two densities are essentially the same.

5.1.5 Minima of the effective potential

The minimum of the effective potential is determined by the equation $V_{\rm eff,\phi} = 0$ which gives

$$\phi_{\rm min} = M\left(\frac{\lambda M_\beta}{M}\right)^{\frac{k}{n+k}}\left(\frac{k\rho}{\sigma n M^4}\right)^{\frac{1}{n+k}} \tag{5.15}$$

The chameleon mass at the minimum is given by

$$\begin{aligned} m_\phi^2 \equiv V_{\rm eff,\phi\phi}(\phi_{\rm min}) &= \tfrac{k(n+k)\rho}{\lambda^2 M_\beta^2}\left(\tfrac{\lambda M_\beta}{\phi_{\rm min}}\right)^{k+2} \\ &= M^2 k(n+k)(\sigma n/k)^{\frac{k+2}{n+k}}\left(\tfrac{\rho}{M^4}\right)^{\frac{n-2}{n+k}}\left(\tfrac{\lambda M_\beta}{M}\right)^{\frac{k(n-2)}{n+k}} \end{aligned} \tag{5.16}$$

where we have used that in contrast to the standard chameleon where $m_\phi^2 = V_{,\phi\phi}$ we now have to take in account the contribution from the term $\beta_{,\phi\phi}\,\rho$. But we can ignore the term $\rho\beta^2{}_{,\phi}$ which is valid as long as $\beta(\phi) \ll 1$. From (5.16) we see that the field will be a chameleon for $n > 2$.

5.1.6 An equivalent formulation

We redefine the field by introducing $\chi = \frac{M_\beta}{\phi}M_p$. Then the coupling (for $k = 1$) becomes that of the SCM

$$\beta(\chi) = \left(\frac{\lambda\chi}{M_p}\right)^k \tag{5.17}$$

Our power law potential (5.4) becomes

$$V(\chi) = \sigma M^4 \left(\frac{M_*}{\chi}\right)^n \tag{5.18}$$

where $M_* = \frac{M_\beta M_p}{M}$. When $M_\beta = \frac{M^2}{M_p}$ we have $M_* = M$ and the potential is identical to the Rattra-Peebles potential often used in the SCM. With this choice for M_β, the full action can be written

$$\begin{aligned} S &= \int dx^4\sqrt{-g}\left[\frac{RM_p^2}{2} - \frac{1}{2}\left(\frac{M}{\chi}\right)^4 (\partial\chi)^2 - V(\chi)\right. \\ &- \left.\mathcal{L}_m\left(e^{2\left(\frac{\lambda\chi}{M_p}\right)^k} g_{\mu\nu}, \psi_i\right)\right] \end{aligned} \tag{5.19}$$

and we see that (for $k = 1$) it is only the kinetic terms that distinguish our model from the SCM. The fine-tuning in the coupling sector is removed and we are left with only one fine-tuned mass-scale in the action.

The field equation is given by

$$\begin{aligned} \Box\chi - \tfrac{2}{\chi}(\nabla_\mu\chi)^2 &= \left(\tfrac{\chi}{M}\right)^4 V_{\text{eff},\chi} \\ V_{\text{eff}}(\chi) &= M^4\left(\tfrac{M}{\chi}\right)^n + \rho e^{\left(\frac{\lambda\chi}{M_p}\right)^k} \end{aligned} \tag{5.20}$$

which is significantly more complicated to work with than (5.5) so we will use the original formulation.

5.1.7 The Coupling Scale

In the background today, taking $\lambda = 1$, we have

$$\frac{\phi_b}{M_\beta} \sim \left(\frac{M}{M_\beta}\right)^{\frac{n}{n+k}} \left(\frac{M_{DE}}{M}\right)^{\frac{4}{n+k}}. \tag{5.21}$$

For the model to be in agreement with experiments we must require $\beta(\phi_b) \ll 1$ in the background today. This constrains

$$M_\beta \ll M_{DE}\left(\frac{M}{M_{DE}}\right)^{\frac{n-4}{n}} \tag{5.22}$$

showing the need to fine-tune M_β. We fix M_β by the requirement that the equivalent action (5.19) is of the same form as the SCM when $M = M_{DE} \sim (1mm)^{-1}$. This fixes

$$M_\beta = \frac{M^2}{M_p} \sim H_0 \tag{5.23}$$

This choice also makes sure that the coupling $|\beta_{,\phi_c}|M_p$ of a $\rho_c = 1g/cm^3$ body is of order 1 when $M = M_{DE}$. The term $|\beta_{,\phi}|M_p$ plays the same role in this model as β does in the SCM, but now this factor is dynamical. In the rest of this article we take $M_\beta = H_0$ so that

$$\beta(\phi) = \left(\lambda \frac{H_0}{\phi}\right)^k \tag{5.24}$$

will be our choice for the coupling.

5.2 Spherical Solutions to the field equation

The field equation in a static spherical symmetric metric with weak gravity reads

$$\ddot{\phi} + \frac{2}{r}\dot{\phi} = V_{,\phi} + \rho\beta_{,\phi} \tag{5.25}$$

where we have assumed $\beta(\phi) \ll 1$. We study solutions inside and outside a spherical body of constant density ρ_c (e.g. the earth) in a background of a very low density $\rho_b \ll \rho_c$. We set

$$\rho = \begin{cases} \rho_c \text{ for } r < R \\ \rho_b \text{ for } r > R \end{cases} \tag{5.26}$$

and the boundary conditions

$$\begin{array}{rcl} \left.\frac{d\phi}{dr}\right|_{r=0} & = & 0 \\ \left.\frac{d\phi}{dr}\right|_{r=\infty} & = & 0 \end{array} \tag{5.27}$$

The first condition follows from the spherical symmetry around $r = 0$ and the second one implies that the field converges to the minimum of the effective potential, ϕ_b, in the far-away background. If $m_c R \ll 1$, the chameleon act approximately as a linear scalar field whereas in the case $m_c R \gg 1$ the full non-linearity of the field equation comes into play.

5.2.1 Case 1: The Thick-shell $m_c R \ll 1$

The field to converges to ϕ_b in the background provided it satisfies $\phi(0) \equiv \phi_i \ll \phi_c$ and the approximation $V_{\text{eff},\phi} \approx \beta_{,\phi}\,\rho_c$ is valid inside the body. Since this driving force is relatively small, we approximate $\beta_{,\phi}\rho_c \approx \beta_{,\phi_i}\rho_c$. Solving the field equation is now straightforward and the solution reads

$$\phi \approx \phi_i - \frac{|\beta_{,\phi_i}|\rho_c r^2}{6} \text{ for } 0 < r < R \tag{5.28}$$

where we have used absolute values since $\beta_{,\phi} < 0$. This solution corresponds to the thick-shell solution in the SCM, which is not surprising since the

non-linearities in the field equation are negligible. Outside the body we assume that the linear approximation is valid leading to a Yukawa profile $\phi = \phi_b + \frac{ARe^{-m_b r}}{r}$. Matching the two solutions at $r = R$ leads to

$$A = \frac{|\beta_{,\phi_i}|\rho_c R^2}{3} \tag{5.29}$$

with ϕ_i determined through

$$\phi_i - \frac{|\beta_{,\phi_i}|\rho_c R^2}{2} = \phi_b \tag{5.30}$$

Defining $m_i^2 = \rho_c \beta_{,\phi\phi}(\phi_i)$, the chameleon mass at the centre of the object, this last expression can be rewritten as

$$(m_i R)^2 = 2(k+1)\left(1 - \frac{\phi_b}{\phi_i}\right) \tag{5.31}$$

and the chameleon takes a value at the centre of the body corresponding to a mass $m_i \sim \frac{1}{R}$. This also shows that the approximation used inside the body is valid since the field undergoes a $\frac{\phi(R)-\phi(0)}{\phi(0)} \lesssim \mathcal{O}(1)$ change. The initial value, ϕ_i, can be rewritten in a more compact fashion for $\phi_i \gg \phi_b$ as

$$\phi_i = \phi_c \left(\frac{(m_c R)^2}{2(n+k)}\right)^{\frac{1}{k+2}}. \tag{5.32}$$

If $m_c R$ is really small we have $\phi_i \approx \phi_b$ and the field inside the body is just a small perturbation in the background. To summarize, the solution is

$$\begin{array}{lcll} \phi & = & \phi_i - |\beta_{,\phi_i}|\frac{\rho_c r^2}{6} & \text{for } 0 < r < R \\ \phi & = & \phi_b + \frac{|\beta_{,\phi_i}|}{4\pi}\frac{M_1 e^{-m_b r}}{r} & \text{for } R < r \\ \phi_i & = & \phi_b + \frac{|\beta_{,\phi_i}|\rho_c R^2}{2}. & \end{array} \tag{5.33}$$

The far-away field is proportional to the coupling $\beta_{,\phi}$ evaluated inside the body (or equivalently at the surface), just like for the SCM. Let us mention that two bodies with $m_c R \ll 1$ attract each other with a force

$$F_\phi = 2\beta_{,\phi_i^{(1)}}\,\beta_{,\phi_i^{(2)}}\,M_p^2 \frac{GM_1M_2(1+m_b r)e^{-m_b r}}{r^2}. \tag{5.34}$$

The relative strength to gravity can be read off as $2\beta_{,\phi_i^{(1)}}\,\beta_{,\phi_i^{(2)}}\,M_p^2$ which is maximal for bodies where $\phi_i \approx \phi_b$. If a body increases in size the strength of the fifth-force decreases. In contrast with the SCM, this suppression appears even for bodies without a thin-shell ($m_c R \ll 1$). See fig(5.1) for a plot of a $m_c R \ll 1$ profile compared to the analytical approximation found above.

The approximations used above differs from the true solution by less than $\sim 10\%$ for $m_c R \lesssim 0.01$. Note that outside the body we have assumed that the

Yukawa profile is a good approximation. When $\phi_i \gg \phi_b$ we have $\phi(R) \gg \phi_b$ meaning that the approximation $V_{\text{eff},\phi} \approx m_b^2(\phi - \phi_b)$ is not valid right outside $r = R$. In these cases, the driving term $V_{,\phi}$ can be neglected relative to the friction term, leading to the same $1/r$-profile. This approximation is valid up to the region where $m_b r \sim 1$ or equivalently $\phi \sim \phi_b$ which leads to the Yukawa solution used above. As $m_b R \ll 1$, we can add the exponential factor to the solution outside $r = R$. The numerical results show that the analytical solutions found above match the actual solutions to a good level of accuracy.

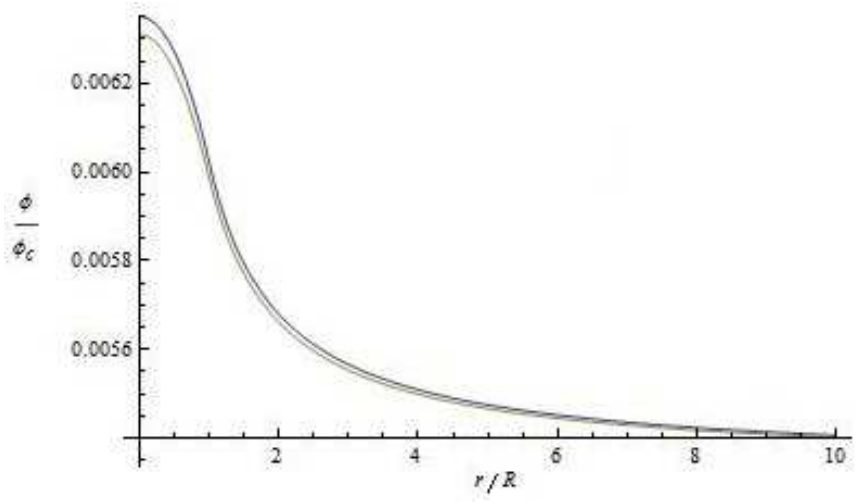

Figure 5.1: Numerical field profile for $n = 10$, $k = 1$ and $m_c R = 10^{-3}$ together with the analytical approximation. The analytical approximation is seen to be a very good match to the actual solution.

5.2.2 Case 2: The Thin-shell $m_c R \gg 1$

When $m_c R \gg 1$ the field decreases very fast inside the body unless it is very close to the minimum, and the field at $r = R$ typically has to be very close to ϕ_c in order to converge to ϕ_b in the background. This is similar to the thin-shell solution in the SCM. Right outside a thin-shelled body the approximation $V_{\text{eff},\phi} \approx V_{,\phi}$ is valid and we must solve

$$\ddot{\phi} + \frac{2}{r}\dot{\phi} \approx n\sigma M^3 \left(\frac{\phi}{M}\right)^{n-1} \quad \text{for } R < r < R^* \tag{5.35}$$

where R^* is the point where the coupling term, $\rho_b \beta_{,\phi}$, becomes relevant again. When $n = 1$ or $n = 2$ we can solve (5.35) as it stands. In these cases the field is not a chameleon. In the general case we will need certain approximations to find a solution.

In Fig. 5.2) we plot a thin-shelled solution for the earth in the cosmological background (density equal to the average cosmological density) and $n = 10$.

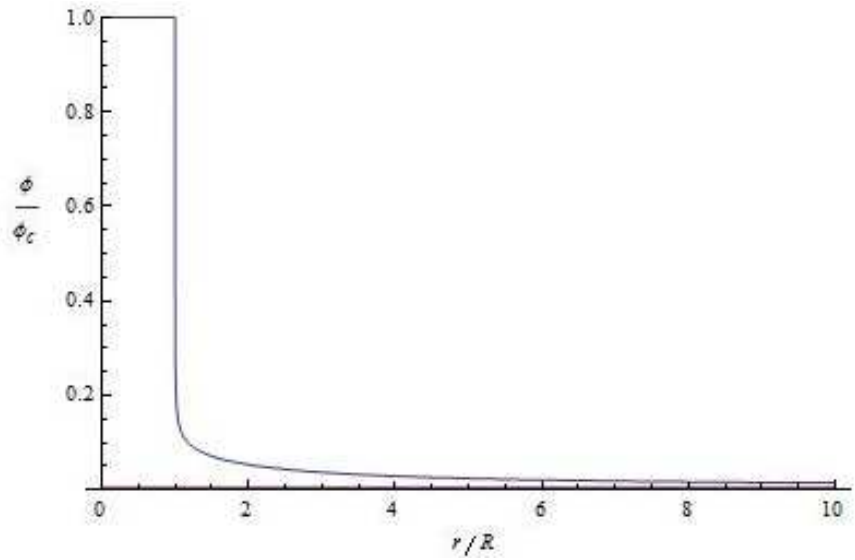

Figure 5.2: The Thin-shell profile for the earth when $n = 10$, $k = 1$ and $m_c R = 10^6$.

Inside the body the field is very close to the minimum and remains there throughout most of the body, except near the surface where the field undergoes a $\mathcal{O}(1)$ change. Linearizing the effective potential around ϕ_c: $V_{\text{eff},\phi} = m_c^2(\phi - \phi_c)$, we can find the solution close to $r = 0$ that matches the initial condition

$$\begin{aligned} &\phi = \phi_c \left(1 - \tau \frac{\sinh(m_c r)}{m_c r}\right) \quad \text{in } 0 < r < R \\ &\tau = \frac{\phi_c - \phi(0)}{\phi_c} \ll 1. \end{aligned} \tag{5.36}$$

The solution is valid as long as the linear term in the Taylor expansion of $V_{\text{eff},\phi}$ dominates over the higher order terms, which gives the condition

$$\begin{aligned} &\left|\frac{\phi - \phi_c}{\phi_c}\right| < \frac{2}{|n-k-3|} \qquad \text{for } n - k - 3 \neq 0 \\ &\left|\frac{\phi - \phi_c}{\phi_c}\right| < \left(\frac{6}{(k+1)(k+2)}\right)^{1/2} \quad \text{for } n - k - 3 = 0. \end{aligned} \tag{5.37}$$

The largest value of $|\phi - \phi_c|$ inside the body occurs at $r = R$ and we will later check that this value satisfies the condition above. Note that, in contrast with the SCM, we do not have an explicit thin-shell solution inside the body. Defining $\delta \equiv \tau \frac{\sinh(m_c R)}{m_c R}$ we have that the field value and derivative at $r = R$

satisfy

$$\begin{aligned} \phi_R &= (1-\delta)\phi_c \\ \dot{\phi}_R &= -\delta m_c \phi_c \end{aligned} \tag{5.38}$$

Outside the body the potential is very steep, so the field drops very quickly and the friction term $\frac{2}{r}\dot{\phi}$ is negligible compared to the driving force $V_{,\phi}$, implying that

$$\ddot{\phi} \approx V_{,\phi} \tag{5.39}$$

To simplify the analysis we define $\psi \equiv \frac{\phi}{\phi_c}$, $x = \frac{r}{R}$ and $\frac{d}{dx} \equiv '$ so that we can write the equations in a dimensionless form as

$$\psi'' = \frac{(m_c R)^2}{n+k}\psi^{n-1} \tag{5.40}$$

which has the solution

$$\begin{aligned} \psi &= \frac{\psi_R}{[1+a(r/R-1)]^{\frac{2}{n-2}}} \\ a &= \frac{m_c R(n-2)}{\sqrt{2n(n+k)}}(1-\delta)^{\frac{n}{2}-1}. \end{aligned} \tag{5.41}$$

Matching to the solution for $r < R$, using (5.38), we find

$$\frac{\delta^2}{(1-\delta)^n} = \frac{2}{n(n+k)} \tag{5.42}$$

which determines δ [2]. Numerically we find $\delta \approx 0.086$ for $(n = 10, k = 1)$ and $\delta \approx 0.200$ for $(n = 4, k = 1)$ for all $m_c R > 10$ in very good agreement with the formula above. If we now go back and put this value for δ into (5.37) we see that the linear approximation is valid for all reasonable values of (n, k). As an example, take $n = 4$, upon using (5.42) we find $\delta^2 \approx \frac{1}{2(k+4)}$ which in (5.37) gives the condition

$$1 < \frac{8(k+4)}{(k-1)^2} \quad \rightarrow \quad k < 12. \tag{5.43}$$

As field rolls down along the potential, it reaches a point $r = R^*$ where the driving force satisfies [3]

$$F_{driving} = \frac{(m_c R)^2}{n+k}\psi^{n-1} < 1 \tag{5.44}$$

[2] This may seems strange since when δ is determined the full solution in $0 < r < \infty$ is known (at least from a numerical point of view), but this is derived without considering the behaviour at large r yet. What this result really states is that the solution that converges to ϕ_b in the background will have to corresponds to an initial value of order δ at $r = R$. This is confirmed by the numerics.

[3] In the case where $m_b R \gg 1$ the field will have settled at the minimum before this happens. But the far field, $\phi - \phi_b$, in these cases will be exponentially suppressed and is not very relevant.

and from here on the dynamics of ψ are determined by the friction term which we have neglected. The field equation reads

$$\psi'' + \frac{2}{x}\psi' \approx 0 \text{ for } R^* < r \tag{5.45}$$

with the solution

$$\psi \approx \psi_b + \frac{AR^*}{r} \text{ for } R^* < r \tag{5.46}$$

for some A. This solution is valid until we reach the region where the driving force has to be taken into account again. This is the case when $m_b r \sim 1$ or equivalently $\psi \sim \psi_b$ and alters the solution by adding a Yukawa exponential $e^{-m_b r}$ to the $1/r$ term. Again since $m_b R^* < 1$ we can incorporate this by adding this term to (5.46) as

$$\psi \approx \psi_b + \frac{AR^* e^{-m_b(r-R^*)}}{r} \text{ for } R^* < r < \infty \tag{5.47}$$

The matching of (5.41) and (5.47) at $r = R^*$, defining $\Delta = \frac{R^*-R}{R}$, implies the identifications

$$\begin{aligned} \psi_b + A &= \frac{\psi_R}{(1+a\Delta)^{\frac{2}{n-2}}} \\ A &= \frac{\psi_R}{(1+a\Delta)^{\frac{2}{n-2}}} \frac{(1+\Delta)a}{1+a\Delta} \frac{2}{n-2} \end{aligned} \tag{5.48}$$

When $m_b R < 1$ we have $\psi(R^*) = A + \psi_b \gg \psi_b$ which leads to

$$\begin{aligned} \Delta &= \frac{2}{n-4} \\ AR^* &= \frac{BR}{(m_c R)^{\frac{2}{n-2}}} = \frac{BR}{(m_b R)^{\frac{2}{n-2}}}\psi_b \\ B &= \left(\frac{n(n+k)}{2}\right)^{\frac{1}{n-2}} \left(\frac{n-2}{n-4}\right)^{\frac{n-4}{n-2}} \end{aligned} \tag{5.49}$$

where we have used $a\Delta \gg 1$ in order to simplify the solutions. This derivation does not apply for $n = 4$. A similar derivation shows that (5.49) is valid for $n = 4$ when one takes the limit $n \to 4$ in the expression for B. Let us summarize the solutions we have found:

$$\begin{aligned} \phi &\approx \phi_c && \text{for} && r < R \\ \phi &\approx \frac{(1-\delta)\phi_c}{(1+a(r/R-1))^{\frac{2}{n-2}}} && \text{for} && R < r < R^* \\ \phi &\approx \phi_b + \frac{\phi_c B}{(m_c R)^{\frac{2}{n-2}}} \frac{R e^{-m_b(r-R^*)}}{r} && \text{for} && R^* < r. \end{aligned} \tag{5.50}$$

Defining the effective coupling in the thin-shell case via

$$\phi = \phi_b + \frac{\beta_{\text{eff}}}{4\pi M_p} \frac{M_1 e^{-m_b r}}{r} \qquad \text{for} \qquad R^* < r \tag{5.51}$$

we have that

$$\beta_{\text{eff}} = \frac{4\pi M_p}{M_1} (MR)^{\frac{n-4}{n-2}} \left(\frac{n-2}{n-4}\right)^{\frac{n-4}{n-2}} (2\sigma)^{-\frac{1}{n-2}}$$

which is independent of the parameters λ and k describing the coupling $\beta(\phi)$. To compare these results to the SCM, we define a thin-shell factor via

$$\beta_{\text{eff}} = |\beta_{,\phi_c}| M_p \frac{3\Delta R}{R} \tag{5.52}$$

and we find

$$\frac{\Delta R}{R} = \frac{\phi_c}{|\beta_{,\phi_c}| \rho_c R^2} \frac{B}{(m_c R)^{\frac{2}{n-2}}} \sim \frac{1}{(m_c R)^{\frac{2(n-1)}{n-2}}} \tag{5.53}$$

This factor determines how much of the mass of the body contributes to the fifth-force. As $m_c R \gg 1$, we have $\frac{\Delta R}{R} \ll 1$ and thus $\beta_{\text{eff}} \ll |\beta_{,\phi_c}| M_p$. If we extend this definition and set $\beta_{\text{eff}} = |\beta_{,\phi_i}| M_p$ when $m_c R \ll 1$ then (5.51) is valid for all bodies. See fig. (5.3) for a plot of the effective coupling as a function of the radius of the body. We note that for the special case when $n = 4$ the far-away field can be written as

$$\phi \approx \phi_b + \frac{\phi_b}{m_b} \frac{e^{-m_b r}}{r} \qquad \text{for} \qquad R^* < r \tag{5.54}$$

which is completely independent of the parameters ρ_c and R describing the body, and depends only on the background. Likewise β_{eff} only depends on the mass of the body. This is also in agreement with the SCM.

In the extreme case where $m_c R \to \infty$ we find that the field outside the body is the same as if there were no body present. This is the thin-shell effect in a nutshell: Increasing the coupling to infinity leads to a completely shielded body. In [10] the same effect was found: the exterior profile of a thin-shelled body is independent of the composition of the body (and the coupling). It depends only on the radii R, and the potential parameters: The stronger the coupling the more effective this mechanism.

Note that for really large $m_c R$ we have a very large gradient at $r = R$ that may cause problems in laboratory experiments using a very small separation between objects (like Casimir, Eöt-Wash etc.). We are mostly interested in the cases where the field has a large range outside planets (like the earth) together with a thin-shell $m_c R \gg 1$. From $\frac{m_c}{m_b} = \left(\frac{\phi_c}{\phi_b}\right)^{\frac{n-2}{2}} = \left(\frac{\rho_c}{\rho_b}\right)^{\frac{n-2}{2(n+k)}}$ we see that having $k \ll n$ and $n \gg 1$ gives the largest ratio $\frac{m_c}{m_b} \sim \left(\frac{\rho_c}{\rho_b}\right)^{\frac{1}{2}}$. For the case of the earth $\rho_c \sim 1 g/cm^3$ in a background of the average solar system density $\rho_b \sim 10^{-24} g/cm^3$ we find $\frac{m_c}{m_b} \sim 10^{12}$. And it is possible that the field has a range as large (not taking experimental bounds into account)

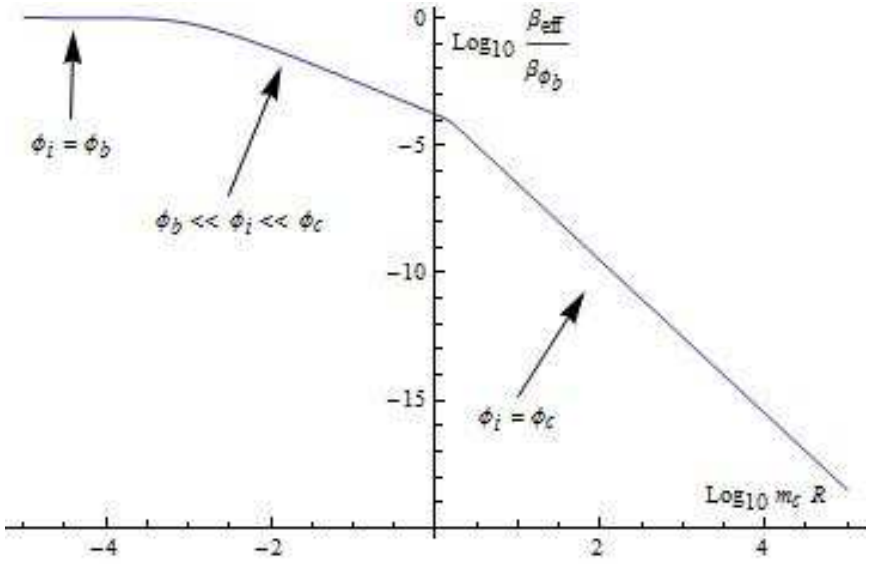

Figure 5.3: The effective coupling (for $n = 4$) for a sphere with constant density. When the body is very small the field inside the body is the same as the background, ϕ_b, leading to a big coupling. Then as the radius gets bigger the field inside the body starts moving away from the background and the coupling decreases. Finally when we reach $m_c R > 1$, the field inside the body settles at ϕ_c, but develops a thin-shell and the coupling starts to decrease like $1/R^3$.

as $m_b^{-1} \sim 10^{15} m \sim 10^4 Au$ and at the same time having a thin-shelled earth $m_c R \gg 1$. This is the same as found in the SCM [1].

In the SCM, the coupling is easily identified as the parameter that multiplies ϕ in the matter-Lagrangian. Here we have a coupling that varies from place to place and is in general given by β_{eff} defined above. For a test particle in a region where $\phi \sim \phi_0$ the coupling is $|\beta_{,\phi}(\phi_0)| M_p$. The coupling becomes smaller in high-density environments and the highest value is achieved when $\phi = \phi_b$, the cosmological field-value. The coupling on earth is much smaller than the cosmological coupling. One can say that the chameleon effect in this model is twofold: First the coupling decreases as the environment gets denser and secondly for big objects only a thin-shell near the surface contributes to the fifth force.

This scenario presents a way of having a strong cosmological coupling, which vanishes close to a thin-shelled object, and it may be possible to have a more rapid growth of matter perturbations on cosmological scales than GR predicts even though the chameleon force is undetectable on earth as found in many other dark energy models ($f(R)$, SCM, etc).

In fig. (5.4) we plot the $n = k = 1$ thin-shelled solution. In order to produce the field profiles for highly thin-shelled objects ($m_c R > 100$) we could not start the numerical simulation at $r = 0$ since the initial value is typically too close to ϕ_c. Upon using the relation (5.38) and (5.42) we were able to start the simulation at $r = R$ allowing us to produce the field profiles shown here.

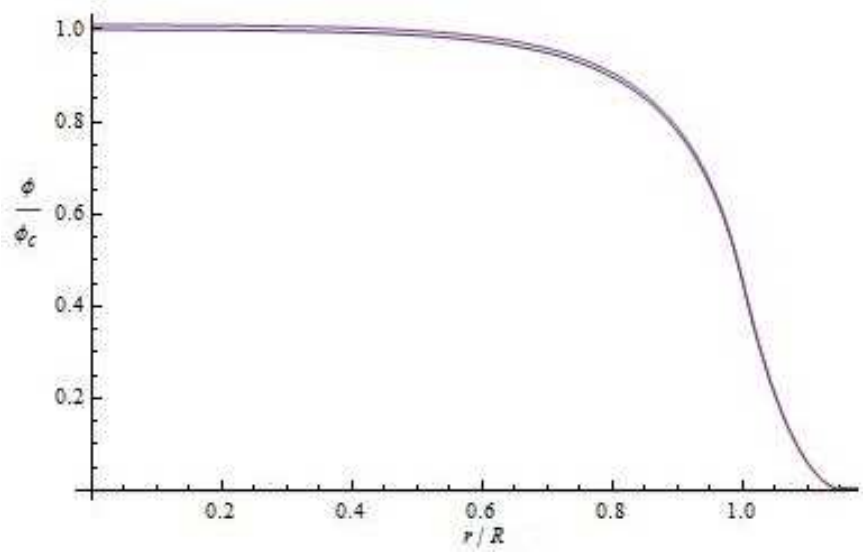

Figure 5.4: Thin-shell profile for $n = k = 1$ (the non-chameleon case). The background has a larger mass than the body and the field reaches the minimum within a thin-shell outside the surface.

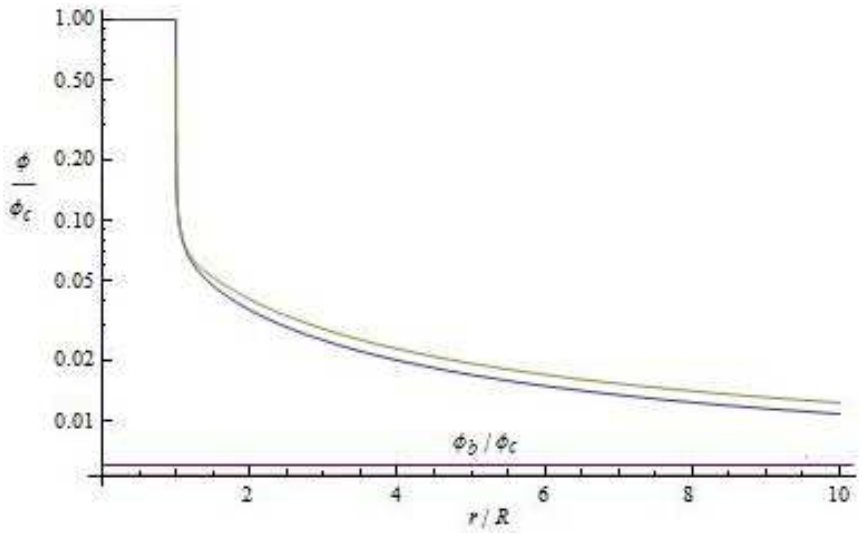

Figure 5.5: The Thin-shell profile for the earth when $n = 10$, $k = 1$ and $m_c R = 10^6$ together with the analytical approximation. The horizontal line shows ϕ_b, the minimum in the background. The error between the numerical solution and the analytical approximation was less than 10% in the whole range.

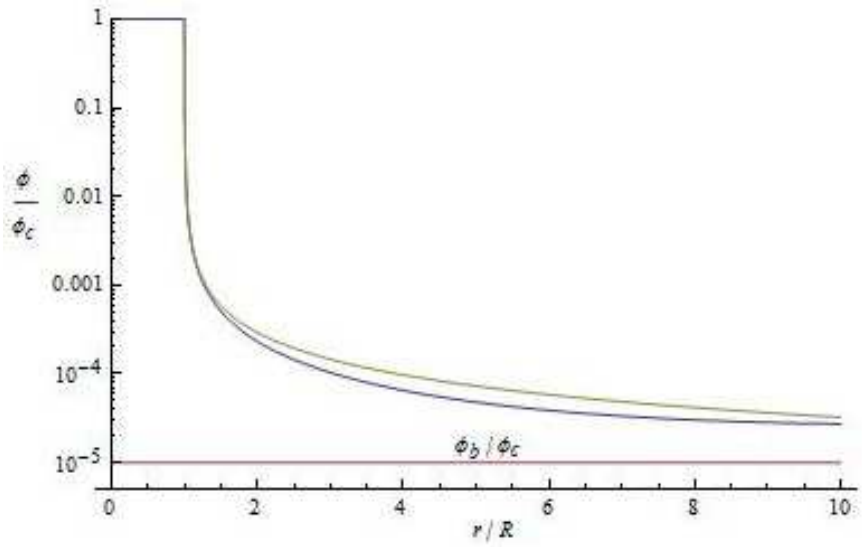

Figure 5.6: The Thin-shell profile for the earth when $n = 4$, $k = 1$ and $m_c R = 10^4$ together with the analytical approximation. The horizontal line shows ϕ_b, the minimum in the background. The error between the numerical solution and the analytical approximation was less than 10% in the whole range.

5.3 The Chameleon force

The geodesic equation in the Jordan Frame reads

$$\ddot{x}^\mu + \tilde{\Gamma}^\mu_{\alpha\nu}\dot{x}^\alpha\dot{x}^\nu = 0 \tag{5.55}$$

Using (5.9) this can be rewritten in terms of the Einstein frame connection Γ and ϕ as

$$\ddot{x}^\mu + \Gamma^\mu_{\alpha\nu}\dot{x}^\alpha\dot{x}^\nu = -\beta_{,\phi}\,\phi^{,\mu} - 2\beta_{,\phi}\,\dot{x}^\nu\dot{x}^\mu\phi_{,\nu} \tag{5.56}$$

In the non-relativistic limit the last term can be neglected and the chameleon force on a test particle is given by

$$\frac{\vec{F_\phi}}{m} = -\beta_{,\phi}\,\vec{\nabla}\phi \tag{5.57}$$

This is attractive since both $\beta_{,\phi}$ and $\frac{d\phi}{dr}$ are negative outside a spherical object as shown in the section about solutions to the field-equations.

5.3.1 Chameleonic Force between two parallel plates

We consider the force between two identical parallel plates of radius R_p whose surfaces are separated by a distance $d \ll R_p$ and the system is in a laboratory vacuum [10], [12]. In practice the 'vacuum' will have a non zero pressure corresponding to a very low, but non-zero density ρ_b. Because the plates are very close to each other we can treat the plates as infinite flat slabs and take plate 1 to occupy the region $x < -d/2$ and plate 2 to occupy the region $x > d/2$.

We use a subscript s when talking about the quantities defined at the surface of the plates, subscript b in the background and subscript c inside the plates. For example the field-value at the surface of the plates is referred to as ϕ_s, $V(\phi_c) \equiv V_c$ and so on. Also a subscript 0 is used to refer to the quantities where $\dot{\phi} = 0$ between the plates, because of the symmetry this is at the point $x = 0$. Finally we assume that the chameleon mass satisfies $m_c R_p \gg 1$ so that the true non-linear nature of the chameleon comes into play. With the conditions stated at the beginning,we have that ϕ obeys

$$\frac{d^2\phi}{dx^2} = V_{,\phi} + \beta_{,\phi}\,\rho_b \tag{5.58}$$

between the plates, and

$$\frac{d^2\phi}{dx^2} = V_{,\phi} + \beta_{,\phi}\,\rho_c \tag{5.59}$$

inside either plate. Integrating the equations above yields

$$\begin{aligned} \dot{\phi}^2 &= 2(V(\phi) - V_0 + \rho_b(\beta(\phi) - \beta_0)) \quad \text{for } -d/2 < x < d/2 \\ \dot{\phi}^2 &= 2(V(\phi) - V_c + \rho_c(\beta(\phi) - \beta_c)) \quad \text{for } x^2 > d^2/4. \end{aligned} \tag{5.60}$$

Where we have used that deep inside the plate we have $\phi(\pm\infty) \approx \phi_c$ and $\frac{d\phi(\pm\infty)}{dx} = 0$. Matching at $x = \pm d/2$ we find that the coupling at the surface is given by

$$\beta_s \equiv \beta(\phi_s) = \frac{V_c - V_0 + \rho_c\beta_c - \rho_b\beta_0}{\rho_c - \rho_b}. \tag{5.61}$$

If the second plate were removed $\phi_0 = \phi_b$, and the coupling at the surface (β_{s0}) would be given by (5.61), with $\phi_0 \to \phi_b$. The perturbation, $\delta\beta_s = \beta_s - \beta_{s0}$, in $\beta(\phi_s)$ due to the presence of the other plate is therefore

$$\delta\beta_s = \frac{V_b - V_0 + \rho_b(\beta_b - \beta_0)}{\rho_c} \tag{5.62}$$

where we have used $\rho_c \gg \rho_b$. Since $m_c R_p \gg 1$ the perturbation deep inside the bodies are suppressed exponentially. Using (1) we find that the attractive force on one plate due to the presence of the other is given by

$$\frac{F_\phi}{A} = \rho_c \int_{d/2}^{d/2+D} dx \frac{d\delta\beta(\phi)}{dx} \approx -\rho_c\delta\beta_s \tag{5.63}$$

which, using (5.61), gives

$$\frac{F_\phi}{A} = V_0 - V_b + \rho_b(\beta_0 - \beta_b) = V_{eff}(\phi_0) - V_{eff}(\phi_b) \tag{5.64}$$

We have to calculate the field value ϕ_0 midway between the plates. This is done by integrating (5.60) over the region $-d/2 < x < 0$, using that $\frac{d\phi}{dx} < 0$ in this region when taking the square root. This gives the equation for ϕ_0

$$\int_{\phi_0}^{\phi_s} \frac{d\phi}{\sqrt{V(\phi) - V_0 + \rho_b(\beta(\phi) - \beta_0)}} = \frac{d}{\sqrt{2}} \tag{5.65}$$

This is a general expression, and can be used for any coupling and potential. Specialising to our case where $\beta(\phi) = \left(\lambda\frac{H_0}{\phi}\right)^k$ and $V(\phi) = \sigma M^4 \left(\frac{\phi}{M}\right)^n$, we change variables to $z = \phi/\phi_0$ and define $y_s = \phi_s/\phi_0$ giving

$$\int_1^{y_s} \frac{dz}{\sqrt{z^n - 1 + \frac{n}{k}\left(\frac{\phi_b}{\phi_0}\right)^{n+k}(z^{-k} - 1)}} = Md\sqrt{\frac{\sigma}{2}}\left(\frac{\phi_0}{M}\right)^{\frac{n-2}{2}}. \tag{5.66}$$

Here we can have several cases.

Case 1: $\phi_0 \approx \phi_c$

This case corresponds to very small separations $m_b d \ll 1$. We set $\phi_0 = \phi_c(1-\delta)$ and rewrite the right hand side of (5.66) as $\frac{m_c d}{\sqrt{2n(n+k)}}$. The integral can now be evaluated

$$\int_1^{1+\delta} \frac{dz}{\sqrt{n(z-1)}} = \frac{2\sqrt{\delta}}{\sqrt{n}} \tag{5.67}$$

resulting in

$$\delta = \frac{(m_c d)^2}{8(n+k)}. \tag{5.68}$$

This case only applies when the separation d is much smaller than the thickness of the plates t, since we have assumed $m_c t \gg 1$. The chameleon force becomes

$$\frac{F_\phi}{A} = V_c \left[1 - \frac{n(m_c d)^2}{8(n+k)}\right] \tag{5.69}$$

Case 2: $\phi_0 \approx \phi_b$

This corresponds to the case where the field drops all the way down to the minimum in between the bodies. Since this case corresponds to $m_b R > m_b d > 1$ the force is exponentially suppressed. We put $\phi_0 = \phi_b(1+\delta)$ where we assume $\delta \ll 1$. This allows us to approximate $\left(\frac{\phi_b}{\phi_0}\right)^{n+k} \approx 1-(n+k)\delta$ and since $\phi_c \gg \phi_b$ we can take $y_s \to \infty$ and the integral (5.66) can be written

$$\int_1^\infty \frac{dz}{\sqrt{z^n - 1 + \frac{n}{k}\left(1-(n+k)\delta\right)\left(\frac{1}{z^k}-1\right)}} = \frac{m_b d}{\sqrt{2n(n+k)}}. \tag{5.70}$$

In the limit $\delta \to 0$ the left hand side diverges. Upon using a power series expansion of the integrand near $z = 1$

$$z^n - 1 + \frac{n}{k}\left(\frac{\phi_b}{\phi_0}\right)^{n+k}(z^{-k}-1) \approx n(n+k) \times \tag{5.71}$$

$$\left[\delta(z-1) + \tfrac{1}{2}\left(1-\delta(k+1)\right)(z-1)^2 + \frac{(n-k-3)-a\delta}{6}(z-1)^3 + ...\right] \tag{5.72}$$

where $a = (k+1)(k+2)$, we see that the second term is the divergent part when $\delta = 0$. This term dominates in the region $1+2\delta < z < \left|\frac{n-k}{n-k-3}\right|$ and for $0 < \delta \ll 1$ provide the dominating contribution to the integral. We can therefore approximate the integral by

$$\int_{1+2\delta}^{\left|\frac{n-k}{n-k-3}\right|} \frac{dz}{\sqrt{\frac{n(n+k)}{2}}(z-1)} \approx \frac{\sqrt{2}\ln(2\delta)}{\sqrt{n(n+k)}} \tag{5.73}$$

This gives

$$\delta \approx \frac{1}{2} e^{-\frac{m_b d}{2}} \tag{5.74}$$

and shows that the chameleon force

$$\frac{F_\phi}{A} \approx V_{eff,\phi\phi}(\phi_b)\frac{(\phi_0-\phi_b)^2}{2} \approx \frac{m_b^2\phi_b^2}{8} e^{-m_b d} \tag{5.75}$$

is indeed exponentially suppressed by the factor $m_b d \gg 1$.

Case 3: $\phi_c \gg \phi_0 \gg \phi_b$

In this last case we can neglect the third term in the square root of (5.66) and also take $y_s \to \infty$. This enables us to evaluate the integral analytically

$$\int_1^\infty \frac{dz}{\sqrt{z^n - 1}} = \frac{\Gamma\left(\frac{1}{2}\right)\Gamma\left(\frac{1}{2} - \frac{1}{n}\right)}{|\Gamma\left(-\frac{1}{n}\right)|}. \tag{5.76}$$

The Γ-function satisfies $\Gamma(\epsilon) \approx \frac{1}{\epsilon} - \gamma_E$ for $\epsilon \ll 1$ with $\gamma_E \approx 0.577$ being the Euler-Gamma constant. This gives

$$S_n \equiv \frac{\Gamma\left(\frac{1}{2}\right)\Gamma\left(\frac{1}{2} - \frac{1}{n}\right)}{|\Gamma\left(-\frac{1}{n}\right)|} \approx \frac{\pi}{n} \text{ for large } n. \tag{5.77}$$

We can now find an explicit expression for ϕ_0

$$\phi_0 = M\left(\sqrt{\frac{2}{\sigma}}\frac{S_n}{Md}\right)^{\frac{2}{n-2}} \tag{5.78}$$

and the chameleon force

$$\frac{F_\phi}{A} \approx \sigma M^4 \left(\sqrt{\frac{2}{\sigma}}\frac{S_n}{Md}\right)^{\frac{2n}{n-2}}. \tag{5.79}$$

We see that the force follows a power law where the drop-off is faster than $1/d^2$ as found in the similar situation in the SCM. The Casimir-force falls off as $1/d^4$ making Casimir experiments (with large plate-separations) a good way of constraining the chameleon. See fig(5.7) for a plot of the dependence of the force (or more accurately, the pressure F_ϕ/A) as a function of the distance between the plates.

5.3.2 Chameleon Force between two spherical thin-shelled bodies

We consider the force between two bodies, with thin-shells, that are separated by a distance $r \gg R_1, R_2$. Given than $d \gg R_1, R_2$ we can consider the monopole moment of the field emanating from the two bodies only.

We denote by ϕ_1 (ϕ_2) the field outside body one (two) when body two (one) is absent. To a good accuracy we have $\phi_1 \approx \phi_{c1}$ the minimum inside body 1. In between the bodies, we can superimpose the far-away fields from the two bodies. As the distance is large, the perturbation $\delta\phi_1$ in the field inside the body two due to the presence of body one satisfies $\delta\phi_1 \ll \phi_2$. The combined field close to the surface of body two is approximately given by $\phi_2 + \delta\phi_1$.

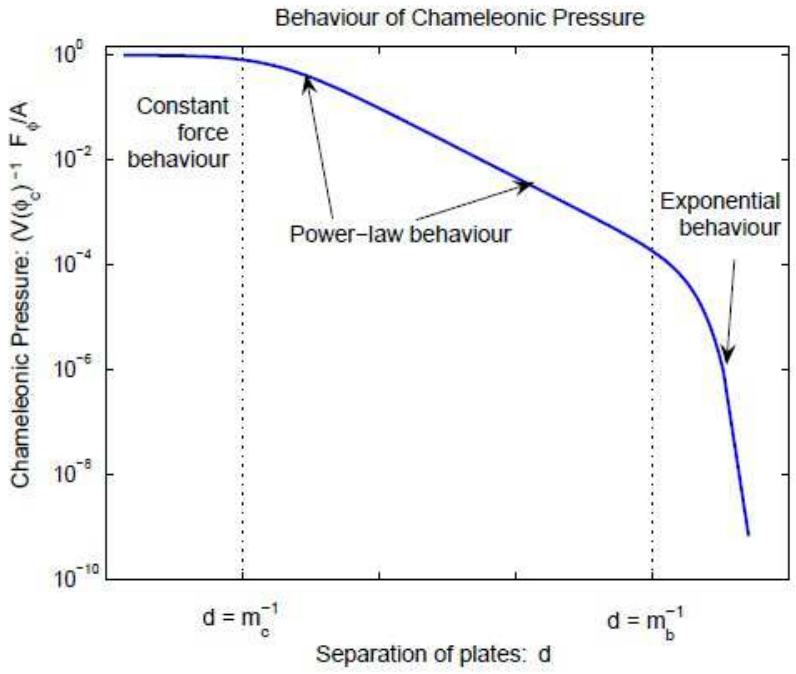

Figure 5.7: General behaviour of the chameleon pressure $\frac{F_\phi}{A}$ as a function of the plate separation d.

Using the geodesic equation, $dF_\phi = -\beta_{,\phi}\,\nabla\phi dm$, we have that the total force on body two due to body one is

$$F_\phi \approx -\beta_{,\phi_{c2}} \int_{\text{body two}} \nabla\delta\phi_1 dm \tag{5.80}$$

Next we have that the perturbation $\delta\phi_1$ is given by the far field of body one evaluated at body two

$$\delta\phi_1 = \frac{\beta_{\text{eff1}}}{4\pi M_p}\frac{M_1 e^{-m_b r}}{r} \tag{5.81}$$

Because of the big mass of the chameleon inside body two, the perturbation created by body one is attenuated , and ,as in the SCM, only a thin-shell close to the surface contributes to the force. We model this by setting

$$F_\phi = 2\beta_{\text{eff1}}\beta_{,\phi_{c2}}\, M_p \left(\frac{\Delta R}{R}\right)_2 \frac{GM_1M_2(1+m_b r)e^{-m_b r}}{r^2} \tag{5.82}$$

where $\left(\frac{\Delta R}{R}\right)_2$ models the effect of this thin-shell.

Likewise the force on body one due to body two is given by the same expression with $1 \to 2$. Up to a $\mathcal{O}(1)$ factor we have

$$\frac{\Delta R}{R} = \frac{\phi_c}{\rho_c|\beta_{,\phi_c}|R^2(m_c R)^{\frac{2}{n-2}}} \sim \frac{1}{(m_c R)^{2+\frac{2}{n-2}}} \tag{5.83}$$

which is also $\frac{\beta_{\text{eff}}}{|\beta_{,\phi_c}|M_p}$. The force between two thin-shelled objects is then, up to a $\mathcal{O}(1)$ constant, given by

$$F_\phi = 2\beta_{\text{eff1}}\beta_{\text{eff2}}\frac{GM_1M_2(1+m_b r)e^{-m_b r}}{r^2} \tag{5.84}$$

In the thick-shell case ($m_c R \ll 1$) the whole body contributes to the force [4] giving

$$F_\phi = 2(\beta^{(1)}_{,\phi_i}\, M_p)(\beta^{(2)}_{,\phi_i}\, M_p)\frac{GM_1M_2(1+m_b r)e^{-m_b r}}{r} \tag{5.85}$$

5.4 Bounds on the parameters

We will constrain the parameters λ and M (or σ) by looking at the effect our model has on local gravity experiments. The experiments considered here bound the chameleon coupling in different regions. The Eöt-Wash experiment (and other fifth-force searches) are usually the best way to get good bounds when $|\beta_{,\phi_c}|M_p \sim 1$. Casimir type experiments are often the best way to bound the highly coupled, $|\beta_{,\phi_c}|M_p \gg 1$, region. Finally the PPN and BBN bounds constrain the extremely high coupled region which are invisible to the Casimir type experiments due to the extremely short range of the chameleon.

[4] The field-equation is quasi-linear in this case and the superposition principle holds.

5.4.1 PPN bounds

For experiments using the deflection of light by large bodies, the only Post-Newtonian Parameter (PPN) at play is the Eddington-parameter γ. The Eddington-parameter is defined in the Jordan-frame by $\tilde{g}_{ij} = (1 - 2\gamma\tilde{\Psi})\delta_{ij}$ when $\tilde{g}_{00} = -1 - 2\tilde{\Psi}$ [67]. Transforming to the Einstein-frame we find

$$\gamma = \frac{\Psi_E - \beta(\phi)}{\Psi_E + \beta(\phi)} \approx 1 - \frac{2\beta(\phi)}{\Psi_E} \tag{5.86}$$

The back reaction on the gravitational potential from the chameleon is in most interesting cases negligible, and since $\beta(\phi) \ll 1$ the Jordan-frame and Einstein-frame potential are the same. The best bounds on this parameter comes from the Cassini-experiment [21] and reads $|\gamma - 1| < 2.3 \cdot 10^{-5}$. The gravitational potential for the sun is $\Psi_{sun} = 10^{-6}$ and the field near the surface of the sun satisfies $\phi \approx \phi_c$ giving us the bounds shown in Fig. (5.8). This experiment only restricts the parameters in which $|\beta_{,\phi_c}|M_p \gg 1$.

5.4.2 BBN bounds

Since our chameleon couples to matter via the conformal transformation (5.2), the masses of the standard model particles have a ϕ-dependence of the form $m = m_0 \exp\beta(\phi)$. Bounds on particle masses restrict a variation of this type to be below the 10% level since Big-Bang Nucleosynthesis (BBN). Since in our model $\dot{\phi} < 0$, $\beta(\phi)$ is an increasing function of time so we must require

$$\beta(\phi_{today}) \lesssim 0.1 \text{ and } \beta(\phi_{BBN}) \lesssim 0.1 \tag{5.87}$$

The last condition is satisfied as long as the chameleon has settled at the minimum before the time of BBN. The condition today translates into the bound

$$\lambda \lesssim 10^{30} \left(\frac{M}{M_{DE}}\right)^{\frac{n-4}{n}} \text{ for } n \neq 4 \tag{5.88}$$

$$\lambda \lesssim 10^{30}\sigma^{-\frac{1}{4}} \text{ for } n = 4 \tag{5.89}$$

The k dependence is weak, and we have that this is satisfied as long as the PPN bound above is satisfied.

5.4.3 Eöt-Wash bounds

The University of Washington's Eöt-Wash experiment [66] is designed to search for deviations from the $1/r^2$ drop-off of Newton's law. The experiment uses a rotating torsion balance to measure the torque on a pendulum. The torque on the pendulum is induced by an attractor which rotates with a frequency ω. The attractor has 42 equally spaced holes, or missing masses,

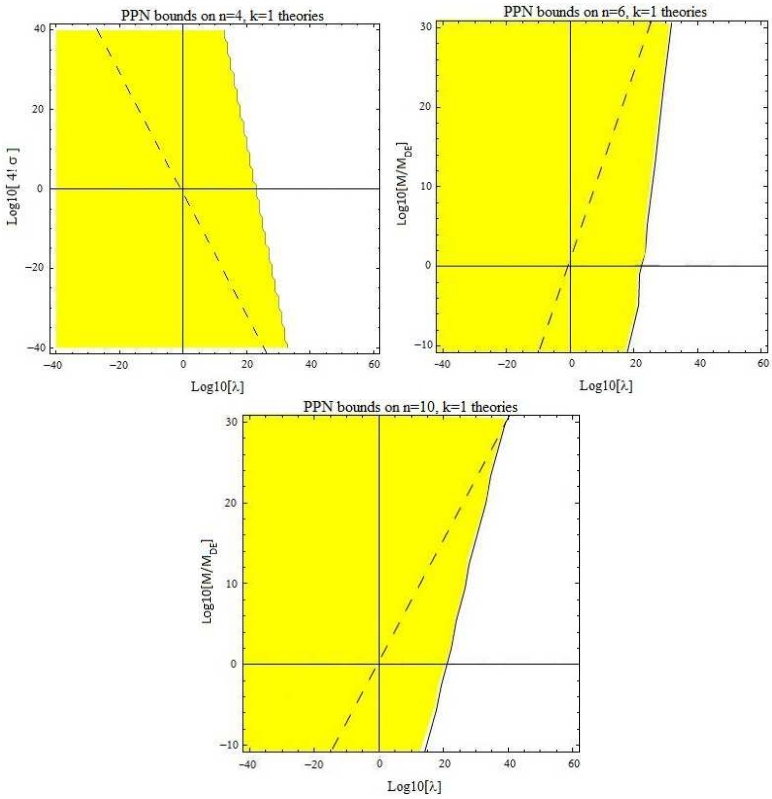

Figure 5.8: PPN constraints on chameleon theories coming from experimental bounds on the Eddington-parameter in light-deflection experiments. The shaded area shows the regions of parameter space that are allowed by the current data. The solid horizontal black lines indicate the cases where M and σ take 'natural values'. The solid vertical lines show when $M_\beta = H_0$. The dashed-black line indicates when $|\beta,_{\phi_c}|M_p = 1$ for $\rho_c = \mathcal{O}(1g/cm^3)$. The amount of allowed parameter space increases with n.

bored into it. As a result, any torque on the pendulum, which is produced by the attractor, will have a characteristic frequency which is some integer multiple of 21ω. This characteristic frequency allows any torque due to background forces to be identified. The attractor is manufactured so that, if gravity drops off as $1/r^2$, the torque on the pendulum vanishes. The experiment has been running with different separations between the pendulum and attractor. The experiment has been running for typically $55\mu m = d$. Both the attractor and the pendulum are made out of molybdenum with a density of about $\rho_c = 10g/cm^3$ and are $t = 0.997mm$ thick. Electrostatic forces are shielded by placing a $d_{shield} = 10\mu m$ thick, uniform BeCu sheet between the attractor and the pendulum. The density of this sheet is $\rho_{shield} = 8.4g/cm^3$. As discussed in [10] the role played by this sheet is crucial when testing for chameleon fields in the strong coupling regime. If the coupling is strong enough, the sheet will itself develop a thin-shell. When this occurs the effect of the sheet is not only to shield electrostatic forces, but also to block any chameleon force originating from the attractor. Following the analogy of our model with the SCM this effect is given by an extra suppression of $e^{-m_{shield}d_{shield}}$. And, in effect, this will make a larger part of the parameter space allowed in the strong coupled case, and will not affect the experiment when $|\beta,_{\phi_c}|M_p \sim 1$. The force per unit area between the attractor and pendulum plates due to a scalar field with matter coupling λ and constant mass m, where $1/m \ll 0.997mm$ is given by (9.30)

$$\frac{F_\phi}{A} = \alpha \frac{G\rho_c^2 e^{-md}}{2m^2} \tag{5.90}$$

where $\alpha = 8\pi\lambda^2$ and d is the separation of the two plates. The strongest bound on α coming from the Eöt-Wash experiment is $\alpha < 2.5 \cdot 10^{-3}$ for $1/m = 0.4 - 0.8mm$ which constrains $\lambda < 10^{-2}$.

When the pendulum and attractor have thin-shells the force is given by the expressions derived in section III. The vacuum used in these experiments has a pressure of $p = 10^{-6}$ Torr which means that the chameleon mass in the background, m_b, is non-zero and for the largest couplings we will have a $e^{-m_b d}$ suppression. Hence the experiment cannot detect a very strongly coupled chameleon. The BeCu sheet produces a force on the pendulum. As the sheet is uniform, this resulting force leads to no detectable torque. If neither the pendulum nor the attractor have thin-shells then we must have $m_b d \ll 1$ and the chameleon force is just $2\beta,^2_{\phi_i} M_p^2$ times the gravitational one. Since this force drops off as $1/r^2$, it will be undetectable in this experiment. In this case, however, λ is constrained by other experiments such as those that look for Yukawa forces with larger ranges as discussed below.

Even though we have formulae for the force, we have used numerics to calculate the bounds. This gives more accuracy in the regions where our approximate formulae do not apply. As mentioned above, the rotation of

one plate relative to the other induces a torque. This can be shown to be given by [12]

$$\tau_\phi = \frac{d\mathcal{V}_\phi}{d\theta} \approx e^{-m_{\text{shield}} d_{\text{shield}}} a_T \int_d^\infty \frac{F_\phi(x)}{A} dx \tag{5.91}$$

where $a_T = \frac{dA}{d\theta}$ is a constant that depends on the experimental setup. For the 2006 Eöt-Wash experiment this constant is $a_T = 3 \cdot 10^{-3} m^2$. The bounds derived from the experiment can also be expressed in terms of this torque as $\tau_\phi(d = 55\mu m) < 0.87 \cdot 10^{-17}\text{Nm}$, which we used to compute the bounds numerically. We also compared the numerical results and the analytical expression in the regions where they both apply. Our results are shown in fig. (5.9). In these plots the shaded region is allowed by the current bounds.

When $n = 4$, we can see that a natural value of σ is ruled out for $\lambda = 1$. As n becomes larger than 10, the case $\lambda \sim 1$ and $M \sim M_{DE}$ becomes allowed.

The area of allowed parameter space grows with increasing n. Indeed when the potential is steeper, the mass of the chameleon increases, and the thin-shell effect is present for a larger part of the parameter space.

The setup and the behaviour of a chameleon in the experiment is more thoroughly explained in [12].

5.4.4 Fifth-force searches

In the Irvine-experiment [40] the inverse-square distance dependence of the Newtonian gravitational force law was tested. One experiment used a torsion balance consisting of a 60-cm-long copper bar suspended at its midpoint by a tungsten wire, to compare the torque produced by copper masses 105 cm from the balance axis with the torque produced by a copper mass 5 cm from the side of the balance bar, near its end. The produced torques due to the masses at 105 cm and 5 cm have been measured. Letting $R_{Measured}$ be the measured ratio of the two torques and R_{Newton} the Newtonian prediction it was found that

$$\left| \frac{R_{Measured}}{R_{Newton}} - 1 \right| = (1.2 \pm 7) \cdot 10^{-4} \tag{5.92}$$

If the walls of the vacuum chamber do not have thin-shells the field inside the chamber, as discussed below (5.31), settles at a value where $m_{\text{chamber}} \sim R_{\text{chamber}}^{-1}$ and R_{chamber} being the size of the chamber. The experiment here bounds

$$2\beta_{,\phi_i^{(1)}} \beta_{,\phi_i^{(2)}} M_p^2 \lesssim 10^{-3} \tag{5.93}$$

with ϕ_i determined by (5.30). The vacuum chamber used was held at a pressure $p = 3 \cdot 10^{-8}\text{torr}$ which corresponds to a background density $4.6 \cdot$

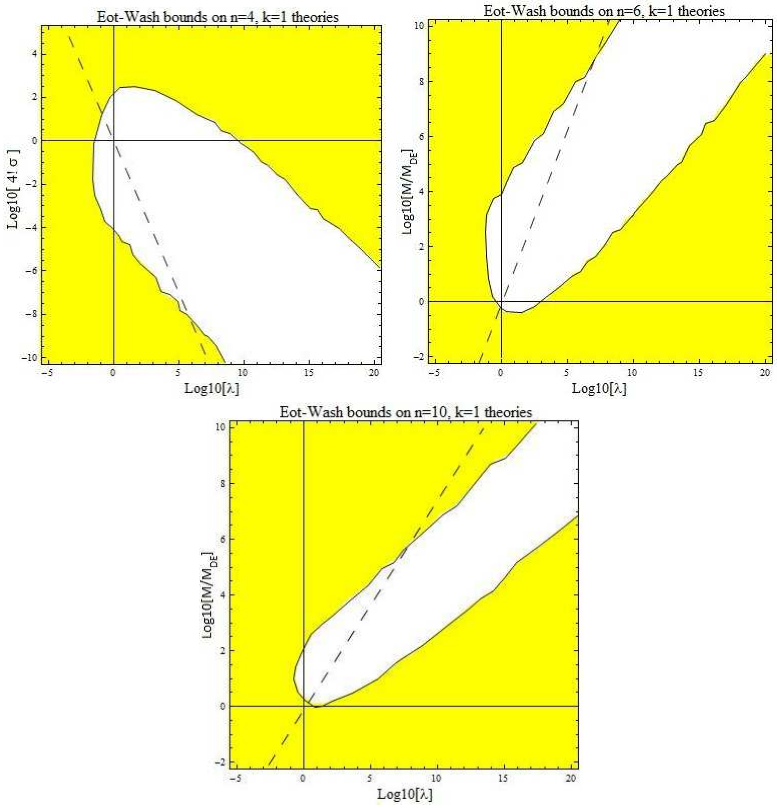

Figure 5.9: Constraints on chameleon theories coming from Eöt-Wash bounds on deviations from Newton's law. The shaded area shows the regions of parameter space that are allowed by the current data. The solid horizontal black lines indicate the cases where M and σ take 'natural values'. The solid vertical lines show when $M_\beta = H_0$. The dashed-black line indicates when $|\beta_{,\phi_c}|M_p = 1$ for $\rho_c = \mathcal{O}(1g/cm^3)$. The amount of allowed parameter space increases with n.

$10^{-14}g/cm^3$ (at $T = 300K$). When the walls of the chamber and therefore the test-masses have thin-shells the chameleon sits at the minimum of its effective potential inside the chamber. The chameleon mass $m_{chamber}$ will for $m_{\rm test}R_{test} \sim 1$ typically be much less than the inverse size of the chamber and the bounds becomes

$$2\beta_{\rm eff1}\beta_{\rm eff2} \lesssim 10^{-3} \tag{5.94}$$

with $\beta_{\rm eff}$ is the thin-shell effective coupling given by (5.52). For the highly coupled cases $m_{\rm chamber}R_{chamber} \gg 1$ there will be an extra $e^{-m_{\rm chamber}d}$ suppression of the torque where d is the separation of the test-masses. This experiment provides the best bounds for the chameleon in the linear regime since the more accurate Eöt-Wash experiment is, by design, unable to detect the linear chameleon ($F_\phi \propto 1/r^2$). See fig. (5.10) for the resulting bounds.

5.4.5 Casimir bounds

Casimir force experiments provide an excellent way of bounding chameleon field parameters when the scalar field is strongly coupled to matter. Casimir force experiments measure the force per unit area between two test masses separated by a distance d. It is generally the case that d is small compared to the curvature of the surface of the two bodies and so the test masses can be modeled, to a good approximation, as flat plates and the results derived in section III apply. The Casimir force between two parallel plates is:

$$\frac{F_{Casimir}}{A} = \frac{\pi^2}{240d^4} \tag{5.95}$$

Even though the most accurate measurements of the Casimir force have been made using one sphere and one slab as the test bodies, this setup has a more complicated geometry and will not be discussed in this paper. We will focus on the experiments which use two flat slabs as test bodies.

In all cases, apart from $n = 4$ and $m_c d \gg 1$, the chameleon force per area grows more slowly than d^4 as $d \to 0$. When $n = 4$ and $m_c d \gg 1$, $m_b d \ll 1$ we have $F/A \propto d^{-4}$. It follows that the larger the separation, d, the better Casimir force searches constrain chameleon theories. Additionally, these tests provide the best bounds when the test masses do have thin-shells as this results in a strongly d dependent chameleon force.

Note that if the background chameleon mass is large enough that $m_b d \gg 1$ then F/A is suppressed by a factor $e^{-m_b d}$. This shows that the experiments cannot detect the strongest coupled chameleons. For these extreme cases the post-newtonian corrections (and BBN bounds) constrain these theories. See [13] for a detailed analysis of the Casimir force in the SCM.

To date, the most accurate measurements of the Casimir force over separations $d = 0.16 - 1.2\mu m$ have been made by Decca et al. in a series of three

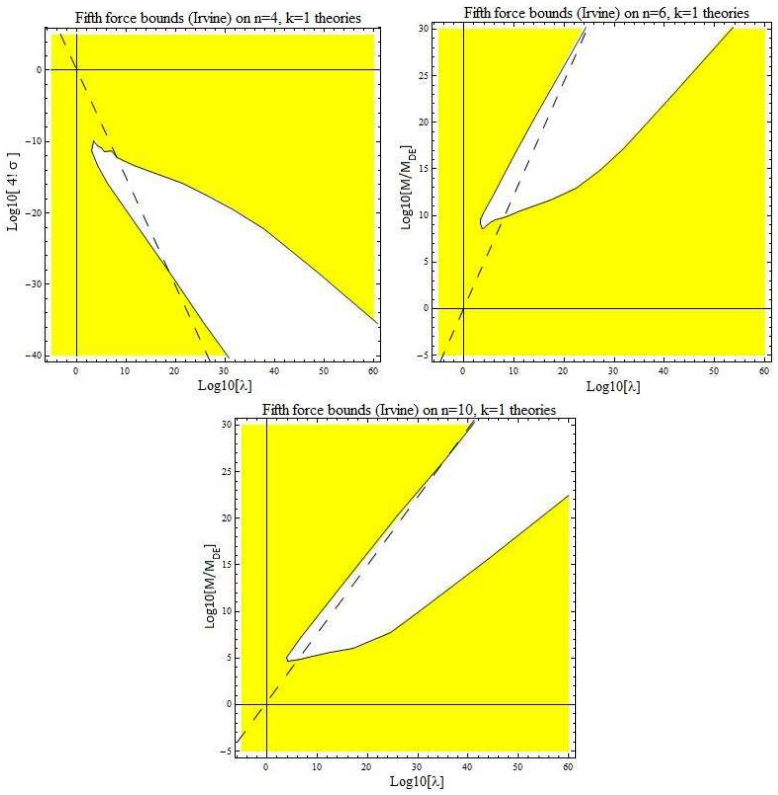

Figure 5.10: Constraints on chameleon theories coming from experimental fifth-force searches (the Irvine-experiment). The shaded area shows the regions of parameter space that are allowed by the current data. The solid horizontal black lines indicate the cases where M and σ take 'natural values'. The solid vertical lines show when $M_\beta = H_0$. The dashed-black line indicates when $|\beta_{,\phi_c}|M_p = 1$ for $\rho_c = \mathcal{O}(1g/cm^3)$.

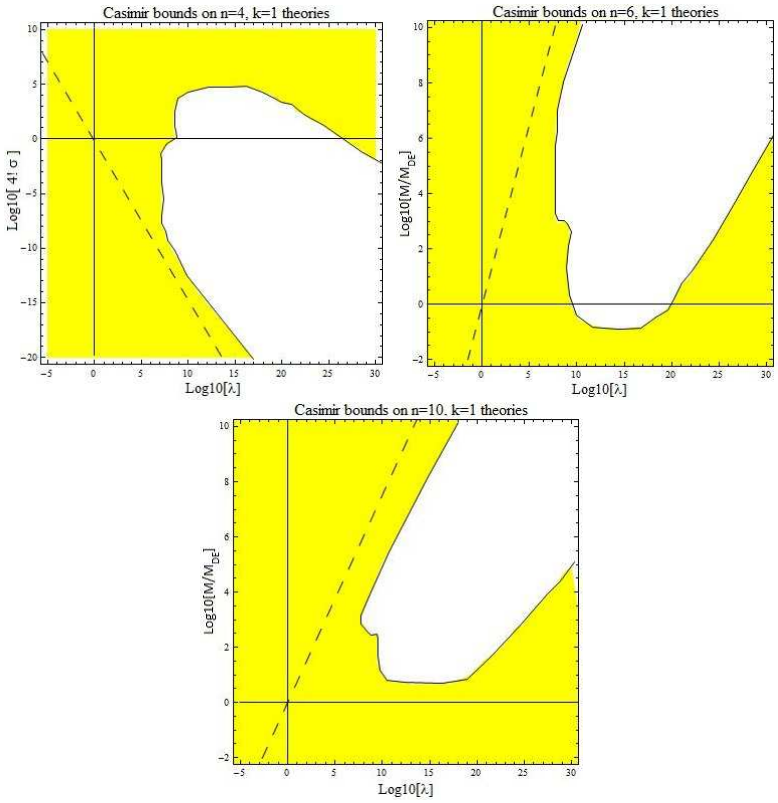

Figure 5.11: Constraints on chameleon theories coming from experimental searches for the Casimir force. The shaded area shows the regions of parameter space that are allowed by the current data. The solid horizontal black lines indicate the cases where M and σ take 'natural values'. The solid vertical lines show when $M_\beta = H_0$. The dashed-black line indicates when $|\beta,_{\phi_c}|M_p = 1$ for $\rho_c = \mathcal{O}(1g/cm^3)$. The amount of allowed parameter space increases with n.

experiments taking place between 2003 and 2007 [71, 72, 73]. We define $P = \frac{F}{A}$ to be the total measured pressure between two parallel plates. Using their most recent experiment, described in Ref. [73], Decca et al. found the following 95% confidence intervals on $\Delta P = P - P_{casimir}$: at $d = 162nm$, $|P| < 21.2mPa$, at $d = 400nm$, $|P| < 0.69mPa$ and at $d = 746nm$, $|P| < 0.35mPa$. The resulting bounds are shown in fig(5.11). The area of allowed parameter space is seen to grow with n and k: The thin-shell condition $m_c R \gg 1$ is more easily satisfied in this case.

5.4.6 Combined bounds

The chameleon theories considered in this work have a four-dimensional parameter space, spanned either by M and λ ($n > 4$), or by σ and λ ($n = 4$).

We combine the constraints found in sections above to bound the values of λ and M (or σ) for different n and k. We plotted the constraints for $n = 4, 6, 10$ and $k = 1$ in Fig. fig. (5.12). In these figures we have included all the bounds coming from the Eöt-Wash experiment, as well as those coming from Casimir force searches. We also include the bounds (labeled Irvine) coming from another search for Yukawa forces. The BBN constraints are weaker than the PPN constraints and are not shown here. In general, the larger n (and k) is, the larger the region of allowed parameter space. This is because, in a fixed density background, the chameleon mass, m_c, scales as $M^{-\frac{(n-4)(2+k)}{n+k}}\sigma^{\frac{2+k}{n+k}}$ and so m_c increases with n and k since the exponents are monotonous functions of n, k. The larger m_c is, in a given background, the stronger the chameleon mechanism, and a stronger chameleon mechanism tends to lead to looser constraints. The chameleon mechanism also becomes stronger in the limits $M \to 0$ or $\sigma \to \infty$, and all of the constraints are more easily satisfied in these limits. The interesting region of the parameter space is when $M \sim M_{DE}$ and $\lambda \sim 1$. We have chosen to show as much of the parameter space as possible and also include the cases $M = M_p$ (which corresponds to $\log_{10}(M/M_{DE}) = 30$) and $M_\beta = M_p$ (which corresponds to $\log_{10}\lambda = 60$). When λ is very small, the chameleon mechanism is so weak that, in all cases, the chameleon behaves like a standard (non-chameleon) scalar field and the bounds depends solely on the value of $|\beta_{,\phi_b}|M_p$. It is clear that $\lambda \gg 1$ (which implies $|\beta_{,\phi_c}|M_p \gg 1$) is very much allowed for a large class of chameleon theories. This is in agreement with what was found for the SCM in [10].

5.5 Conclusions

We have studied a scalar-tensor theory with an field dependent coupling (assumed to be of the form of an inverse power-law) and a power-law potential.

Our main result is that this theory exhibits the thin-shell mechanism found in the original chameleon theory [1]. Thus, the theory presented is a chameleon field theory. As we have shown, many of the familiar properties of the standard chameleon model carry over to this new setup.

If we look at the bounds computed here we see that the natural values $M = M_{DE}$ for $n \neq 4$ or $\sigma = \frac{1}{4!}$ for $n = 4$ together with $\lambda \sim 1$ are ruled out by the Eöt-Wash experiment for $n \lesssim 10$, but are allowed for a slightly lower M. We also have shown that there exist a large region in parameter space which is allowed by experiments and in which the coupling to matter in a high density environment: $|\beta_{,\phi_c}|M_p \gg 1$. These results are equivalent to what was found in the SCM, and is due to the thin-shell effect.

Assuming that the scalar field plays the role of dark energy, we need to fine-tune the mass-scale in the coupling sector, namely we have to demand that $M_\beta \sim H_0$. It should be noted that even though this mass scale has

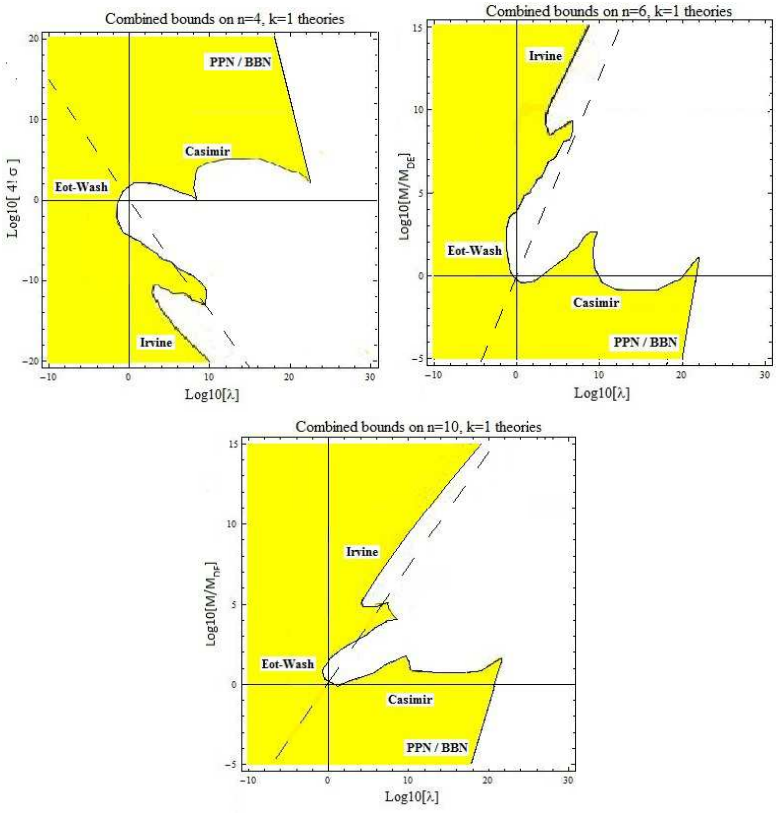

Figure 5.12: Combined constraints on chameleon theories. The shaded area shows the regions of parameter space that are allowed by the current data. The solid horizontal black lines indicate the cases where M and σ take 'natural values'. The solid vertical lines show when $M_\beta = H_0$. The dashed-black line indicates when $|\beta_{,\phi_c}|M_p = 1$ for $\rho_c = \mathcal{O}(1g/cm^3)$. The amount of allowed parameter space increases with n.

an unnatural small value it is not strictly this scale which determines the coupling strength to gravity: It is given together with the local field value ϕ_0 as $|\beta_{,\phi_0}|M_p$ which can be of order unity or larger. If we redefine the field by $\chi = \frac{H_0}{\phi} M_p$ then this fine-tuning is removed and the resulting action has only one fine-tuned mass-scale. Thus the models proposed here are fine-tuned in the same manner as the SCM.

In cosmology the field is well behaved and can act as a dark-energy field causing the late time acceleration of the universe in the same manner as the SCM. The evolution of the density parameters when the field is slow rolling along the attractor is very close to that of ΛCDM.

Chapter 6

The Powerlaw Coupling

6.1 Introduction

In the previous chapter we considered the inverse powerlaw coupling, $\beta(\phi) = \left(\frac{\lambda H_0}{\phi}\right)^m$ with $m > 0$. We focused on this case since the powerlaw coupling (6.2) had already been given a treatment in [11]. We begin by considering their approach.

6.2 The Thin-shell approach

The thin-shell solution in the SCM consist of having $\phi \approx \phi_c$ in $0 < r < R_r$ and letting the field grow only in the thin-shell $R_r < r < R$. Since the field grows in this shell the approximation

$$V_{\text{eff},\phi} \approx \rho\beta_{,\phi} \tag{6.1}$$

is valid in the thin-shell. The approach in [11] was to find solution in this shell and match them to the solution in $0 < r < R_r$ and $r > R$. By performing this matching one finds that this is not possible for $m > 2$. This show that there is no explicit 'geometrical' thin-shell inside the body as found by solving the field-equation in the SCM. But this does not mean that there do not exists a chameleon mechanism in these models. We will show the existence of a chameleon mechanism, which is completely analogous to the SCM and the models considered in the previous chapter. Thus, $m > 1$ theories are indeed chameleon field theories apposed to what was claimed in [11]. It should be noted that they were only interested in $\mathcal{O}(1)$ values for λ, and for $m > 1$ theories we generally need to tune $\lambda \gg 1$ to have a viable model.

The results in this article convinced us that there was no thin-shell effects in the powerlaw couplings, we therefore started to look at the inverse powerlaw coupling. It was only after the completion of the previous section we had time to go back and check the results in this article.

6.3 The powerlaw coupling

We consider the scalar-tensor theory (5.1) with the powerlaw coupling

$$\beta(\phi) = \left(\frac{\lambda\phi}{M_p}\right)^m \quad m > 1 \tag{6.2}$$

and the Ratra-Peebles potential

$$V(\phi) = M^4 \left(\frac{M}{\phi}\right)^n \tag{6.3}$$

The field equation, in a static spherical symmetric metric, is given by

$$\frac{d^2\phi}{dr^2} + \frac{2}{r}\frac{d\phi}{dr} = V_{,\phi} + \rho\beta_{,\phi}\, e^{\beta(\phi)} \tag{6.4}$$

Experimental bounds (e.g. BBN bounds) requires $\beta(\phi) \ll 1$ and we can safely put $e^{\beta(\phi)} = 1$ when solving the field equation.

6.3.1 Minimum of the effective potential

From $V_{,\phi} + \rho\beta_{,\phi} = 0$ we find

$$\phi_{\min} = \left(\frac{m\rho}{nM^4}\left(\frac{\lambda M}{M_p}\right)^m\right)^{-\frac{1}{m+n}} M \tag{6.5}$$

The ratio between the minimum, ϕ_c, inside a body of density ρ_c, and the minimum in the background ϕ_b (where $\rho = \rho_b$) is given by

$$\frac{\phi_b}{\phi_c} = \left(\frac{\rho_c}{\rho_b}\right)^{\frac{1}{m+n}} \tag{6.6}$$

The chameleon mass of small oscillations around the minimum value, $m^2_{min} = V_{\text{eff},\phi\phi}(\phi_{min})$ is

$$\begin{aligned} m^2_{\min} &= m(m+n)\frac{\rho\lambda^2}{M_p^2}\left(\frac{\lambda\phi_{min}}{M_p}\right)^{m-2} \\ &= m(m+n)\left(\frac{n}{m}\right)^{\frac{m-2}{m+n}}\left(\frac{\rho}{M^4}\right)^{\frac{n+2}{m+n}}\left(\frac{\lambda M}{M_p}\right)^{\frac{m(n+2)}{m+n}} M^2 \end{aligned} \tag{6.7}$$

6.3.2 Spherical solutions to the field-equation

We will look at solutions inside and outside a spherical body of constant density ρ_c (e.g. the earth) in a background of a very low density $\rho_b \ll \rho_c$. That is we set

$$\rho = \begin{cases} \rho_c \text{ for } r < R \\ \rho_b \text{ for } r > R \end{cases} \tag{6.8}$$

together with the usual boundary conditions

$$\begin{aligned} \left.\frac{d\phi}{dr}\right|_{r=0} &= 0 \\ \left.\frac{d\phi}{dr}\right|_{r=\infty} &= 0 \\ \phi(r\to\infty) &= \phi_b \end{aligned} \tag{6.9}$$

The thick-shell: $\phi_i \gg \phi_c$

In this regime the field equation will be quasi-linear and we can approximate $V_{\text{eff},\phi} \approx \rho_c \beta_{,\phi_i}$ inside the body[1]. The solution reads

$$\phi = \phi_i + \frac{\rho_c \beta_{,\phi_i} r^2}{6} \quad \text{for} \quad 0 < r < R \tag{6.10}$$

Outside the body the linear approximation, $V_{\text{eff},\phi} = m_b^2(\phi - \phi_b)$, is valid and the solution that converges to ϕ_b in the far background is given by

$$\phi = \phi_b - \frac{ARe^{-m_b r}}{r} \tag{6.11}$$

Matching at $r = R$, assuming $m_b R \ll 1$, we find

$$AR = \frac{M_1 \beta_{,\phi_i}}{4\pi} \tag{6.12}$$

$$\phi_i + \frac{\rho_c \beta_{,\phi_i} R^2}{2} = \phi_b \tag{6.13}$$

where M_1 is the mass of the body. The field-profile outside the body can then be written

$$\phi = \phi_b - \frac{\beta_{,\phi_i}}{4\pi} \frac{M_1 e^{-m_b r}}{r} \tag{6.14}$$

The thin-shell: $\phi_i \approx \phi_c$

When the field starts out close to the minimum, we can linearize the effective potential around ϕ_c: $V_{\text{eff},\phi} = m_c^2(\phi - \phi_c)$. The solution that satisfy the boundary conditions is

$$\phi = \phi_c + \delta\phi_c \frac{\sinh(m_c r)}{m_c r} \tag{6.15}$$

$$\delta = \frac{\phi_i - \phi_c}{\phi_c} \ll 1 \tag{6.16}$$

We start by assuming that this solution is valid all the way to $r = R$. By matching to the solution in $r > R$ given by (6.11) we find

$$A = (\phi_b - \phi_c)\left(1 + \frac{\tanh(m_c R)}{m_c R}\right) \tag{6.17}$$

$$\delta = \frac{\phi_b - \phi_c}{\phi_c \cosh(m_c R)} \tag{6.18}$$

[1]Note that this solution is only strictly when $m_c R \ll 1$ in such as way that the source term $\rho_c \beta_{,\phi_i} < \phi_i$. There do exist some intermediate regime between thick-shells and thin-shells, but we will not consider this here since the main point is to show the existence of a chameleon mechanism.

where we have assumed $m_b R < 1$ since we are interested in a long-ranged chameleon. A generalization of this result to $1 \lesssim m_b R$ is easily found by using the same procedure as above. The assumption $\phi_i \approx \phi_c$ which is equivalent to $\delta \ll 1$ is seen by the above formula to require $m_c R \gg 1$ since $\frac{\phi_b}{\phi_c} = \left(\frac{\rho_c}{\rho_b}\right)^{\frac{1}{n+m}} \gg 1$. With this result we have

$$A \approx \phi_b - \phi_c \tag{6.19}$$

and the profile outside the body can be written

$$\phi = \phi_b - \frac{\beta_{,\phi_c}}{4\pi} \frac{3(\phi_b - \phi_c)}{\rho_c \beta_{,\phi_c} R^2} \frac{M_1 e^{-m_b r}}{r} \tag{6.20}$$

Defining the thin-shell factor

$$\frac{\Delta R}{R} = \frac{(\phi_b - \phi_c)}{\rho_c \beta_{,\phi_c} R^2} \approx \frac{\phi_b}{\phi_c} \frac{(m+n)}{(m_c R)^2} \tag{6.21}$$

the effective coupling, defined through $\phi = \phi_b - \frac{\beta_{\rm eff}}{4\pi M_p} \frac{M e^{-m_b r}}{r}$, is given by

$$\beta_{\rm eff} = \beta_{,\phi_c} M_p \frac{3\Delta R}{R} \tag{6.22}$$

and when $\frac{\Delta R}{R} \ll 1$ the effective coupling will be suppressed. The thin-shell condition $\frac{\Delta R}{R} \ll 1$ is satisfied whenever $(m_c R)^2 \gg (m+n)\frac{\phi_b}{\phi_c} = (m+n)\left(\frac{\rho_c}{\rho_b}\right)^{\frac{1}{m+n}}$. This clearly shows the existence of a chameleon mechanism, if our assumptions can be shown to be valid.

To validate the derivation above we need to show that the solution (6.15) is valid all the way to $r = R$. The Taylor expansion of the effective potential is given by the series

$$V_{{\rm eff},\phi} = m_c^2(\phi - \phi_c) + V_{{\rm eff},\phi\phi\phi}|_{\phi=\phi_c} \frac{(\phi - \phi_c)^2}{2} + ... \tag{6.23}$$

We have only used the linear term, and this is valid as long as the linear term dominates over the higher order terms. Since ϕ is increasing inside the body we need only show that this is true at $r = R$. This condition becomes

$$\left|\frac{\phi - \phi_c}{\phi_c}\right| \ll \left|\frac{2}{n - m - 3}\right| \tag{6.24}$$

for[2] $n - m - 3 \neq 0$. From

$$\frac{\phi(R) - \phi_c}{\phi_c} = \frac{\phi_b - \phi_c}{\phi_c} \frac{\tanh(m_c R)}{m_c R} \approx \frac{\phi_b}{\phi_c} \frac{1}{m_c R} \tag{6.25}$$

[2]The reason this condition diverges for $n = m + 3$ is because the second term in the Taylor expansion vanishes. The same analysis using the next order term gives a similar equation with another $\mathcal{O}(1)$ term on the r.h.s.

where we have used $\tanh(x) \approx 1$ for large x and $\phi_b \gg \phi_c$. The condition (6.24) can be written

$$\frac{\phi_b}{\phi_c}\frac{1}{m_c R} \ll \frac{2}{(n-m-3)} \tag{6.26}$$

And we see that when (dropping any $\mathcal{O}(1)$ factors)

$$m_c R \gg \frac{\phi_b}{\phi_c} = \left(\frac{\rho_c}{\rho_b}\right)^{\frac{1}{n+m}} \tag{6.27}$$

the solution (6.15) will indeed by valid all the way to $r = R$.

6.3.3 The Chameleon force

Lets consider two thick-shelled bodies separated by a distance $r \gg R_1, R_2$ where R_1 (R_2) is the radius of curvature of body 1 (2). We denote the field-value inside body 1 (2) as $\phi_{i^{(1)}}$ ($\phi_{i^{(2)}}$). Since the field equation is linear in the thick-shell case we need only the solution outside body 1 in order to calculate the force. The attractive chameleon force becomes

$$F_\phi \approx M_2 \beta_{,\phi_i^{(2)}} \frac{d\phi_1}{dr} = 2\beta_{,\phi_i^{(1)}} M_p \beta_{,\phi_i^{(2)}} M_p \frac{GM_1M_2}{r^2}(1+m_b r)e^{-m_b r} \tag{6.28}$$

For $m_b^{-1} < r$ this force is gravitational with strength $2(\beta_{,\phi_i^{(1)}} M_p)(\beta_{,\phi_i^{(2)}} M_p)$. The maximum value occurs for bodies where $\phi_i \approx \phi_b$, i.e. when the field inside the body is just a small perturbation in the background. Likewise the minimum value happens for bodies where $\phi_i \approx \phi_c$.

Let us now consider the force between two thin-shelled bodies, which we take to be identical for simplicity. The same derivation as above gives us

$$F_\phi = 2(\beta_{,\phi_c} M_p)^2 \left(\frac{3\Delta R}{R}\right)^2 \frac{GM_1M_2}{r^2}(1+m_b r)e^{-m_b r} \tag{6.29}$$

which is suppressed by the factor $\left(\frac{3\Delta R}{R}\right)^2 \ll 1$. The analogy with the SCM is very transparent, and the thin-shell factor is on exactly the same form (compare (6.21) with (3.43)). The natural continuation is to go on and calculate the experimental bounds for this coupling, but due to limitations in time this will be omitted here.

However, we will compute the LLR bounds for $m = 2$ and $m = 3$ since these results will come handy later on when studying the cosmological effects of the powerlaw coupling.

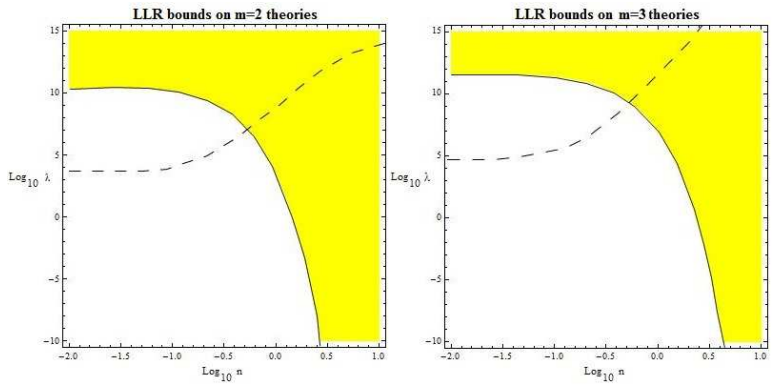

Figure 6.1: Lunar Laser Ranging bounds for the powerlaw coupling. The shaded region is allowed by the experiment. The dashed line shows when $\beta_{,\phi_b} M_p = 1$, i.e. when the coupling in background (solar-system) is of order 1. The region below (above) this dashed line corresponds to a coupling which is weaker (stronger) than gravity.

6.3.4 LLR bounds for the powerlaw coupling

Measurements of the difference in free-fall acceleration of the Moon and the Earth towards the Sun constraints this to be less than one part in 10^{13} [54], that is

$$\frac{|a_{moon} - a_{earth}|}{a_N} \lesssim 10^{-13} \tag{6.30}$$

where a_N is the Newtonian acceleration. When the Moon has a thin-shell (which implies that the Sun and the Earth also has a thin-shell), we find

$$\frac{|a_{moon} - a_{earth}|}{a_N} \approx 18\beta_{,\phi_c}^{(E)} \beta_{,\phi_c}^{(M)} M_p^2 \left(\frac{\Delta R}{R}\right)_S \left[\left(\frac{\Delta R}{R}\right)_M - \left(\frac{\Delta R}{R}\right)_E\right] \tag{6.31}$$

where E, M and S stands from earth, moon and sun respectively. The resulting bounds were calculated numerically and are shown in figure (6.1).

Chapter 7

Cosmology of Chameleons with Field-dependent Couplings

7.1 Introduction

The origin of dark energy (DE) responsible for the cosmic acceleration today is still a mystery. Although a host of independent observations have supported the existence of dark energy over the past decades, no strong evidence was found yet implying that dynamical DE models are better than a cosmological constant. The first step towards understanding the origin of DE would be to detect some clear deviation from the ΛCDM model observationally and experimentally. Models such as quintessence based on minimally coupled scalar fields provide a dynamical equation of state of DE different from $\omega = -1$. Still it is difficult to distinguish these models from ΛCDM in current observations pertaining to the cosmic expansion history only, such as the supernovae Ia observations. Even if we consider the evolution of matter perturbations δ_m in these models, the growth rate of δ_m is similar to that in ΛCDM. Hence one cannot generally expect large differences with ΛCDM at both the background and the perturbation levels. There is another class of DE models in which gravity is modified with respect to General Relativity (GR). Chameleon models falls in under this last class since gravity is modified by the addition of a fifth-force.

In chameleon models a scalar field(s) properties depend on the environment. First proposed by Khoury and Weltman [1], and employs a combination of self-interaction and couplings to matter of the scalar-field to avoid the most restrictive of the current bounds. In the models that they proposed, which from now on will be referred to as the standard chameleon model, a scalar field couples to matter with gravitational strength, in harmony with general expectations from string theory, whilst, at the same time, remaining relatively light on cosmological scales. In the literature the chameleon model is typically studied using a constant coupling to matter. However as we have shown in the previous chapter, the chameleon mechanism also exist for the field-dependent powerlaw couplings.

The modified evolution of the matter density perturbations δ_m can provide an important tool to distinguish generally modified gravity DE models (and in particular chameleon-models), from DE models inside GR like the ΛCDM model [82]. In fact the effective gravitational constant G_{eff} which appears in the source term driving the evolution of matter perturbations can change significantly relative to the gravitational constant G in the usual GR regime. A useful way to describe the perturbations is to write the growth function $f = \frac{d\log\delta_m}{\log a}$ as $f = \Omega_m(z)^\gamma$ where Ω_m is the density parameter of non-relativistic matter (baryonic and dark matter). One has $\gamma \approx 0.55$ in the ΛCDM-model [83, 84]. It was emphasized that while γ is quasi-constant in standard (non-interacting) DE models inside GR with $\gamma \approx 0.55$, this needs not be the case in modified gravity models. For example for the model proposed by Starobinsky [80] it was found in [81] that the present value of the growth index γ can be as small as $\gamma = 0.40 - 0.43$ together with

large slopes. This allows to clearly discriminate this model from ΛCDM. An additional important point is whether γ can exhibit scale dependence (dispersion). When this happens the resulting matter power spectrum is expected to have a scale dependence which is not found in ΛCDM.

In this paper we shall study the cosmology of chameleon models with field-dependent couplings. First look at the background evolution and then look at the dependence of the growth index γ on scales relevant to the linear regime of the matter power spectrum. This last part will be very similar to what we did in the chapter 'On the growth of matter perturbations in chameleon models'.

7.2 The Chameleon Action

We consider the scalar-tensor model described by the following action

$$S = \int dx^4\sqrt{-g}\left[\frac{RM_p^2}{2} - \frac{1}{2}(\partial\phi)^2 - V(\phi)\right] + S_{\rm matter}(\tilde{g}_{\mu\nu}, \psi_i) \tag{7.1}$$

where g is the determinant of the Einstein-frame metric $g_{\mu\nu}$, R is the Ricci-scalar and ψ_i are the different matter-fields. The matter fields couple to $\tilde{g}_{\mu\nu}$ which is related to $g_{\mu\nu}$ via a conformal rescaling on the form

$$\tilde{g}_{\mu\nu} = A(\phi)^2 g_{\mu\nu} \tag{7.2}$$

We will, for simplicity, focus on the case where all the matter-fields couple with the same $A(\phi)$ and define $\log A(\phi) \equiv \beta(\phi)$. The standard chameleon model (SCM) [1] corresponds to the choice

$$\begin{aligned} \beta(\phi) &= \left(\tfrac{\lambda\phi}{M_p}\right)^p \\ V(\phi) &= M^4 \exp\left(\tfrac{M}{\phi}\right)^n \end{aligned} \tag{7.3}$$

with $p = 1$. The cosmology of this model was studied in [14]. We will look at $p > 1$ and $p < 0$, but since the former case is very similar to $p = 1$ we will focus on the case $p < 0$ when discussing the cosmological evolution of the field. However the results are, with suitable modifications, also valid for the case $p > 1$. When $p < 0$ the mass-scale of the coupling must be tuned appropriately and we cannot allow $n < 0$ to have a chameleon mechanism present. We consider

$$\begin{aligned} \beta(\phi) &= \left(\lambda\tfrac{M_\beta}{\phi}\right)^m \\ V(\phi) &= M^4 \exp\left(\tfrac{\phi}{M}\right)^n \end{aligned} \tag{7.4}$$

where $m = -p > 0$, $n > 0$ and M_β is a mass-scale. The local gravity bounds for this model was investigated in the previous section[1] and shows the need to fine-tune $M_\beta \sim H_0$.

7.3 The Chameleon Potential

To have a chameleon mechanism we need an effective potential, $V_{\text{eff}} = V(\phi) + \rho e^{\beta(\phi)}$, which has a local minimum. The simplest type of potential that has this property is

$$V(\phi) = M^4 \left(\frac{\phi}{M}\right)^n \tag{7.5}$$

but when doing cosmology it is more convenient to use the exponential potential (7.4). When $\phi \ll M$ the exponential potential reduces to (7.5) and will generally be the case in the late universe. To get the correct density for dark energy today we need to choose $M^4 = \Lambda \sim 10^{-48} GeV^4 \rightarrow M \approx 10^{-3} eV$.

7.4 The Coupling Scale

We start with the action eq(7.1) and make a field-redefinition $\chi = M_p \frac{M_\beta}{\phi}$ with $M_\beta = \frac{M^2}{M_p} \sim H_0$. The action transforms as

$$\begin{aligned} (\partial\phi)^2 &\rightarrow \left(\tfrac{M}{\chi}\right)^4 (\partial\chi)^2 \\ V(\phi) &\rightarrow M^4 \exp\left(\tfrac{M}{\chi}\right)^n \\ \beta(\phi) &\rightarrow \left(\tfrac{\lambda\chi}{M_p}\right)^m \end{aligned} \tag{7.6}$$

When $m = 1$ we recover the SCM with a non-standard kinetic-term. The original formulation (7.1) have two fine-tuned mass-scales $M_\beta \sim H_0$ and M, but with this transformation we are left with an action with only a single fine-tuned mass-scale M. This model does not solve the fine-tuning problem, but it does not do any worse that the SCM or ΛCDM. In the following we take $M_\beta = \frac{M^2}{M_p} \approx 10^{-42}$ GeV.

7.5 Minima's of the effective potential

The minimum of the effective potential V_{eff} is given by

$$x^{n+p} e^{x^n} = \frac{m\rho_m}{nM^4} \left(\frac{\lambda M}{M_p}\right)^m \tag{7.7}$$

[1] Note that our bounds are in terms of the powerlaw potential and not the powerlaw exponential. However since these potentials are equal in the limit $\phi \ll M$ we expect similar results, ref. the SCM and the two potentials considered there.

where $x = \frac{\phi_{min}}{M}$. In the case $M \lesssim \phi$

$$\phi_{min} \approx M \log \left[\frac{m\rho_m}{nM^4} \left(\frac{\lambda M}{M_p} \right)^m \right]^{\frac{1}{n}} \tag{7.8}$$

and when $\phi \ll M$

$$\phi_{min} = M \left[\left(\frac{\lambda M}{M_p} \right)^m \frac{m\rho_m}{nM^4} \right]^{1/(n+m)} \tag{7.9}$$

The chameleon mass in the background, $m_\phi^2 \equiv V_{\rm eff,\phi\phi}(\phi_{\rm min})$, is given by

$$\begin{aligned} m_\phi^2 &= 3\Omega_m H^2 \lambda^m \left(\frac{M_p}{M} \right)^{2-m} m(n+m) \\ &\times \left[\left(\frac{M}{\phi} \right)^{m+2} + \frac{n}{m+m} \left(\frac{\phi}{M} \right)^{n-m-2} \right] \end{aligned} \tag{7.10}$$

The transition from $\phi_{min} > M$ to $\phi_{min} < M$ takes place when the r.h.s. of eq(7.7) becomes of less than 1:

$$\frac{\rho_m}{\rho_{m0}} \approx \left(10^{30} \lambda^{-1} \right)^m \tag{7.11}$$

where we have used $M^4 \approx \rho_{m0}$. For $m = 1$ and $\lambda = \mathcal{O}(1)$ we find $z \approx 10^{10}$, i.e. around the time of BBN. For $m > 1$ and $\lambda = \mathcal{O}(1)$ we will always have $\phi_{min} \ll M$ and the chameleon potential behaves like a cosmological constant $V \approx M^4$ at all times. We can now show that the field has a super-Hubble mass:

The function $g(x) = \frac{1}{x^{m+2}} + \frac{n}{n+m} x^{n-m-2}$ has a minimum bigger than 0 for $n > m + 2$ and the minimum value is of order 1 when $(n, m) = \mathcal{O}(1)$. The lowest value of the density parameter Ω_m is at the Planck-time where $\Omega_m \approx 10^{-28}$. Thus,

$$\begin{aligned} \frac{m_\phi^2}{H^2} &= 3m(n+m)\Omega_m \left(\frac{M_p}{M} \right)^{2-m} \lambda^m g\left(\frac{\phi}{M} \right) \\ &> \lambda^m 10^{30(2-m)-28} \end{aligned} \tag{7.12}$$

Which for $m = 1$ gives $\frac{m_\phi^2}{H^2} > 100\lambda \gg 1$ for all times when $\mathcal{O}(1) \lesssim \lambda$. Larger m requires a fine-tuning $\lambda \gg 1$ in order for this to be true.

7.6 Cosmological Evolution

We consider a flat FLRW background

$$ds^2 = -dt^2 + a(t)^2(dx^2 + dy^2 + dz^2) \tag{7.13}$$

The corresponding Friedmann equations are given by

$$3H^2 = 8\pi G\left(\rho_m A(\phi) + \rho_r + \frac{1}{2}\dot{\phi}^2 + V(\phi)\right) \tag{7.14}$$

$$\dot{H} = -4\pi G\left(3\rho_m A(\phi) + 4\rho_r + \dot{\phi}^2\right) \tag{7.15}$$

The matter-density ρ_m is defined as the density in the Einstein-frame which satisfy the usual continuity equation

$$\dot{\rho}_m + 3H\rho_m = 0 \tag{7.16}$$

The density-parameters will be given by

$$\begin{aligned} \Omega_m &= \frac{\rho_m A(\phi)}{3M_p^2 H^2} = \Omega_{m,0}(1+z)^3 \frac{A}{A_0} \\ \Omega_\phi &= \frac{V(\phi)+\frac{1}{2}\dot{\phi}^2}{3M_p H^2} \end{aligned} \tag{7.17}$$

When ϕ is slowrolling this last relation can be written $\Omega_{\phi,0}\frac{V(\phi)}{V(\phi_0)}$. The field equation for ϕ is

$$\begin{aligned} &\ddot{\phi} + 3H\dot{\phi} + V_{\text{eff},\phi} = 0 \\ &V_{\text{eff}} = V(\phi) + \rho e^{\beta(\phi)} \end{aligned} \tag{7.18}$$

The analysis below will be very close up to the treatment given in [14] for the SCM.

7.6.1 Attractor solution

We show the existence of an attractor solution where the chameleon follow the minimum of its effective potential $\phi = \phi_{min}(t)$. Suppose the field is at the minimum at some time t_i. Then a time later due to the red shifting of the matter density the minimum ϕ_{min} has moved to a slightly smaller value. The characteristic timescale for this evolution is the Hubble time $1/H$. Meanwhile the characteristic timescale of the evolution of ϕ is given by $1/m_\phi$. When $m_\phi \ll H$ the response-time of the chameleon is much larger than $1/H$, the chameleon cannot follow the minimum and starts to lag behind. But if $m_\phi \gg H$ then the response-time of the chameleon is much smaller than $1/H$, the chameleon will adjust itself and adiabatically start to oscillate about the minimum. This can also be seen from the analogy of eq(7.18) with a driven harmonic oscillator å

$$\ddot{x} + 2\zeta\omega\dot{x} + \omega^2 x = 0 \tag{7.19}$$

This equation will have a solution which oscillates with a decreasing amplitude as long as $\zeta < 1$ which in our case reduces to $\frac{2m_\phi}{3H} > 1$. In order for us to have any control over the evolution of ϕ and for the field to satisfy bounds from BBN etc. we must require that $\frac{m_\phi^2}{H^2} \gg 1$ at least since $z \sim 10^{15}$ if we consider arbitrary initial conditions. As shown above, when $\mathcal{O}(1) \lesssim \lambda$ the field will always satisfy this condition.

7.6.2 Dynamics of ϕ along the attractor

The attractor solution is given by ϕ_{min} which in the late universe ($\phi_{min} \ll M$) is given by

$$\phi = \phi_0 (1+z)^{\frac{3}{m+n}} \tag{7.20}$$

which is decreasing with time. When the field follows the attractor, $\phi \approx \phi_{min}$ and $V_{\text{eff},\phi} \approx 0$. Taking the time-derivative yields

$$\dot{\phi} \approx -3H \frac{V_{,\phi}}{m_\phi^2} \tag{7.21}$$

and the slow-roll condition

$$\frac{\dot{\phi}^2}{2V} = \frac{9H^2}{2m_\phi^2} \frac{1}{\Gamma} \ll 1 \tag{7.22}$$

with $\Gamma = \frac{V m_\phi^2}{V_{,\phi}^2}$. For our potential eq(7.5) we find

$$\Gamma = 1 + \frac{n+m}{n} \left(\frac{M}{\phi} \right)^n > 1 \tag{7.23}$$

When the field follows the minimum it will be slow-rolling whenever the condition $m_\phi^2 \gg H^2$ is satisfied. The equation of state for a minimal coupled scalar field is given by $\omega_{usual} = \frac{\dot{\phi}^2 - 2V}{\dot{\phi}^2 + 2V} \approx -1$ when the field is slow-rolling. But we are not dealing with a minimal coupled scalar field so we must calculate the equation of state from $\dot{\rho_\phi}/\rho_\phi = -3H(1+\omega_{\text{eff}})$. This yield together with eq(7.21)

$$\omega_{\text{eff}} = -1 + \frac{1}{\Gamma} \tag{7.24}$$

when the chameleon is slow-rolling along the minimum. In the time before BBN, $\phi \gg M$, $\Gamma \approx 1$ and the chameleon acts as dust. After the transition to $\phi \ll M$, $\Gamma \gg 1$ and $\omega \approx -1$ which will be the case today. See fig(7.4) for a typical evolution of the effective equation of state. Comparing this with the usual equation of state

$$\omega_{usual} = \frac{\dot{\phi}^2 - 2V}{\dot{\phi}^2 + 2V} \approx -1 + \frac{1}{\Gamma} \frac{H^2}{m_\phi^2} \tag{7.25}$$

which is much closer to -1 than ω_{eff}.

7.6.3 Reaching the attractor

We consider releasing the field at some time t_i with $\dot{\phi} = 0$ for simplicity at some initial value ϕ_i and would like to show that the attractor is reached for a large span of initial conditions. We can have two cases here

Undershooting: $\phi_i \gg \phi_{min}(t_i)$

In this case the field equation reads

$$\ddot{\phi} + 3H\dot{\phi} \approx -V_{,\phi} \tag{7.26}$$

which is the same equation as in quintessence. In this case the driving term will dominate over the friction term when $V_{,\phi\phi} \gg H^2$ driving the field down towards the minimum. When m_ϕ^2/H^2 all the way back to the Planck-time this will always be the case, but if this is not the case the field will be fixed at ϕ_i until the Hubble factor has had time to be sufficiently redshifed. The field will drop to, and go past, $\phi = \phi_{min}$. Here the approximation eq(7.26) cannot be used anymore, but the field will usually have to much kinetic energy to settle at the minimum and will be driven past the minimum. In this model, apposed to the SCM, the further past the minimum the field is driven the stronger the factor $\beta_{,\phi}\,\rho_m$ becomes, even though ρ_m is very small in the radiation era it will eventually kick in and drive the field up again. We will also have a contribution from the decoupling of relativistic matter which will be discussed in the next section. This will make the field oscillate around the minimum, and as long as $m_\phi^2/H^2 \gg 1$ the amplitude of the oscillations will be damped, making sure that the field quickly settles at the minimum. When the energy density in ϕ is kinetic-dominated, as it is when dropping past the minimum, we have $\ddot{\phi} \approx -3H\dot{\phi}$ which gives $\dot{\phi} \sim a^{-3}$. Integrating this relation, and using the initial value $\dot{\phi}_i^2 = 6\Omega_\phi^{(i)} H_i^2 M_p$, gives

$$\phi(t) = \phi_i - \sqrt{6\Omega_\phi^{(i)}} \left[1 - \left(\frac{t_i}{t}\right)^{1/2}\right] M_p \tag{7.27}$$

When $t \to \infty$ this expression converges to $\phi_\infty = \phi_i - \sqrt{6\Omega_\phi^{(i)}} M_p$. Here we can have two cases: If $\phi_\infty > 0$ and $\rho_m |\beta_{,\phi_\infty}| \ll 3H\dot{\phi}$ then the field stops at $\phi_{stop} \sim \phi_\infty$. This typically happens when $m_\phi \lesssim H$. When $m_\phi^2 \gg H^2$ we have $\phi_\infty < 0$ and the field will stop when the driving-term $\rho_m \beta_{,\phi}\, e^{\beta(\phi)}$ becomes larger than the friction term[2] $3H\dot{\phi}$. After this the field will evolve as in the overshoot solution described below.

Overshooting: $\phi_i \ll \phi_{min}(t_i)$

In this case the potential term $V_{,\phi}$ can be ignored and the ϕ-equation becomes

$$\ddot{\phi} + 3H\dot{\phi} \approx \beta_{,\phi} T^\mu_\mu \tag{7.28}$$

where we have restored the trace of the energy-momentum tensor. In the radiation-dominated era this trace is very small since radiation does not

[2] We have restored the exponential factor since in some cases the field will drop to a field value where $\beta(\phi) > 1$.

contribute to the trace and the field would be almost frozen at its initial value. But as discussed in [14] as the universe expands and cools the different matter-species decouple from the radiation heat bath when their mass satisfies $m \sim T$. This gives rise to a trace-analomy where the trace of the EM-tensor gets non-zero for about one e-fold of expansion leading to a 'kick' in the chameleon pushing it to larger field-values. This trace can be written for a single matter-species as [14]:

$$T_{\mu}^{\mu(i)} = -\frac{45}{\pi^4} H^2 M_p^2 \frac{g_i}{g*(T)} \tau(m_i/T) \tag{7.29}$$

where the τ-function is given by

$$\tau(x) = x^2 \int_x^{\infty} \frac{\sqrt{y^2 - x^2} dy}{e^y \pm 1} \tag{7.30}$$

and $\pm$ refers to bosons and fermions respectively. See fig(7.1) for a plot of

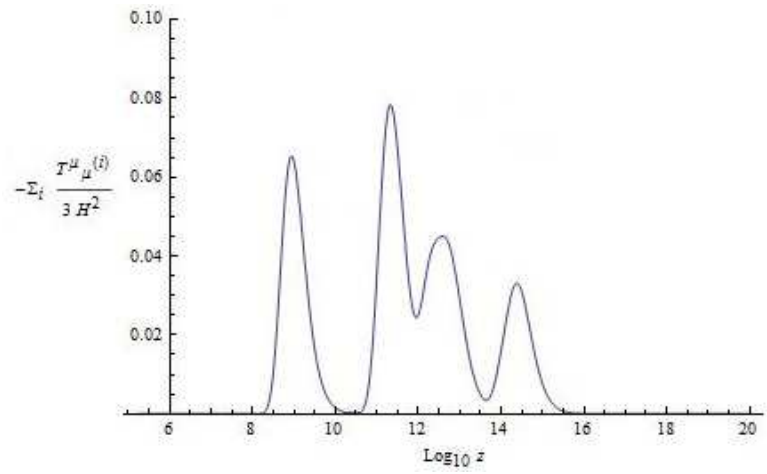

Figure 7.1: The trace of the EM-tensor, $-T_{\mu}^{\mu}/(3H^2M_p^2)$, in the radiation dominated era for all the different matter species decoupling from the radiation heat bath.

$T_{\mu}^{\mu}/(3H^2M_p^2)$ in the radiation era. The plot shows that each kick contributes to the field equation as an effective matter-density $\Omega_{\mathrm{m\ eff}} \sim \mathcal{O}(0.01)$. By using a delta-function source (see [14]) as the kick we can show that the result is to push the field up a distance

$$\Delta\phi = \mathcal{O}\left(|\beta_{,\phi_i}| M_p^2 \frac{g_i}{g*(m_i)}\right) \tag{7.31}$$

where ϕ_i is the field-value before the kick sets in. Since $\frac{M_p}{\phi_i} > 1$, which must be true or else the energy-density in ϕ will be the dominating one,

and $\beta_{,\phi} \propto \frac{1}{\phi^{m+1}}$ the lower ϕ_i the higher the field will be kicked and in most cases the kick from the top-quark, the $W^{\pm}$ and Z-bosons will drive the field up and above the minimum independently of the initial value. When above the minimum the resulting kicks will be balanced by the term $V_{,\phi}$ which drives the field down again making the field oscillate above the minimum before eventually settling down at the minimum. In contract with the SCM where the field gets kicked almost the same amount every time a new particle species freezes out, we here have that the field gets pushed up less and less every time since $|\beta_{,\phi}|$ decreases when the field is kicked up. Also since the field typically will be oscillating above the minimum after a couple of kicks, we will have $\beta(\phi) < \beta(\phi_{min})$ and BBN bounds on particle mass variation are more easily satisfied than in the SCM. The closer to $\phi = 0$ we start the more effective this kick-mechanism is in driving the field closer to the minimum and is an effect of having a dynamical coupling. Because of this effect it is desired to have the chameleon starting out below its effective potential and have these 'kicks' bringing it up to the minimum. The initial value will of course depend on the how the chameleon behaves under inflation. If the chameleon couples to the inflaton and sits at the minimum at the onset of inflation, then after the inflaton decays to reheat the universe the density of matter-species coupled to the chameleon will decrease rapidly since most of the energy will go to radiation. This will lead to a release of the field at a value well above the minimum, where the undershoot solution applies. If $m_\phi^2 \gg H^2$ then the field will typically settle at the minimum before the time of BBN.

Due to $m_\phi^2 \gg H^2$ the field will eventually converge to the minimum since the amplitude of the oscillations are damped. This can be showed explicitly as done in [14], the derivation there is general and applies to our case as well.

7.6.4 BBN bounds

Because of the conformal coupling eq(7.2), a constant mass scale m_0 in the matter-frame is related to a ϕ-dependent mass scale $m(\phi)$ in Einstein-frame by the rescaling $m(\phi) = m_0 e^{\beta(\phi)}$. A variation in ϕ lead to variations in the various masses

$$\left|\frac{\Delta m}{m}\right| \approx \Delta\beta(\phi) \tag{7.32}$$

Big-bang nucleosynthesis constrains the variation in $m(\phi)$ from the time of nucleosynthesis until today to be less than 10%. Since the minimum, ϕ_{min}, is a decreasing function of time $\beta(\phi)$ will be increasing with time and if the field is at the minimum at BBN the bound is satisfied for all $\lambda \lesssim 10^{30}$. When the field is not at the minimum we get the bound $\beta(\phi_{BBN}) \lesssim 0.1$. As discussed above, as long as $m_\phi^2/H^2 \gg 1$ this bound will almost always be satisfied. Due to numerical limitations we have not been able to simulate the extreme

cases $\phi_i \sim H_0 \to \beta(\phi_i) \sim 1$ which corresponds to the case $\phi_i^{(SCM)} \sim M_p$, but for a large range in initial condittions the field always satisfied BBN bounds as long as $m_\phi^2 \gg H^2$ was satisfied.

7.6.5 CMB bounds

Another important restriction on chameleon theories comes out from considering the isotropy of the CMB [74]. A difference in a the value of ϕ today and the value it had during the epoch of recombination would mean that the electron mass at that epoch differed from its present value $\frac{\Delta m_e}{m_e} \approx \Delta\beta(\phi)$. Such a change in m_e would, in turn, alter the redshift at which recombination occurred, z_{rec}:

$$\frac{\Delta z_{rec}}{z_{rec}} \approx \Delta\beta(\phi) \tag{7.33}$$

WMAP bounds z_{rec} to be within 10% of the value that has been calculated using the present day value of m_e, [14]. Denoting ϕ_0, ϕ_{rec} and ϕ_{BBN} with the field value today, at recombination and BBN respectivitly. Then $\phi_0 < \phi_{rec} < \phi_{BBN} \to \beta_0 > \beta_{rec} > \beta_{BBN}$ and this bound will always be weaker then the bound coming from BBN.

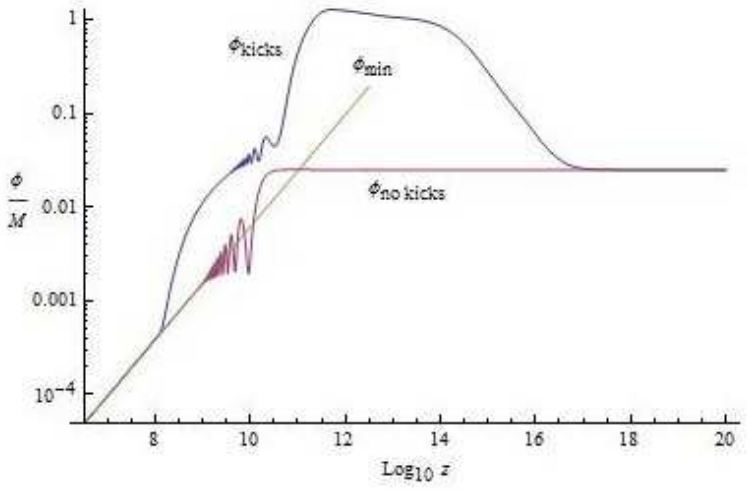

Figure 7.2: $\phi(z)$ calculated numerically with and without the kicks together with the minimum of the effective potential. We used $m = 1$, $\lambda = 1$ and the exponential potential $V = M^4 \exp(\phi^4/M^4)$ with the initial value $\phi_i = 10^{-2}M$. We see that the the kicks-solution does not reach the minimum until $z \approx 10^8$, but because of the large mass $m_\phi^2 \gg H^2$ when $\phi \sim \phi_{\min}$ it starts to follow the minimum right away.

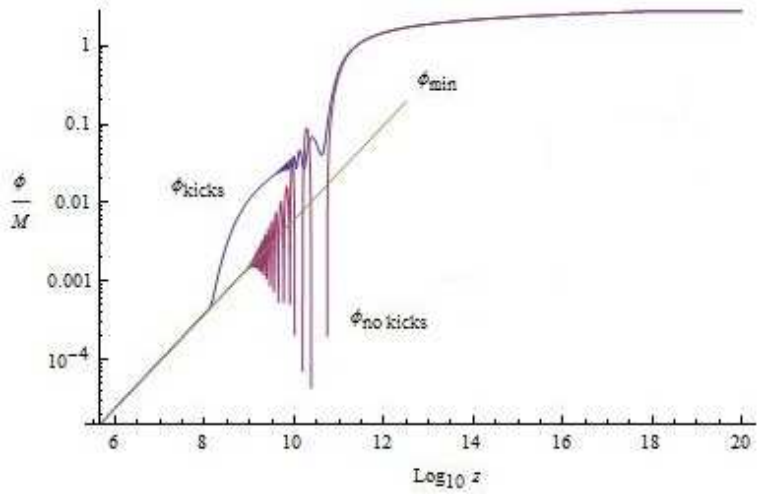

Figure 7.3: $\phi(z)$ calculated numerically with and without the kicks together with the minimum of the effective potential. We used $m = 1$, $\lambda = 1$ and the exponential potential $V = M^4 \exp(\phi^4/M^4)$ with the initial value $\phi_i = 1.1M$. Here $M = 10$MeV, much higher than the required value $M = 10^{-3}$eV due to numerical limitations. We see that the no kicks solution oscillates very rapidly, but when the kicks are included the oscillations are balanced out.

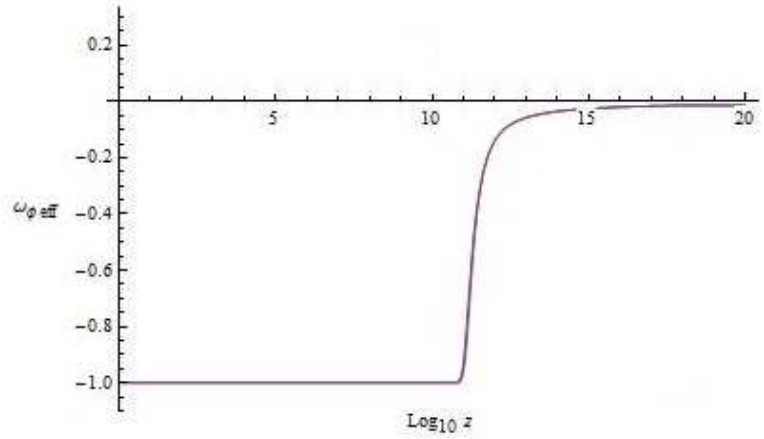

Figure 7.4: The effective equation of state for the chameleon when $m = 1$, $\lambda = 1$ and the exponential potential $V = M^4 \exp(\phi^4/M^4)$ with the initial value $\phi_i = 1.1M$. We see that the chameleon acts as a matter-fluid during the period before BBN, but then quickly drops to $\omega = -1$.

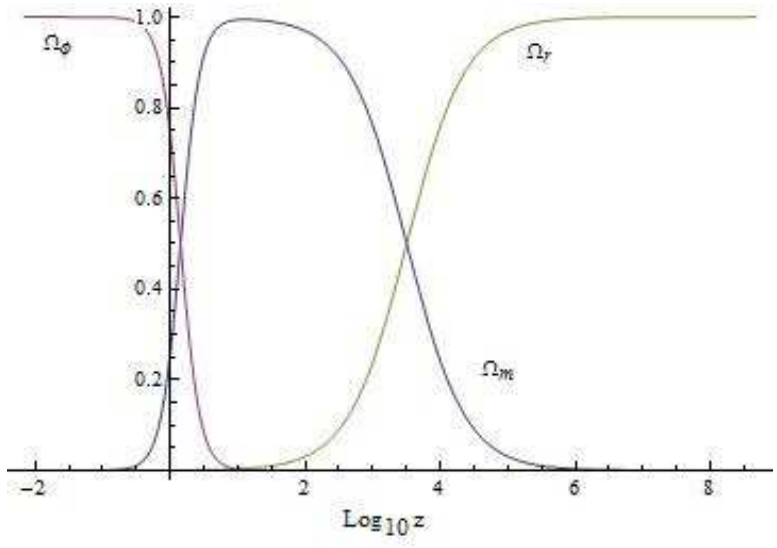

Figure 7.5: The density parameters in the late universe where the chameleon plays the role of dark energy. The deviation from ΛCDM is usually much less than 1% as long as the chameleon has settled at the minimum.

7.7 The Perturbations

We start by consider a general scalar-tensor model eq(7.1) with universal matter-coupling $\log A(\phi) = \beta(\phi)$ and a potential $V(\phi)$. In deriving the perturbation we will work in units of $M_p = \frac{1}{\sqrt{8\pi G}} \equiv 1$. We will consider the Jordan-frame matter-density satisfying

$$\dot{\rho}_m + \left(3H - \frac{d\beta}{d\phi}\dot{\phi}\right)\rho_m = 0 \tag{7.34}$$

since this choice will simplify the field equation. In terms of the Einstein-frame density ρ_m^{EF} this choice corresponds to $\rho_m = A(\phi)\rho_m^{EF}$. This is just a matter of convenience since $A \approx 1$ in the late universe whenever the model is viable. With this choice the field equation reads

$$\ddot{\phi} + 3H\dot{\phi} + V_{,\phi} + \frac{d\beta}{d\phi}\rho_m = 0 \tag{7.35}$$

The most general metric in FLRW spacetime with scalar perturbations is given by

$$ds^2 = -(1+2\alpha)dt^2 - 2aB_{,i}dtdx^i + a^2\left((1+2\psi)\delta_{ij} + 2\gamma_{,i;j}\right)dx^i dx^j \tag{7.36}$$

where the covariant derivative is given in terms of the three-space metric which in the case of a flat background reduces to δ_{ij}. In the gauge-ready

formulation [16], the scalar perturbations equations are (we consider $\mathrm{M_p} \equiv 1$)

$$\dot{\chi} + H\chi - \alpha - \psi = 0 \quad (7.37)$$

$$\kappa + \frac{\Delta}{a^2}\chi - \frac{3}{2}(\rho_m v + \dot{\phi}\delta\phi) = 0 \quad (7.38)$$

$$\delta\ddot{\phi} + 3H\delta\dot{\phi} + (V_{,\phi\phi} - \frac{\Delta}{a^2})\delta\phi + \beta_{,\phi\phi}\,\rho_m\delta\phi +$$
$$\beta_{,\phi}\,(2\alpha\rho_m + \delta\rho_m) + 2\alpha V_{,\phi} - \dot{\phi}(\dot{\alpha} - 3H\alpha + \kappa) = 0 \quad (7.39)$$

$$\dot{v} - \alpha + \beta_{,\phi}\,(\dot{\phi}v - \delta\phi) = 0 \quad (7.40)$$

$$\delta\dot{\rho}_m + 3H\delta\rho_m - \rho_m\left(\kappa - 3H\alpha + \frac{\Delta}{a^2}v\right) - \beta_{,\phi}\,(\rho_m\delta\dot{\phi} \quad (7.41)$$

$$+\delta\rho_m\dot{\phi}) - \beta_{,\phi\phi}\,\rho_m\dot{\phi}\delta\phi = 0 \quad (7.42)$$

$$H\kappa + \frac{\Delta}{a^2}\psi - \left(-\delta\rho_m + \alpha\dot{\phi}^2 - \dot{\phi}\delta\dot{\phi} - V_{,\phi}\delta\phi\right)/2 = 0 \quad (7.43)$$

$$\dot{\kappa} + 2H\kappa + 3\alpha\dot{H} + \frac{\Delta}{a^2}\alpha - \left(\delta\rho_m - 4\alpha\dot{\phi}^2 + 4\dot{\phi}\delta\dot{\phi} - 2V_{,\phi}\delta\phi\right)/2 = 0 \quad (7.44)$$

with

$$\chi = a(B + a\dot{\gamma}) \quad (7.45)$$

$$\kappa = 3(-\dot{\psi} + H\alpha) - \frac{\Delta}{a^2}\chi \quad (7.46)$$

and Δ being the co-moving covariant three-space Laplacian. The choice of a gauge will simplify the system and we will work in the so-called co-moving gauge ($v = 0$) where we can closed the system for the two variables $(\delta\phi, \delta_m)$. Here $\delta\phi$ is the perturbation in the chameleon field and δ_m is the matter-density perturbations defined by

$$\delta_m \equiv \frac{\delta\rho_m}{\rho_m} - \frac{\dot{\rho}_m}{\rho_m}v \equiv \frac{\delta\rho_m}{\rho_m} \quad \text{in the co-moving gauge,} \quad (7.47)$$

In Fourier space we have

$$\ddot{\delta}_m + 2H\dot{\delta}_m - \frac{1}{2}\rho_m\delta_m + \delta\phi\left(U_{,\phi} - \beta'[6H^2 + 6\dot{H} - \frac{k^2}{a^2} + 2\dot{\phi}^2]\right) - \beta'\delta\ddot{\phi}$$
$$- \delta\phi\left(\beta''[2H\dot{\phi} - U_{,\phi} - \beta'\rho_m] + \beta'''\dot{\phi}^2\right) - \delta\dot{\phi}\left(5\beta'H + 2\dot{\phi} + 2\beta''\dot{\phi}\right) = 0 \quad (7.48)$$

$$\delta\ddot{\phi} + (3H + 2\beta'\dot{\phi})\delta\dot{\phi} + \beta'\rho_m\delta_m - \dot{\phi}\dot{\delta}_m \quad (7.49)$$
$$+\left(U_{,\phi\phi} + \frac{k^2}{a^2} - 2\beta'^2\rho_m - 2\beta' U_{,\phi} + \beta''[2\dot{\phi}^2 + \rho_m]\right)\delta\phi = 0$$

where k is a co-moving wavenumber and $' \equiv \frac{d}{d\phi}$. It should be noted that the equation above are derived in full generality, without specifying the exact form of β and V, and can be used when studying any scalar-tensor theory given by the action eq(7.1). When the field is slow rolling along the minimum $\phi \approx \phi_{\min}$, and for scales within the Hubble radius, $\frac{k^2}{a^2} > H^2$, we can simplify the equations to

$$\begin{aligned} \ddot{\delta_m} + 2H\dot{\delta_m} &= \tfrac{3}{2}\Omega_m H^2 \left(1 + \frac{2\beta^2_{,\phi}}{1+\frac{\lambda^2_{pert}}{\lambda^2_\phi}} \right) \\ \delta\phi &= \tfrac{3}{4\pi^2}|\beta_{,\phi}|\Omega_m H^2 \delta_m \frac{\lambda^2_\phi}{1+\frac{\lambda^2_{pert}}{\lambda^2_\phi}} \end{aligned} \tag{7.50}$$

where we have introduced the length scale $\lambda_{pert} = \frac{2\pi a}{k}$ of the perturbation and the critical length scale for the chameleon $\lambda_\phi = \frac{2\pi}{m_\phi}$. Restoring $M_p^{-2} \equiv 8\pi G$ we can write this equation on the same form as in ΛCDM

$$\ddot{\delta_m} + 2H\dot{\delta_m} = 4\pi G_{\text{eff}} \rho_m \delta_m \tag{7.51}$$

where

$$G_{\text{eff}} = G\left[1 + \frac{2|\beta_{,\phi}\, M_p|^2}{1 + \frac{\lambda^2_{pert}}{\lambda^2_\phi}}\right] \tag{7.52}$$

and G is the Newtonian gravitational constant. The quantity G_{eff} encodes the modification of gravity due to the chameleon in the weak-field regime.

The perturbations will also exhibit an oscillating term which we have averaged out in the equations above by taking $< \phi >= \phi_{\min}$. This is valid since this term will be time-decreasing and hence negligible for small redshifts. In some $f(R)$-models however, this oscillating term can grow to infinity because the mass of the scalaron is not bounded above. The divergence of this mass can be removed by adding a UV-term [57].

7.7.1 The Growth Factor

In studying perturbations, it is convenient to introduce the growth-factor $f = \frac{d\log(\delta_m)}{d\log(a)}$. In ΛCDM $f \to 1$ at high redshifts and $f \to 1$ in an Einstein-de Sitter universe. It is important to find a characteristics in the perturbations that can discriminate between different DE models and the ΛCDM. It was noted in [51], [52] that writing the growth factor as

$$f = \Omega_m^\gamma \tag{7.53}$$

can be a parametrization that is useful for this purpose. In ΛCDM we have to a good accuracy $\gamma \approx 0.55$ for redshifts $z \lesssim 10$. Of course in some models

γ will vary to much for it to be considered a constant, and we can also have a scale dependence, so we should write $\gamma = \gamma(z, k)$.

We will be most interested in scales k relevant to the galaxy power spectrum [50]

$$0.01 h Mpc^{-1} \lesssim k \lesssim 0.2 h Mpc^{-1} \tag{7.54}$$

or

$$\frac{10}{h} Mpc \lesssim \lambda_{pert} \lesssim \frac{200}{h} Mpc \tag{7.55}$$

where $h = 0.72 \pm 0.08$ corresponds to the uncertainty in the Hubble factor today. These scales are also in the linear regime of perturbations.

7.7.2 The Critical Length scale λ_ϕ

In eq(7.50) we can have three cases. First when $\lambda_\phi \ll \lambda_{pert}$ we find $G_{\rm eff} = G$ and the perturbations are in the GR regime.

Secondly when $\lambda_\phi \gg \lambda_{pert}$ we find $G_{\rm eff} = G(1 + 2|\beta_{,\phi}\, M_p|^2)$ and the matter-perturbations will feel a stronger gravitational constant than in GR. Note that $\beta_{,\phi}$ is in general a dynamical quantity and will increasing with time when the chameleon follows the minimum.

The last case is $\lambda_\phi \sim \lambda_{pert}$ where

$$G_{\rm eff} = G\left(1 + 2|\beta_{,\phi}\, M_p|^2 \frac{\lambda_\phi^2}{\lambda_\phi^2 + \lambda_{pert}^2}\right) \tag{7.56}$$

and the perturbations will exhibit a scale dependence which was discussed in [39] in the case of the SCM.

Let us first consider the inverse power coupling $\beta(\phi) = \left(\frac{\lambda H_0}{\phi}\right)^k$ with the potential $V(\phi) = M^4 \exp\left(\frac{\phi}{M}\right)^n$. The range of the chameleon in the background today can be written in terms of the coupling $|\beta_{,\phi_b}|M_p$ as

$$\lambda_\phi = 2\pi \sqrt{\frac{k}{n(n+m)}} \left(\frac{M_p}{M}\right)^{\frac{(n-2)}{2(n-1)}} |\beta_{,\phi_b}\, M_p|^{-\frac{(n-2)}{2(n-1)}} \frac{1}{M} \tag{7.57}$$

which gives

$$\frac{\lambda_\phi}{1pc} \sim 10^{-5-\frac{15}{n-1}} |\beta_{,\phi_b}\, M_p|^{-\frac{(n-2)}{2(n-1)}} \tag{7.58}$$

This shows that if the chameleon is to have a super parsec range, then the coupling must satisfy

$$|\beta_{,\phi_b} M_p| < 10^{-10} \tag{7.59}$$

which is to small to affect the linear perturbations. This can change if we could take $n < 0$, but then the effective potential does not have a minimum and the model is no longer a chameleon.

If we instead look at the power-law coupling $\beta(\phi) = \left(\frac{\lambda\phi}{M_p}\right)^m$ together with the potential $V(\phi) = M^4 \exp\left(\frac{M}{\phi}\right)^n$ we find

$$\frac{\lambda_\phi}{1pc} \sim 10^{-5+\frac{15}{n+1}} |\beta_{,\phi_b} M_p|^{-\frac{(n+2)}{2(n+1)}} \tag{7.60}$$

For $n < 1$ we can have $\lambda_\phi = \mathcal{O}(1Mpc)$ together with $|\beta_{,\phi_b} M_p| \sim 1$ today. This regime was studied in the case of the SCM in [39]. Here our chameleon can affect the growth of the linear perturbations. Se fig(7.6) and fig(7.7) for a plot of the growth factor γ measured today. The plot shows the three regimes:

- (i): Phase space where $\gamma < 0.43$ for all relevant scales. This is the scalar regime.
- (ii): Phase space where γ is dispersed between $0.43 < \gamma < 0.55$.
- (iii): Phase space where $\gamma \approx 0.55$ for all relevant scales. This is the GR regime.

We see that when local gravity constraints are satisfied, the perturbations are in the GR regime with no signature on the matter perturbations or at the background evolution. If we consider a coupling to dark matter only then the local constraints are avoided and the strongest bounds are the BBN bounds.

7.8 Conclusions

We have shown the existence of an attractor solution for the chameleon models with a powerlaw coupling. This attractor is reached for a large span of initial conditions and as long as $m_\phi^2 \gg H^2$ the model is in agreement with BBN bounds on particle mass variations. Along the attractor the chameleon is slowrolling and can account for the late time acceleration of the universe. The potential is fine-tuned in the same manner as a cosmological constant.

In the case of the inverse power-law coupling (7.4), the linear perturbations are not affected by the chameleon since its range is in general to small

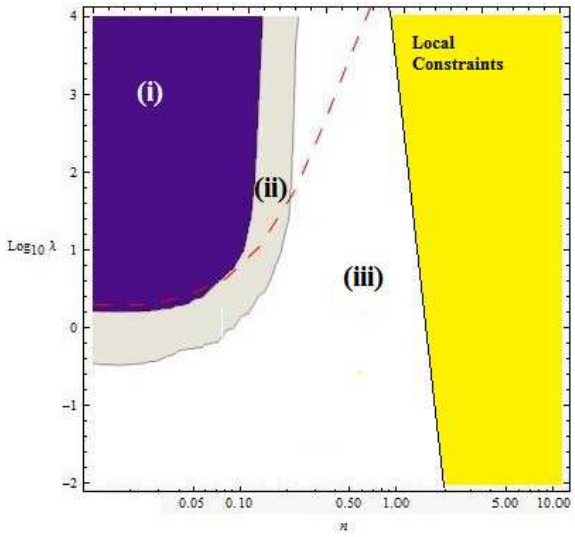

Figure 7.6: The three regimes for the growth factor γ_0 for the quadratic coupling $\beta(\phi) = \left(\frac{\lambda\phi}{M_p}\right)^2$. The dashed line shows $|\beta_{,\phi_b} M_p| = 1$, i.e. when the coupling in the (cosmological) background today is of order 1. The shaded region on the r.h.s. shows the local constraints (LLR bounds).

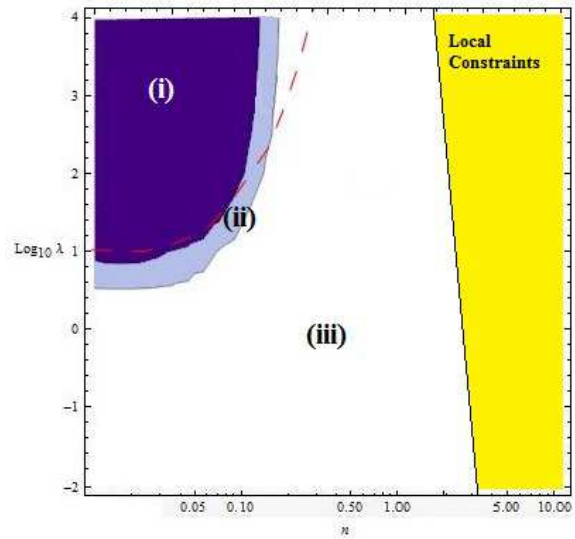

Figure 7.7: The three regimes for the growth factor γ_0 for the cubic coupling $\beta(\phi) = \left(\frac{\lambda\phi}{M_p}\right)^3$. The dashed line shows $|\beta_{,\phi_b} M_p| = 1$, i.e. when the coupling in the (cosmological) background today is of order 1. The shaded region on the r.h.s. shows the local constraints (LLR bounds).

compared to cosmic scales, and if the range is large enough the coupling is in general to small to produce an observable effect. This is not the case for the power-law coupling. If $n < 1$ the range of the chameleon can be as large as $\mathcal{O}(1Mpc)$ together with a matter-coupling of order unity and the matter perturbation will grow faster than in ΛCDM. We can also have a dispersion for scales within the linear regime. However, it must be emphasized that gravity constraints force us to have a gravitational coupling of the chameleon field to dark matter only in order to have this ΛCDM deviating growth.

With this consideration we have shown that the growth of matter perturbations allow to discriminate between our models and ΛCDM while the background evolution is completely similar to that in ΛCDM. The reason is the fifth-force acting on the growth of matter perturbations on cosmic scales.

If future observations will measure the growth function $\gamma(z, k)$ with high accuracy and find significant deviations from ΛCDM, for which $\gamma \approx 0.55$, is quasi-constant and scale independent, then our model can account for this. It would then be interesting to investigate how to discriminate our models with other DE models where similar departures from ΛCDM can take place. Since the effective gravitational constant is ϕ-dependent in the models considered here, it can in principle allow us to discriminate them from the SCM by measuring the red-shift dependence of γ.

We have not had time to study the effects on the matter power spectrum, and leave this for a future work.

Chapter 8

Conclusions

8.1 Summary and conclusion

The main purpose of this thesis has been to investigate different types of couplings in chameleon models, and the main result is that there do exist a much larger range of models that have the thin-shell suppression property of the standard chameleon model (SCM). The thin-shell effect is the property that only a small fraction of a body will contribute to the fifth-force, and because of this mechanism it is possible for the chameleon to couple to matter with gravitational strength and still be in agreement with experiments.

The crucial difference between the models we have considered: The powerlaw coupling (PLC) and the inverse powerlaw coupling (IPLC), and the SCM is the obvious fact that the coupling in the former models is field-dependent. This makes sure that the coupling will tune itself to smaller values in a high density environment than in a low density environment even without a thin-shell effect. The thin-shell effect comes in addition for really large objects.

Using the same potential (where it is possible) in the SCM and in the IPLC we found the same value for the effective coupling $\beta_{\text{eff}} = |\beta_{,\phi_c} M_p| \frac{3\Delta R}{R}$. Thus, a (hypothetical) measurement of the fifth-force between two thin-shelled bodies will not be able to distinguish the two models.

The PLC and IPLC can be distinguished from the SCM if one is able to make a measurement of the fifth-force between two objects in a low-density environment that have thick-shells (like in the satelitte experiments SEE, GG, MICROSCOPE discussed in the introduction). The fifth-force (relative to gravity) in the SCM will in this regime be stronger than that on earth, but will be the same for all thick-shelled objects. In the PLC and IPLC the coupling will depend on the size (density and radii) of the objects, and thus a large object will feel a smaller fifth-force (relative to gravity) than a small object.

As a dark energy fluid both the SCM, the PLC and the IPLC give rise to a background evolution that is very similar to ΛCDM. In the IPLC, the growth of the linear matter perturbations are required to be the same as ΛCDM, but can be quite different in the SCM and PLC. The reason is the appearance of a fifth force acting on the growth of the matter perturbations on cosmic scales, and in the IPLC this fifth-force is always very weak when the field has a large range. However, to have this effect, it must be emphasized that local gravity constraints forces us to have a coupling of the chameleon field to dark matter only.

It was showed that the mass-scale of the coupling in the IPLC had to be tuned to an unnatural low value $M_\beta \sim H_0$. This fine-tuning can however be reduced by introducing a redefinition of the field and the model was shown to be fine-tuned in the same way as the SCM and ΛCDM.

8.1.1 Things for the future

There are several issues with this thesis that can be improved. For example deriving more accurate solutions to the field equations, derive bounds for experiments overlooked in this thesis and if one is really brave: correct all the typos. The experimental bounds for the PLC was not calculated in this thesis due to limitations in time. Because of the similarities with the SCM and the IPLC we don't really expect any new surprising results. For completeness this should of course be done, but it would only be really interesting if we had some experimental data which contradicted general relativity.

Our treatment have been in terms of the simplest type of potentials. One could certainly consider more complicated potentials, but one should have a motivation for doing so.

We have only looked at the weak-field, non relativistic regime. It would be interesting to see how the chameleon would behave in a strong gravitational setting (like neutron stars). This work has been given a treatment within the standard chameleon model [85, 63], but a field-dependent coupling could alter these results. It could also be interesting to see if the chameleon favors the formation of super massive black-holes at the centre of galaxies, or if the presence of a chameleon can alter the mass-radius relationship of white dwarfs.

Perhaps the most interesting continuation would be to look at the the non-linear structure formation within chameleon models. There are starting to come some articles on this subject, but there are still many things left to be solved. An analysis of this kind would require a full N-body simulation though, which is highly non-trivial.

Chapter 9

Appendix

9.1 Spherical solution of the field equation in the BD model

Consider a spherical body, for example a planet, with constant density ρ_c which is embedded in a background density ρ_b. In the case of a planet, the average density outside the body will be very small so we can approximate $\rho_b = 0$. This approximation can also be valid in other cases, the only assumption we need to impose is that $\rho_b \ll \rho_c$.

The field equation (2.50) in a static spherical symmetric metric, assuming $\beta\phi \ll M_p$, reads

$$\frac{d^2\phi}{dr^2} + \frac{2}{r}\frac{d\phi}{dr} = \frac{\beta\rho}{M_p} \tag{9.1}$$

Inside a spherical body with constant density ρ_c the solution reads

$$\phi = \phi_i + \frac{\beta\rho_c r^2}{6M_p} \quad \text{for} \quad 0 < r < R \tag{9.2}$$

where $\phi_i = \phi(0)$. Outside the body, $\rho_b = 0$, and the field equation reads

$$\frac{d^2\phi}{dr^2} + \frac{2}{r}\frac{d\phi}{dr} = 0 \tag{9.3}$$

The solution that converges to ϕ_0 (the cosmological field) in the background is given by

$$\phi = \phi_0 + \frac{AR}{r} \quad \text{for} \quad r > R \tag{9.4}$$

Matching the two solutions at $r = R$ gives us

$$\phi_i = \phi_0 - \frac{\beta\rho_c R^2}{2} \tag{9.5}$$

$$A = -\frac{\beta\rho_c R^2}{3} \tag{9.6}$$

$$\tag{9.7}$$

Now the field-profile for $r > R$ can be written

$$\phi = \phi_0 + 2\beta M_p U(r) \tag{9.8}$$

where $U(r) = -\frac{GM}{r}$ is the gravitational potential outside the body. We assumed $\beta\phi \ll M_p$ in this derivation, and we can now show that this is a good approximation since

$$\frac{\beta(\phi - \phi_0)}{M_p} < 2\beta^2 U(R) \ll 1 \tag{9.9}$$

for $\beta \lesssim \mathcal{O}(1)$ since the gravitational potential is usually less than 10^{-5} for an average planet.

The fifth-force on a test-particle of mass $m_{\rm test}$ outside the body is

$$F_\phi(r) = -m_{\rm test}\frac{\beta}{M_p}\frac{d\phi}{dr} = 2\beta^2 F_{\rm gravity}(r) \tag{9.10}$$

where $F_{\rm gravity}(r)$ is the gravitational force on the test-body.

9.2 Field equation for a minimal coupled scalar-field

Starting with the action

$$S_\Phi = -\int \sqrt{-g}dx^4 \left[\frac{1}{2}(\partial\Phi)^2 + V(\Phi)\right] \tag{9.11}$$

we introduce a small variation $\delta\Phi$ in Φ that vanishes at infinity. This leads to a variation

$$\delta S_\Phi = -\int \sqrt{-g}dx^4 \left[\frac{1}{2}\delta(\nabla_\mu\Phi\nabla^\mu\Phi) + V_{,\Phi}\,\delta\Phi\right] \tag{9.12}$$

$$= -\int \sqrt{-g}dx^4 \left[\nabla_\mu\Phi\nabla^\mu\delta\Phi + V_{,\Phi}\,\delta\Phi\right] \tag{9.13}$$

$$= -\int \sqrt{-g}dx^4 \left[-(\nabla_\mu\nabla^\mu\Phi)\delta\Phi + V_{,\Phi}\,\delta\Phi\right] \tag{9.14}$$

$$= \int \sqrt{-g}dx^4 \left[\Box\Phi - V_{,\Phi}\,\right]\delta\Phi \tag{9.15}$$

in S. Some comments on the derivation: In the second line we have used the fact that derivation and variation commutes. In the third line we have used the identity $\nabla^\mu\Phi\nabla^\mu\delta\Phi = \nabla^\mu\left[\delta\Phi\nabla_\mu\Phi\right] - \delta\Phi\Box\Phi$. The first term on the RHS is a total divergence which by Gauss theorem does not contribute to the variation since $\delta\Phi$ is assumed to vanish at infinity. Demanding that the action is invariant for any $\delta\Phi$ we get the field equation

$$\Box\Phi = V_{,\phi} \tag{9.16}$$

The $\Box$-operator in a flat FLRW metric,

$$ds^2 = -dt^2 + a(t)^2(dx^2 + dy^2 + dz^2) \tag{9.17}$$

is given by

$$\Box\Phi = \nabla_\mu\nabla^\mu\Phi = -\frac{d^2\Phi}{dt^2} + \frac{1}{a^2}\nabla^2\Phi + \Gamma^\mu_{\alpha\mu}\Phi,^\alpha \tag{9.18}$$

The last term is found by using the expression for the Christoffel-symbols (2.22)

$$\Gamma^{\mu}_{\alpha\mu}\Phi,^{\alpha} = \frac{1}{2}g^{\mu\delta}(g_{\mu\delta,\alpha} + g_{\alpha\delta,\mu} - g_{\alpha\mu,\delta})\Phi,^{\alpha} \tag{9.19}$$

$$= \frac{1}{2}g^{ij}(g_{ij,\alpha} + g_{\alpha j,i} - g_{\alpha i,j})\Phi,^{\alpha} \tag{9.20}$$

$$= \frac{1}{2}g^{ij}g_{ij,0}\Phi,^{0} \tag{9.21}$$

$$= -\frac{3}{2a^2}(2a\dot{a})\dot{\Phi} = -3H\dot{\Phi} \tag{9.22}$$

where we have used $\dot{\Phi} = \Phi_{,0} = -\Phi,^{0}$ together with the definition $H \equiv \frac{\dot{a}}{a}$. Thus

$$\Box\Phi = -\ddot{\Phi} - 3H\dot{\Phi} + \frac{1}{a^2}\nabla^2\Phi \tag{9.23}$$

and the field equation becomes

$$\ddot{\Phi} + 3H\dot{\Phi} - \frac{1}{a^2}\nabla^2\Phi + V_{,\Phi} = 0 \tag{9.24}$$

When the scalar-field is homogeneous there is no spatial variation and the equation above reduces to

$$\ddot{\Phi} + 3H\dot{\Phi} + V_{,\Phi} = 0 \tag{9.25}$$

9.3 Fifth-force between two parallel plates due to a linear scalar-field

We consider the fifth-force between two parallel plates due to a linear scalar field with a constant mass m and coupling λ. The two plates are separated by a distance $d \ll R$ where R is the radius of the plates. Because of this condition we can consider the plates as infinite slabs and take plate one to occupy the region $z < 0$ and plate two to occupy the region $z > d$.

Since linearity means the superposition principle holds we need only consider the field emanating from plate 1 in order to calculate the force between the plates. The field-equation for a linear scalar field reads[1]

$$\nabla^2\phi = m^2\phi + \frac{\lambda\rho_c}{M_p} \tag{9.26}$$

[1]The chameleon model with a quadratic potential, $V(\phi) = \frac{1}{2}m^2\phi^2$.

where $\nabla^2 = \frac{d^2}{dz^2}$ because of the symmetry in the setup. The force is given by the same expression as in the chameleon model

$$F_\phi = \int_d^\infty \frac{\lambda\rho_c}{M_p}\nabla\phi dz \tag{9.27}$$

with $\nabla \to \frac{d}{dz}$. The field equation has the solution

$$\phi(z) = Ae^{mz} - \frac{\lambda\rho_c}{M_p m^2} \text{ for } z < 0 \tag{9.28}$$

$$\phi(z) = Be^{-mz} \text{ for } z > 0 \tag{9.29}$$

Matching the two solutions at $z = 0$ gives $B = -A = -\frac{\lambda\rho_c}{2M_p m^2}$. The force on the second plate due to the first is then given by

$$\frac{F_\phi}{A} = \frac{\lambda\rho_c}{M_p}\int_d^\infty \nabla\phi dz = -\frac{\lambda\rho_c}{M_p}\phi(d) \tag{9.30}$$

$$= 8\pi\lambda^2\frac{G\rho_c^2 e^{-md}}{m^2} \tag{9.31}$$

Note that λ parametrizes the strength of the interaction relative to $M_p^{-2} \equiv 8\pi G$. If one wants λ to be the strength relative to gravity, which is just G, one should replace $\lambda \to \frac{\lambda}{8\pi}$ in the result above.

Bibliography

[1] J. Khoury and A. Weltman, Phys. Rev. D **69** (2004) 044026 [arXiv:astro-ph/0309411].

[2] A. Riess et al., AJ 116, 1009 (1998); S. Perlmutter et al., ApJ 517, 565 (1999).

[3] D. Spergel et al., ApJ Supp. **148**, 175 (2003).

[4] A.J. Sanders et al., Meas. Sci. Technol. **10**, 514 (1999).

[5] J. Mester et al., Class. Quant. Grav. **18**, 2475 (2001)

[6] A.M. Nobili et al., Class. Quant. Grav. **17**, 2347 (2000)

[7] James J. Binney, 'Lecture Notes on Classical Fields', http://www-thphys.physics.ox.ac.uk/user/JamesBinney/classf.pdf

[8] Francis E. Low, 'Classical Field Theory: Electromagnetism and Gravitation', Wiley-VCH, ISBN: 0-471-59551-9

[9] Theodore Frankel, 'The geometry of physics: an introduction' 2nd ed. (2004). ISBN 0-521-53927-7

[10] D. F. Mota and D. J. Shaw, Phys. Rev. D **75** (2007) 063501 [arXiv:hep-ph/0608078].

[11] Ph. Brax, C. van de Bruck and A. C. Davis, JCAP **0411** (2004) 004 [arXiv:astro-ph/0408464].

[12] P. Brax, C. van de Bruck, A. C. Davis and D. J. Shaw, Phys. Rev. D **78** (2008) 104021 [arXiv:0806.3415 [astro-ph]].

[13] P. Brax, C. van de Bruck, A. C. Davis, D. F. Mota and D. J. Shaw, Phys. Rev. D **76** (2007) 124034 [arXiv:0709.2075 [hep-ph]].

[14] P. Brax, C. van de Bruck, A. C. Davis, J. Khoury and A. Weltman, Phys. Rev. D **70** (2004) 123518 [arXiv:astro-ph/0408415].

[15] T. P. Waterhouse, arXiv:astro-ph/0611816.

[16] J. c. Hwang, Astrophys. J. **375** (1991) 443.

[17] John D. Norton, 'Einstein's Investigations of Galilean Covariant Electrodynamics prior to 1905', Archive for History of Exact Sciences 59: 45-105, doi:10.1007/s00407-004-0085-6, (2004)

[18] Albert Einstein, 'Relativity: The Special and General Theory' (1920)

[19] C. M. Will, 'Theory and experiment in gravitational physics', Revised edition, Cambridge University Press (1993)

[20] T. Tamaki and S. Tsujikawa, Phys. Rev. D **78** (2008) 084028 [arXiv:0808.2284 [gr-qc]].

[21] B. Bertotti, L. Iess and P. Tortora, Nature **425** (2003) 374.

[22] A. De Felice and S. Tsujikawa, arXiv:1002.4928 [gr-qc].

[23] È.È. Flanagan, Class. Quant. Grav., **21**:3817, (2004)

[24] Ø. Grøn and S. Hervik, 'Einstein's General Theory of relativity', Springer (1997), ISBN: 978-0-387-69199-2

[25] J. K. Webb *et al.*, Phys. Rev. Lett. **87** (2001) 091301 [arXiv:astro-ph/0012539].

[26] J.P. Ostriker and P. Steinhardt, Scientific American, vol. **284**, 1 (2001)

[27] S. Baessler, B. R. Heckel, E. G. Adelberger, J. H. Gundlach, U. Schmidt and H. E. Swanson, Phys. Rev. Lett. **83** (1999) 3585.

[28] Hughes et al., Phys. Rev. lett. **4** no. 1 (1960), pg 342.

[29] P. Brax and C. van de Bruck, Class. Quant. Grav. **20** (2003) R201 [arXiv:hep-th/0303095].

[30] F. Mandl and G. Shaw, 'Quantum field theory', Wiley Publ., ISBN: 0-471-94186-7

[31] G.W. Anderson and S.M. Carroll, astro-ph/9711288.

[32] T. Damour and A.M. Polyakov, Nucl. Phys. B **423**, 532 (1994); Gen. Rel. Grav. 26, 1171 (1994).

[33] G. Huey, P.J. Steinhardt, B.A. Ovrut and D. Waldram, Phys. Lett. B **476**, 379 (2000)

[34] C.T. Hill and G.C. Ross, Nucl. Phys. B **311**, 253 (1988)

[35] J. Ellis, S. Kalara, K.A. Olive and C. Wetterich, Phys. Lett. B **228**, 264 (1989);

[36] G.W. Anderson and S.M. Carroll, astro-ph/9711288.

[37] G. Huey, P.J. Steinhardt, B.A. Ovrut and D. Waldram, Phys. Lett. B **476**, 379 (2000).

[38] C.T. Hill and G.C. Ross, Nucl. Phys. **B311**, 253 (1988); J. Ellis, S. Kalara, K.A. Olive and C. Wetterich, Phys. Lett. B **228**, 264 (1989).

[39] Radouane Gannouji, Bruno Moraes, David F. Mota, David Polarski, Shinji Tsujikawa and Hans Winther. In preperation.

[40] J. K. Hoskins, R. D. Newman, R. Spero and J. Schultz, Phys. Rev. D **32** (1985) 3084.

[41] http://lambda.gsfc.nasa.gov/

[42] B. Jain and J. Khoury, arXiv:1004.3294 [astro-ph.CO].

[43] G. W. Gibbons and S. W. Hawking, Phys. Rev. D **15** (1977) 2752.

[44] R. H. Dick, 'Experimental Relativity', Relativity, Groups and Topology, ed. C. DeWitt and B. DeWitt, pp. 165-313. Gordon and Breach, New York (1964)

[45] R. M. Wald, 'General Relativity', University of Chicago Press (1984)

[46] Ø. Grøn, 'Lecture Notes on the General Theory of Relativity', Springer (2009)

[47] Ø. Elgarøy 'Lecture Notes in Cosmology', University of Oslo (2008)

[48] S. Dodelson, 'Modern Cosmology', Academic Press (2003)

[49] P. Brax, C. van de Bruck, A. C. Davis and A. M. Green, Phys. Lett. B **633** (2006) 441 [arXiv:astro-ph/0509878].

[50] S. Tsujikawa, R. Gannouji, B. Moraes and D. Polarski, Phys. Rev. D **80** (2009) 084044 [arXiv:0908.2669 [astro-ph.CO]].

[51] R. Gannouji, B. Moraes and D. Polarski, arXiv:0907.0393 [astro-ph.CO].

[52] R. Gannouji, B. Moraes and D. Polarski, JCAP **0902** (2009) 034 [arXiv:0809.3374 [astro-ph]].

[53] D. J. Kapner, T. S. Cook, E. G. Adelberger, J. H. Gundlach, B. R. Heckel, C. D. Hoyle and H. E. Swanson, Phys. Rev. Lett. **98** (2007) 021101 [arXiv:hep-ph/0611184].

[54] For a review of experimental tests of the Equivalence Principle and General Relativity, see C.M. Will, *Theory and Experiment in Gravitational Physics*, 2nd Ed., (Basic Books/Perseus Group, New York, 1993); C.M. Will, Living Rev. Rel. 4, 4 (2001).

[55] H. Motohashi, A. A. Starobinsky and J. Yokoyama, arXiv:0905.0730 [astro-ph.CO].

[56] S. Tsujikawa, Phys. Rev. D **77** (2008) 023507 [arXiv:0709.1391 [astro-ph]].

[57] I. Thongkool, M. Sami, R. Gannouji and S. Jhingan, Phys. Rev. D **80** (2009) 043523 [arXiv:0906.2460 [hep-th]].

[58] A. A. Starobinsky, JETP Lett. **86** (2007) 157 [arXiv:0706.2041 [astro-ph]].

[59] A. Upadhye, J. H. Steffen and A. Weltman, Phys. Rev. D **81** (2010) 015013 [arXiv:0911.3906 [hep-ph]].

[60] P. Brax, C. Burrage, A. C. Davis, D. Seery and A. Weltman, arXiv:0911.1267 [hep-ph].

[61] P. Brax, C. van de Bruck, A. C. Davis and D. Shaw, arXiv:0911.1086 [hep-ph].

[62] A. C. Davis, C. A. O. Schelpe and D. J. Shaw, Phys. Rev. D **80** (2009) 064016 [arXiv:0907.2672 [astro-ph.CO]].

[63] S. Tsujikawa, T. Tamaki and R. Tavakol, JCAP **0905** (2009) 020 [arXiv:0901.3226 [gr-qc]].

[64] P. Brax, C. van de Bruck, A. C. Davis, D. F. Mota and D. J. Shaw, Phys. Rev. D **76** (2007) 085010 [arXiv:0707.2801 [hep-ph]].

[65] A. Upadhye, S. S. Gubser and J. Khoury, Phys. Rev. D **74** (2006) 104024 [arXiv:hep-ph/0608186].

[66] E. G. Adelberger [EOT-WASH Group], arXiv:hep-ex/0202008.

[67] K. Hinterbichler and J. Khoury, arXiv:1001.4525 [hep-th].

[68] N. G. Stephen, Journal of Sound and Vibration Volume 310, Issue 3, Page 729-739, (2008)

[69] A. D. Linde, Lect. Notes Phys. **738** (2008) 1 [arXiv:0705.0164 [hep-th]].

[70] P. Binetruy, Supersymmetry: Theory, experiment and cosmology, *Oxford, UK: Oxford Univ. Pr. (2006) 520 p*

[71] R. S. Decca et al., Phys. Rev. Lett. **91**, 050402 (2003).

[72] R. S. Decca et al., Ann. Phys. **318**, 37 (2005).

[73] R. S. Decca et al., Phys. Rev. D **75**, 077101 (2007).

[74] D. Spergel et al., ApJ Supp. **148**, 175 (2003).

[75] C. Burrage, A. C. Davis and D. J. Shaw, Phys. Rev. D **79** (2009) 044028 [arXiv:0809.1763 [astro-ph]].

[76] J. P. Uzan, arXiv:0908.2243 [astro-ph.CO].

[77] Ph. Brax, C. van de Bruck, A. C. Davis, D. J. Shaw and D. Iannuzzi, arXiv:1003.1605 [quant-ph].

[78] J. H. Steffen [GammeV Collaboration], PoS **IDM2008** (2008) 064 [arXiv:0810.5070 [hep-ex]].

[79] A. S. Chou *et al.* [GammeV Collaboration], Phys. Rev. Lett. **102** (2009) 030402 [arXiv:0806.2438 [hep-ex]].

[80] A. A. Starobinsky, JETP Lett. **86**, 157 (2007).

[81] R. Gannouji, B. Moraes and D. Polarski, JCAP **0902**, 034 (2009).

[82] S. M. Carroll, I. Sawicki, A. Silvestri and M. Trodden, New J. Phys. **8**, 323 (2006); T. Faulkner, M. Tegmark, E. F. Bunn and Y. Mao, Phys. Rev. D **76**, 063505 (2007); Y. S. Song, W. Hu and I. Sawicki, Phys. Rev. D **75**, 044004 (2007); R. Bean, D. Bernat, L. Pogosian, A. Silvestri and M. Trodden, Phys. Rev. D **75**, 064020 (2007); Y. S. Song, H. Peiris andW. Hu, Phys. Rev. D **76**, 063517 (2007); Y. S. Song, H. Peiris and W. Hu, Phys. Rev. D **76**, 063517 (2007); L. Pogosian and A. Silvestri, Phys. Rev. D **77**, 023503 (2008); T. Tatekawa and S. Tsujikawa, JCAP **0809**, 009 (2008); H. Oyaizu, M. Lima andW. Hu, Phys. Rev. D **78**, 123524 (2008); K. Koyama, A. Taruya and T. Hiramatsu, arXiv:0902.0618 [astro-ph.CO]; S. Tsujikawa, R. Gannouji, B. Moraes and D. Polarski, Phys. Rev. D **80** (2009) 084044 [arXiv:0908.2669 [astro-ph.CO]].

[83] L. M. Wang and P. J. Steinhardt, Astrophys. J. **508**, 483 (1998).

[84] E. V. Linder, Phys. Rev. D **72**, 043529 (2005); D. Huterer and E. V. Linder, Phys. Rev. D **75**, 023519 (2007).

[85] J. Lindroos, 'Chameleon fields and compact objects', Master Thesis, University of Oslo (2009)